AUS DER KLINIK FÜR PSYCHIATRIE UND PSYCHOTHERAPIE
DIREKTOR: Univ.-Prof. Dr. T. Kircher
DES FACHBEREICHS MEDIZIN DER PHILIPPS-UNIVERSITÄT MARBURG
IN ZUSAMMENARBEIT MIT DEM FB PHYSIK DER PHILIPPS-UNIVERSITÄT MARBURG

Multisensory self-motion processing in humans

INAUGURAL-DISSERTATION
zur Erlangung des Doktorgrades der Naturwissenschaften (Dr. rer. nat.)
am Fachbereich Medizin der Philipps-Universität Marburg

dem Fachbereich Medizin der Philipps-Universität Marburg

vorgelegt von

M. Sc. Elisabeth-Maria Rosenblum aus Osnabrück
Marburg, 2023

Angenommen vom Fachbereich Medizin der Philipps-Universität Marburg am:
25.09.2023

Gedruckt mit Genehmigung des Fachbereichs.

Dekan/in: Prof. Dr. Denise Hilfiker-Kleiner
Referent/in: Prof. Dr. Frank Bremmer
Korreferent/in: Prof. Dr. Benjamin Straube

TABLE OF CONTENTS

I. ABBREVIATIONS

AIC:	Anterior insular cortex
BOLD:	Blood-oxygen-level dependent
EEG:	Electroencephalography
ERP:	Event-related potential
fMRI:	Functional magnetic resonance imaging
FOE:	Focus of expansion
FOV:	Field of view
hMST:	Human medial superior temporal area
hMT:	Human middle temporal visual area
hVIP:	Human ventral intraparietal area
IPL:	Inferior parietal lobule
MST:	Medial superior temporal area
MT:	Middle temporal visual area
SI:	Primary somatosensory cortex
SII:	Secondary somatosensory cortex
VIP:	Ventral intraparietal area
vMMN:	Visual Mismatch negativity
VR:	Virtual reality

II. LIST OF FIGURES

III. LIST OF TABLES

1. INTRODUCTION

The brain estimates and controls our self-motion relative to the environment. In the visual modality, self-motion generates a specific pattern on the retina called 'optic flow' (Warren et al., 1988). This pattern contains information about the traveled distance, travel speed, and travel direction (heading) of the moving organism (Gibson, 1966). However, to create stable perception of the world, the brain combines cues from different sensory modalities, making self-motion perception a multisensory phenomenon. While a large body of literature is devoted to visual and vestibular self-motion perception, the contribution of auditory and tactile information on self-motion perception has rarely been studied.

In my thesis, I have examined specific aspects of tactile self-motion perception (path-integration and heading) in human observers and possible interactions with visually perceived self-motion. In a series of experiments, I simulated visual and tactile self-motion by showing an optic flow stimulus and providing airflow (tactile flow) towards the subjects' foreheads.

In a first behavioral study (study 1), I investigated the influence of behaviorally irrelevant tactile flow on visual self-motion direction perception. Subjects indicated perceived heading in unimodal (unimodal tactile, unimodal visual) conditions as well as *visually* perceived heading in a combined condition (bimodal) where tactile and visual stimuli presented either congruent or incongruent self-motion directions. In a second behavioral study (study 2), in which the tactile flow was introduced as behaviorally relevant, I examined if and how stimuli from both modalities are integrated in the estimation of perceived heading. Finally, in an imaging study (study 3), I investigated the neural correlates of visual and tactile path integration as a function of cognitive task demands.

1.1. Self-motion perception

For effective navigation through the environment, the moving observer must accurately estimate their own motion in space and position relative to objects in the surrounding. Vision is specialized for perception of self-motion by encoding different motion cues. While visual information provides reliable information to sufficiently guide motion through the environment, it cannot, in isolation, be used to guide the motor response required to move in the direction of self-motion (Telford et al., 1995). Information from other sensory modalities is needed to execute motoric actions. Another important and well-studied sensory modality

in the context of self-motion is the vestibular modality (Monkeys: see Gu, 2018 for a review; humans: see Cullen, 2019 for a review). The vestibular system supports a stable percept of the world while the moving observer explores their environment by constantly moving their head and eyes. While the vestibular system encodes information about head motion, the proprioceptive sense provides feedback about muscle and joint position. Proprioception is defined as "the sense of self-movement and body position" (Mergner & Rosemeier, 1998; Tuthill & Azim, 2018) and has been previously demonstrated to play a major role for self-motion. Another modality that has also received attention in the context of self-motion is the auditory modality. For instance, auditory cues can provide information about self-motion by changes e.g., of loudness, the Doppler effect or interaural time differences (Lutfi & Wang, 1999). Tone frequency can provide information about relative distance of objects in the environment (Butler & Flannery, 1980; Coleman, 1963), delivering important information for navigation through space. Importantly, acoustic cues can also provide particular information about heading direction (McKerrow, 2008; Müller & Schnitzler, 2000) and travel distance (Krala et al., 2019; Von Hopffgarten & Bremmer, 2011).

All these sensory modalities, i.e., visual, vestibular, proprioceptive, and auditory, have been comparatively well studied in their role in self-motion perception. On the contrary, the tactile modality has received very little attention. The aim of my thesis was to investigate tactile self-motion perception and its interaction with visual self-motion stimuli to add to the existing, sparse literature on tactile self-motion perception.

1.2. Visual self-motion processing

Guiding motion through a constantly changing environment is one of the visual system's most demanding and important functions. While the organism relies on input from various sensory modalities, it is the visual input that contributes most strongly to the estimation of self-motion parameters (Benson, 1990; Howard, 1982). This was initially demonstrated by studies where subjects were placed inside a "swinging room" (e.g., Aronson & Lee, 1974). Subjects stood inside an experimental room of which the ceiling and walls were constructed to move back and forth, inducing optic flow patterns that would accompany natural forward and backward motion. Already during the first trials, subjects experienced the illusion that they themselves were swaying, demonstrating that strong illusions of self-motion can be induced by visual information alone (Engel et al., 2020, 2021; Student et al., 2022).

Using optic flow in the laboratory can induce an illusion of self-motion, (rotation or translation of the body) which is called *vection* (Kovács et al., 2008). Characteristics of that pattern depend on the speed, distance, and the direction of travel (Lappe et al., 1999). Figure 1 shows a schematic illustration of the egocentric visual flow field generated by linear forward motion of the observer. White arrows indicate the moving direction. More distant points in the environment move much more slowly on the observers' retina (indicated by shorter arrows in Fig. 1). The 'singularity' in the flow field is called the focus of expansion (FOE). During fixed gaze, the FOE specifies the observer's heading direction (red dot in Figure 1).

Figure 1. Schematic illustration of egocentric optic flow patterns that result from straight ahead linear translational motion of the observer when gaze is directed straight ahead. During locomotion, the optical flow field expands from a singular point, the focus of expansion (FOE, red dot). The direction of arrows indicates the direction a particular point in the environment would take over time of translation. The length of the arrows indicates the speed of the motion with longer lines indicating faster motion in the periphery and shorter lines indicating slower motion near to the FOE. Modified from Bremmer, 2008.

The magnitude of optic flow emerging from the scene is dependent on travel speed. During observers' rotation, the rate of optic flow specifies the angular speed as well as the direction of rotation (Warren, 1995). The integration of experienced optic flow over time allows to determine the absolute angle by which the observer has turned. Accordingly, integration of the optic flow over time determines the (angular and translational) distance that the observer has traveled. Path integration is a navigation strategy that integrates this information to continuously update one's current position (Loomis et al., 1999).

Several properties of the visual system enable estimation of self-motion parameters. For example, binocular disparity allows for the perception of depth (Stereopsis). In mammals, stereopsis is based on horizontal and vertical differences of incoming object images between the two retinas as a result of the horizontal separation of the eyes. Stereoscopic information has been shown to enhance the experience of vection from visually simulated self-motion (Andersen & Braunstein, 1985). To be able to explore the current path and to plan for the next step, the moving observer is constantly adjusting their eye position (Matthis et al., 2022). Naturally, optic flow patterns trigger eye movements towards the FOE (Chow et al., 2021). These eye movements also induce shifts of the optic flow patterns, thereby confounding the interpretation of self-motion information (Warren & Hannon 1990; Lappe et al., 1999; Bremmer et al., 2017). Thus, successful navigation depends on the ability to separate optic flow caused by eye movements from motion signals caused by self-motion. The nervous system obtains this by combining incoming sensory information with the information from outgoing motor commands that are used to control the eye-movement. Copies of these out-going commands are referred to as efference copy or corollary discharge (Bremmer et al., 2017; Cullen, 2004; Morris et al., 2012; Sperry, 1950; Von Holst & Mittelstaedt, 1950; for a review see: Subramanian et al., 2019). The concept of efference copies will further be explained below (cf. Section 3.4.3. 'Predictive Coding').

On the neural level, visual self-motion processing is organized in a hierarchy defined by stimulus properties. Figure 2 shows the processing pathway from the point when the visual stimulus reaches the retina along the subcortical hierarchy up to the visual cortex. Light arriving on the retina elicits hyperpolarization of the photoreceptors (rods and cones). By this, incoming light is converted into receptor potentials. These electrical signals are then transferred to bipolar cells which eventually lead to action potentials in retinal ganglion cells and retinal interneurons (such as Horizontal- and Amacrine cells) which interconnected with bipolar cells, carrying neuronal information and modulate information flow. The axons of retinal ganglion cells leave the eye and as a whole form the two optic nerves. First crossing on the level of the optic chiasm, the optic nerve passes the lateral geniculate nucleus (LGN), a subsection of the thalamus. This leads to ipsilateral processing of visual information (information from the left hemifield is processed in the right hemisphere of the brain and vice versa). Finally, the optic tract devolves into visual pathways that reach the striate cortex (i.e., primary visual cortex, area V1 in primates) of the occipital lobe. The spatial organization of visual information

arriving on the retina is maintained up to the striate cortex and beyond ('retinotopy'), with a strong magnification of the foveal space. Early visual areas (striate and extrastriate cortex) have small receptive fields that respond to basal stimulus properties like, for example, specific orientations of bars or gratings. Following a definition by Jose-Manuel Alonso and Yao Chen (2009), a receptive field "is a portion of sensory space that can change neuronal responses when stimulated".

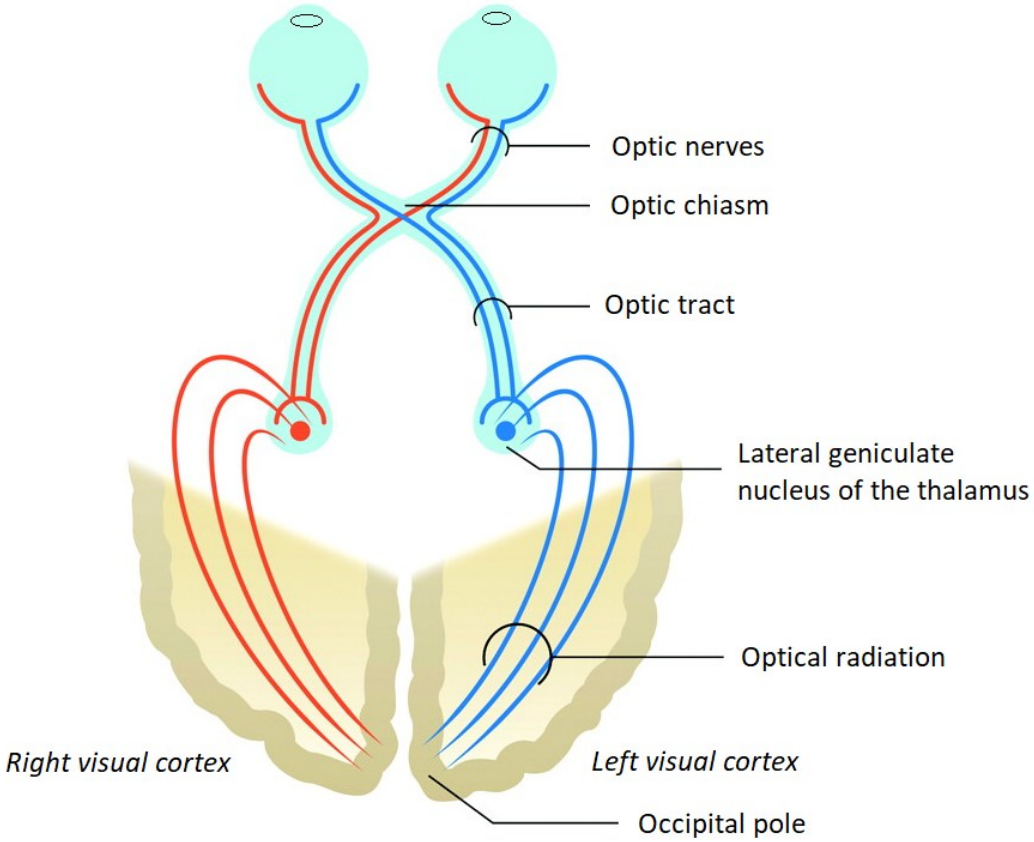

Figure 2. Schematic overview of the hemispheric processing of visual information from both visual fields arriving at the retina. Information from the retina travels to the primary visual cortex through the optic chiasm and subcortical structures of the thalamus. Modified from 'Challenges of the Anatomy and Diffusion Tensor Tractography of the Meyer Loop', Mandelstam, American Journal of Neuroradiology August 2012, 33 (7) 1204-1210; DOI: https://doi.org/10.3174/ajnr.A2652

Visual information leaves the striate cortex towards extrastriate visual cortices and eventually two main pathways. Figure 3 schematically depicts both processing pathways along the cortex. At this higher neural level, the two-streams hypothesis provides a model of sensory processing based on stimulus features (Mishkin et al., 1983). While the ventral stream

reaches area V4 and further connects to the temporal lobe, the dorsal stream leads via area V5, also known as the middle temporal visual area (hMT), to the parietal lobe. Broadly speaking, the ventral pathway (often also called the “what” pathway) is involved in object identification and recognition. Conversely, the dorsal pathway (often referred to as the “where” or “how” pathway) mainly processes information about the objects’ spatial location and their movements relative to the observer.

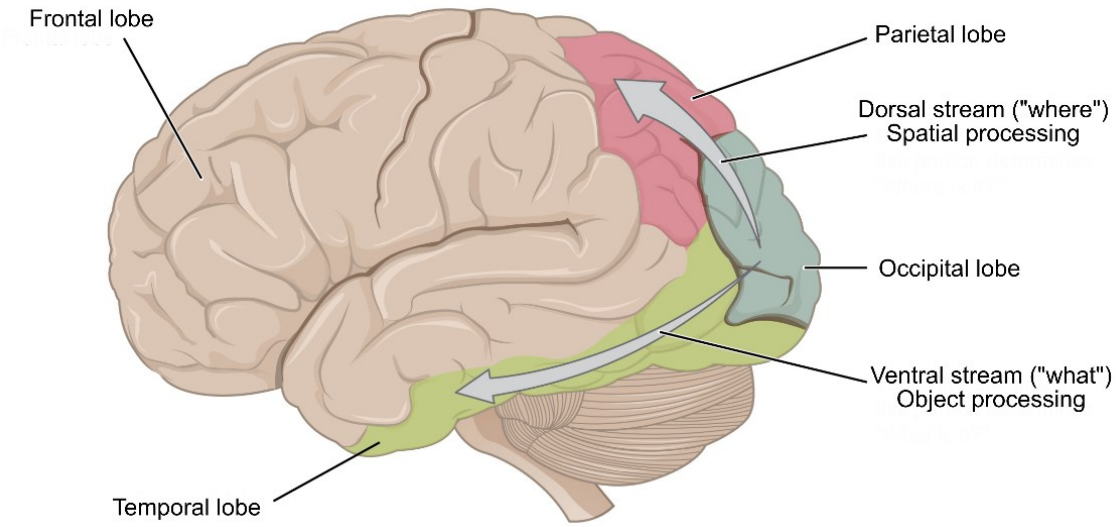

Figure 3. Schematic overview of the dorsal and ventral visual stream. The two-streams hypothesis divides the processing of visual information into two streams that follow different routes in the brain. Both streams originate from primary visual cortex. From there, spatial information (‘where’; i.e., different aspects of the spatial arrangement of the outside world) travels along the dorsal stream and is processed in the parietal lobe. Information for object identification (“what”) follows the ventral stream and is processed in the temporal lobe. Modified from Anatomy & Physiology, Connexions Web site. http://cnx.org/content/col11496/1.6/, Jun 29, 2022.

While early studies proposed a distinct processing in both streams, now a close cross-talk and joint processing between both paths is assumed. In the context of self-motion processing, the areas along the dorsal pathway play a major role in stimulus processing. Neurophysiological studies on non-human primates have identified several areas, based on their response properties, that seem to play a significant role in the analysis of optic flow information, for example the medial superior temporal area (MST) and the ventral intraparietal

area (VIP). These higher order areas have larger-sized receptive fields that respond specifically to certain optic flow properties. Neurons of that areas have been shown to respond to the speed, orientation, and location of visual motion stimuli (MST: Angelaki et al., 2011; Bremmer et al., 2010; Duffy & Wurtz, 1991; Gu et al., 2006, 2012; Lappe et al., 1996; Paolini et al., 2000; Saito et al., 1986, VIP: Bremmer et al., 2002a; Chen et al., 2011; Kaminiarz et al., 2022; Schlack et al., 2002; Shao et al., 2022). These areas are also directly connected to areas that have been implicated in eye, limb, and body movements (MST: e.g., Ilg & Schumann, 2022, VIP: e.g., Nakamura et al., 2001). Imaging studies on humans have identified human equivalents of these areas by employing stimuli that match the preferred stimulation of monkey MST and VIP neurons (hMST: Dukelow et al., 2001; Huk et al., 2002, hVIP: Bremmer et al., 2001; for a review see: Foster et al., 2022).

Vision delivers extensive information to guide motion through the environment, however, it cannot fulfill the complex task of self-motion through the environment alone. As described above, self-motion perception is found to be a multisensory phenomenon. While self-motion perception has been studied in several sensory modalities, one modality has received little attention in the context of self-motion - somatosensation.

1. 3. Tactile self-motion processing

Motion through the environment provides the moving organism with a variety of somatosensory sensations. For example, when riding a bike, wind meets the subjects' face and body, producing the sensation of self-motion (vection). In that scenario, airflow to the face can be considered as information about translational self-motion. Perceived airflow towards the moving observers' face and body scales in strength and location with the speed and heading of self-motion. However, it also provides information about external factors, such as wind in the surrounding and the weather conditions. I will focus in this thesis on the interactions of tactile self-motion information with the visual domain.

The contribution of tactile flow involved in vection has been acknowledged by recent studies on human observers. The majority of studies investigated vection by employing vibrotactile stimuli (Farkhatdinov & Hayward, 2013; Harris et al., 2017; Riecke, 2005; Riecke et al., 2008; Seno et al., 2011). For example, Harris and colleagues (2017) impressively showed that tactile self-motion information provided towards the fingertips was even capable of

overriding self-motion stimuli from the visual and vestibular modality. Only few studies have employed tactile flow as self-motion stimuli. Murata and collegues (2014) could show that perception of self-motion can be driven by airflow towards the participants' body in the absence of visual cues. Accordingly, a few studies have demonstrated that the experience of vection can be facilitated if airflow is added to visual self-motion information. For example, Seno et al. (2011) combined airflow blowing at a constant speed towards the participants' face with optic flow stimuli simulating either forward (expanding dot cloud) or backward (contracting dot cloud) self-motion. Subjects rated their impression of vection. They found that vection perceived from airflow in combination with visually simulated forward self-motion was rated highest. Yahata et al. (2021) compared the vection strength induced by airflows of different temperatures towards the frontal part of the body while participants walked through different environments in a Virtual Reality Set-Up (VR). Visual stimuli consisted of a fire-corridor or a corridor consisting of geometric cubes. Wind was provided at normal temperature, hot temperature, or wind was absent. The combination of hot wind and the fire corridor strongly facilitated perceived vection compared to combinations of other stimulus conditions. These results showed that contextually congruent multisensory information enhances the perception of vection to form one coherent percept of the surroundings. In the context of path integration, a study by Churan et al. (2017) has demonstrated that adding congruent tactile information to visual self-motion information significantly improved the precision of actively reproduced distances in a distance reproduction task. In that study, each trial simultaneously presented either speed-congruent or -incongruent visual and tactile self-motion information. Only the presentation of congruent self-motion speed in both modalities supported response precisions of distance replications. In the context of heading, Feng & Lindeman (2016) provided their subjects with directional wind while solving an orientation task in VR. The speed of airflow was proportional to the subjects' motion velocity in the VR environment and the direction of airflow changed relative to the participants' virtual orientation, providing additional information about position, and heading direction in space. Results showed that this addition of tactile cues caused a significant increase in performance. A few behavioral studies have provided evidence for tactile flow as a valid cue in self-motion perception, however, self-motion perception in the tactile domain is less researched than other sensory modalities.

On a neural level, the perception of touch in mammals is generated by the largest sensory organ, the skin. Six different types of mechanoreceptors encode information about touch

(Hair follicles, Pacinian corpuscles, Meissner corpuscles, Merkel complexes, Ruffini corpuscles, see Delmas et al., 2011). Temperature and pain are mainly encoded free nerve endings of neurons located in the spinal cord (Aδ- and C-fibers; see Prescott & Ratté, 2007). In the face alone, over 17000 nerve endings form mechanosensitive structures signaling different aspects of touch. Physical stimuli such as pressure on the skin or temperature change activate receptors of dorsal root ganglions in the cranial nerves. These nerves convey somatosensory information from the face and head towards the brain. Generally, the neural pathways from early receptors to higher-order processing brain areas preserve neighboring locations of incoming stimulus from the skin when conveying them to the brain (analogous to the retinotopy in early visual processing, cf. section 3.2). In the human brain, incoming somatosensory information first arrives at either the Nucleus ventralis posteromedialis (facial representations) or the Nucleus ventralis posterolateralis (body representations) of the Thalamus. After passing the Thalamus complex, incoming somatosensory information arrives at primary somatosensory cortex which is located on the postcentral gyrus between the central gyrus and the postcentral sulcus (Treede & Baumgärtner, 2019). The primary somatosensory cortex (SI) can be subdivided into different areas according to the functionality in the encoding of stimulus properties. The SI cortex consists of four cytoarchitectonically distinct areas; areas 3a, 3b, 1, and 2 (Brodmann, 1909). Area 3 is engaged into the initial processing of somatosensory information arriving at the cortex directly from the thalamus. Area 3a lies in the fundus of the central sulcus. It mainly encodes proprioceptive information and is involved into the planning of postures and movements. Area 3b in the rostral bank of the postcentral gyrus is engaged in the encoding of touch information in general (Purves et al., 2008). Area 3 is interconnected with areas 1 and 2. Area 1 has been shown to process more complex stimuli, for example in the context of object texture perception by the encoding of direction- and orientation information. Spatial object properties like shape and size have been found to be encoded in area 2 (Bodegård et al., 2001; Grefkes et al., 2013).

The secondary somatosensory cortex (SII), located along the Sulcus lateralis (parietal Operculum) (Eickhoff et al., 2002), already encodes bilateral stimuli, and plays a significant role in the encoding and coordination of more complex, higher-order haptic stimuli (Kuehn & Pleger, 2020; Taoka et al., 2016). The highest processing stage is reached at the posterior parietal cortex which acts as a multimodal association cortex. At this level, sensory information

from different sensory modalities is integrated to form unified percepts and to generate and perform motoric commands (Bremmer et al., 2001; Grefkes et al., 2013).

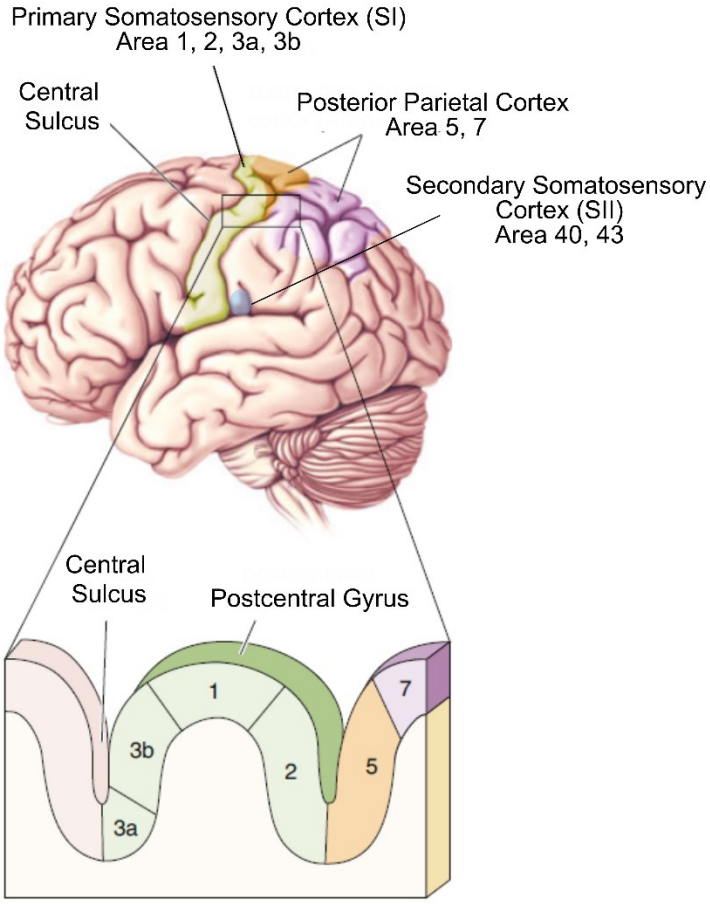

Figure 4. Anatomical overview of somatosensory areas on the cortex. Modified from Bear, M. F., Connors, B. W., & Paradiso, M. A. (2018).

In the macaque monkey, already in 1986, Warren et al. identified that neurons in area SI are tuned to the direction of tactile motion stimuli (Warren et al., 1986). Textured surfaces were moved across the monkeys' skin while neural activity was recorded from area SI. By this, Warren and colleagues identified direction-sensitive neurons responding to movement across the skin in one or more directions in area SI, making this area an important candidate for motion direction perception. Comparable to the properties of motion-selective neurons like in area MT, the motion sensitive neurons in SI have also been shown to be tuned to specific

motion direction (Simoncelli & Heeger, 1998). Human equivalents of macaque areas SI and SII have also been identified by means of fMRI (Bremmer et al., 2001; Disbrow et al., 2000).

By the encoding of mechanoreception, the tactile sense provides information about a multitude of stimulus properties that might be useful for the organism' navigation trough space. However, relying only on one stimulus modality is not a sufficient strategy for successful navigation. In some cases, tactile stimuli might be ambiguous, noisy, or not available, hence it is necessary to consider information from various sensory modalities. In the natural world, integration of various sensory sources of information is key for efficient guidance and for the computation of adequate motor responses. How multisensory information is integrated is subject of many studies and is still not fully understood.

3.4. Multisensory integration of self-motion information

Motion information is conveyed by several sensory sources and is combined to form a coherent percept of the environment (for a review see Angelaki et al., 2009). On the neural level, Wallace, Meredith & Stein (1998) identified different processes by which neural responses elicited by individual stimuli are combined to form one coherent percept. In that sense, multisensory integration is defined as the difference in neural response towards individual stimuli and the neural response to the combination of these stimuli. Generally, multimodal responses are found to be larger than both unimodal responses (known as 'enhancement') or larger than the sum of both unimodal responses (known as 'superadditivity') (Wallace et al., 1998).

Recent studies demonstrated that adding auditory and tactile cues to visual-only cues significantly increased perceived vection (Kruijff et al., 2016; Murovec et al., 2021; Palmisano et al., 2015). However, in the auditory modality, the sensation of auditorily induced vection was found to occur less robust and weaker compared to visually induced vection (Keshavarz et al., 2014; Riecke, 2005; Riecke et al., 2008). By employing auditory self-motion stimuli, studies on human observers have shown that auditory motion cues (in terms of tone pitch scaling with travel speed) can be employed for the estimation of traveled distance (Krala et al., 2019; Von Hopffgarten & Bremmer, 2011). Likewise, for the reproduction of displacement in the azimuth plane, reproduction form visuo-auditory stimuli proved to be more precise than by an auditory target or a visual target alone (Anderson & Zahorik, 2014). For motion processing, neurophysiological (Ahissar et al., 1992; for a review see: Chaplin et al., 2018) and imaging

studies in monkeys (Poirier et al., 2017) have reported on the encoding of the direction of auditory motion in the monkey auditory cortex during the presentation of moving sound stimuli.

Most studies on the perception of self-motion considered visuo-vestibular integration. Among these, a large number of studies reported on the integration of visuo-vestibular heading cues in the perception of heading in non-human primates (Angelaki et al., 2011; Fetsch et al., 2007, 2009) and humans (Crane, 2015; De Winkel et al., 2017; Rodriguez & Crane, 2021). One behavioral study has found that human observers predominantly integrated visual and vestibular cues even in the presence of large spatial discrepancies of up to 90° between heading directions presented in both modalities (De Winkel et al., 2015). For monkeys, one recent neurophysiological study on heading perception has demonstrated that even temporal-incongruent visual-vestibular stimuli are integrated when the visual cue foreruns the vestibular cue with a maximum of 500 ms (Zheng et al., 2021). One reason for this tolerance of spatial and temporal discrepancies in visuo-vestibular self-motion perception might be that in the natural world, such differences practically never occur, making integration of these stimuli in artificial environments the most evident process.

Important insight about potential candidate areas in the integration of multisensory self-motion information is provided by neurophysiological studies on non-human primates. Several cortical areas share self-motion representations across several modalities, e.g., the visual, tactile, and vestibular modality. For example, previous studies in monkeys have suggested that area VIP contributes to multisensory heading perception: It contains neurons that represent the direction and location of incoming stimuli based on visual, tactile as well as vestibular cues (Avillac et al., 2005, 2007; Bremmer et al., 1999; Bremmer et al., 2002a; 2002b; Chen et al., 2013; Duhamel et al., 1998; Fetsch et al., 2007; Gu et al., 2006). Importantly, these neurons response with spatially and action-congruent receptive fields (Avillac et al., 2005, 2007; Bremmer et al., 2002a; Duhamel et al., 1998; Guipponi et al., 2013).

1.3.1. *Reference frames*

Integrating information from various sensory modalities entails that sensory information from different modalities is initially encoded in different frames of reference. Visual information is initially encoded as relative to the eye (i.e., retina-centered), vestibular and auditory information relative to the head and tactile information relative to the body surface.

Integration of sensory information encoded in different reference frames is mandatory for forming one coherent percept of the world. However, the combination of these is complicated by various factors. For example, reference frames have been found to change in dependence to the task (Chen et al., 2018; Sasaki et al., 2020) and across the neural hierarchy (Caruso et al., 2021).

For self-motion information, neurons in area VIP have been found to encode visual stimuli retina-centered (Chen et al., 2013, 2014) and/or head-centered (Duhamel et al., 1997), auditory information retina- and/or head-centered (Mullette-Gillman et al., 2005; Schlack et al., 2005), somatosensory information head centered (Avillac et al., 2005, 2007) and vestibular stimuli intermediate between body- and world-centered (Chen et al., 2013a, 2018). Area VIP is located in the fundus of the intraparietal sulcus and receives projections from, among others, the middle temporal area (MT) (Maunsell & Van Essen, 1983) and area MST (Boussaoud et al., 1990). Humans and non-human primates share common neural representations of self-motion signals. Thus, the investigation of neural responses evoked by self-motion stimuli in non-human primates might serve as an approach to derive putative homologous processes in the human brain.

1.3.2. *Bayes optimal integration*

One theoretical approach describing how information from multiple sensory sources is combined to form a unifying percept is described by the Bayesian theorem. If cues from different sensory modalities share the same origin, their information can be integrated. In this case, according to Bayes Optimal Integration theory (Knill & Pouget, 2004), the system can reduce its uncertainty about the stimulus by exploiting the sensory redundancy. The framework predicts that incoming sensory information is weighted by the reliability of that cues. The integrated sensory percept is then formed from the weighted linear combination of individual cues. This minimizes the variance in the final stimulus estimation, thereby improving the perceptual precision (Alais & Burr, 2004; Ernst & Banks, 2002). On a neurophysiological level, optimal cue integration can be accomplished by populations of neurons that linearly combine unimodal inputs (Gu et al., 2008, for a review see Colonius & Diederich, 2020). A major prediction is that the “optimal observer” accomplishes the combination of sensory cues by taking a weighted average of each unimodal input estimate. Single-cue sensory information is weighted according to its reliability (i.e., inverse variance) (Fetsch et al., 2009; Ma et al.,

2006). One well-founded principle of the Bayesian framework predicts that stimuli presented in spatio-temporal proximity have a higher probability of being integrated (Gepshtein et al., 2005). Numerous psychophysical studies on non-human primates and human observers have demonstrated that multisensory integration can be accurately predicted by the theorem of Bayesian optimal integration (human: Alais & Burr, 2004; Ernst & Banks, 2002; Körding & Wolpert, 2006, monkey: Fetsch et al., 2009; Gu et al., 2008; for a review see: Hou & Gu, 2020). For self-motion, a wealth of published studies has shown that integration of visual and vestibular self-motion cues increases perceptual precision (Butler et al., 2010; De Winkel et al., 2010; Dokka et al., 2015). However, a large number of published studies has also demonstrated Bayes-non-optimal multisensory interaction (Meijer et al. 2019; Rahnev & Denison 2018; Stengard & Van Den Berg 2019).

1.3.3. *Predictive coding*

Integration of optic flow signals becomes considerably complicated when the observer is moving through the environment under natural conditions. For example, optic flow is substantially affected by movements of the body, the head, and the eyes (Lappe et al., 1999a). Furthermore, optic flow is also influenced by motion of objects in the visual field and can be generated by passive movement of the observers or by a moving surrounding (see Section 3.2. "swinging room", Aronson & Lee, 1974, see also Engel et al., 2020, Royden & Hildreth 1996; Warren 1995). Accordingly, the organism must be able to distinguish self-generated from externally induced motion signals. The framework of predictive coding states that we can do so by the attenuation of self-generated sensory signals.

The predictive coding framework is an approach to understand efficient coding in the nervous system by the reduction of redundant information. In that sense, sensory redundancy is reduced by transmitting only unpredicted portions of incoming sensory signals (Rao & Ballard, 1999). The brain contains internal signals (i.e., predictions) related to eye and head movements (i.e., efference copy) that can be used to distinguish self- from externally generated motion signals. This is done by employing information about discrepancies between top-down predictions and actual incoming bottom-up sensory evidence (Friston 2005; Friston & Kiebel, 2009). For instance, vestibular signals from self-generated head motion are inhibited by comparison of an internal prediction of the expected consequences of self-motion with the incoming information about the actual proprioceptive feedback (see Cullen & Zobeiri, 2021).

This allows the nervous system to distinguish self- from externally produced self-motion signals.

One recent neurophysiological study from our group demonstrated that self-motion signals on the level of single neurons are influenced by the perceived sense of agency (Churan et al., 2021) . Monkeys were presented with optic flow stimuli, simulating self-motion in different heading directions. The start of the trial (onset of the optic flow stimulus) could be either self- (initiated by the monkey by button press), or externally (initiated by the experimenter) induced. Single-unit recordings were derived from the macaque area VIP. Results showed shorter response latencies of VIP neurons for optic flow stimuli presented in the self- versus the external condition. The authors speculate that the reduced response latency might be explained by an efference copy mechanism which is used to distinguish self- from externally generated motion signals.

By employing electroencephalography (EEG) on humans and macaque monkeys, two electrophysiological studies from our group have provided evidence on potential neural correlates of predictive coding mechanism in the context of self-motion perception. In the context of heading, Schmitt et al. (2021) identified the visual mismatch negativity component (vMMN) as a correlate of predictive processing of visual heading information across species. Initially, the MMN component as an event-related potential (ERP) was described in the auditory domain as a system that preattentively extracts regularities (‘Standards’) in the environment and signals irregularities (‘Deviants’) (Näätänen & Michie, 1979). For visual heading perception, Schmitt et al. presented their human and monkey observers with standard and deviant trials that differed only in presented heading direction. Heading was simulated as motion over a horizontal plane. For the comparison between deviant and regular (i.e., standard) heading stimuli, the authors found a vMMN in both, humans, and monkeys, which might reflect a common representation of predictions errors across both species.

In the context of path integration, Schmitt et al. (2022) identified suppressed neural activity for self- vs. externally induced visual self-motion signals in human observers. In this study, in each trial, the subjects’ task was to replicate double the length (Active condition) of a previously observed distance (Passive condition). Comparison between the active and passive condition showed an attenuation in the signal for active compared to passive trials. This finding is in line with the predictive coding approach and demonstrates navigation related attenuation of self-induced neural signals in the perception of travelled distance. While a large

body of literature has already reported on the attenuation of visual or visuo-vestibular signals for the efficient self-motion encoding, predictive coding mechanisms in the context of tactile self-motion perception have been not investigated up until now.

1.4. Research questions

Only few studies have investigated the role of tactile flow for the perception of vection. Tactile flow in self-motion research does not appear to be as prevalent in literature as vestibular cues or optic flow. It is worthwhile investigating the role of tactile flow in the perception of different self-motion parameters and to describe potential neural correlates of tactile self-motion perception.

The aim of this dissertation was to investigate the role of the tactile modality and the interaction of visual and tactile information in self-motion perception. In this respect, different parameters of self-motion were investigated in the visual and tactile modality, namely the perception of self-motion direction (heading) and path-integration described as distance perception and distance reproduction. I conducted three studies, in which self-motion in the visual modality was simulated as forward translation over a ground plane. In the tactile modality, air flow towards the subjects' forehead simulated self-motion, as perceived during e.g., bike ride.

Study 1 investigated the influence of a tactile self-motion heading stimulus on visually perceived heading. In this study, tactile flow was introduced as a distractor stimulus. In study 2, heading was investigated from visual and tactile flow. The weighting of stimuli from both modalities was investigated by applying different computational models. Heading perception was tested as a function of varying head- and eye position. By this, reference frames in the encoding of self-motion stimuli were investigated. Study 3 investigated neural correlates of visual and tactile path integration by means of fMRI. Subjects solved a path integration task in two different tasks differing in cognitive demands. By this, a possible influence of predictability and cognitive demands on self-motion perception were probed.

2. STUDY 1

The study has been published as:

Rosenblum, L., Grewe, E., Churan, J., & Bremmer, F. (2022). Influence of Tactile Flow on Visual Heading Perception. Multisensory Research, 35(4), 291-308. https://doi.org/10.1167/jov.21.9.1915

2.1. Abstract

The integration of information from different sensory modalities is crucial for successful navigation through an environment. Among others, self-motion induces distinct optic flow patterns on the retina, vestibular signals, and tactile flow, which contribute to determine travelled distance (path integration) or movement direction (heading). While the processing of combined visual-vestibular information is subject to a growing body of literature, the processing of visuo-tactile signals in the context of self-motion has received comparatively little attention. Here, we investigated whether visual heading perception is influenced by behaviorally irrelevant tactile flow. In the visual modality, we simulated an observer's self-motion across a horizontal ground plane (optic flow). Tactile self-motion stimuli were delivered by air flow from head-mounted nozzles (tactile flow). In blocks of trials, we presented only visual or tactile stimuli and subjects had to report their perceived heading. In another block of trials, tactile and visual stimuli were presented simultaneously, with the tactile flow within +/-40° of the visual heading (bimodal condition). Here, importantly, participants had to report their perceived visual heading. Perceived self-motion direction in all conditions revealed a centripetal bias, i.e., heading directions were perceived as compressed towards straight-ahead. In the bimodal condition, we found a small but systematic influence of task-irrelevant tactile flow on visually perceived headings as function of their directional offset. We conclude that tactile flow is more tightly linked to self-motion perception than previously thought.

2.2. Introduction

The integration of information from different sensory modalities is crucial for successful navigation through an environment including the estimation of self-motion parameters like

travelled distance (path integration) or direction of self-motion (heading). Self-motion generates distinct optic flow patterns on the retina (Lappe and Rauschecker, 1993, 1994; Warren and Hannon, 1988) which are linked to the direction of motion in a complex way (Bremmer et al., 2017; Lappe et al., 1999; Matthis et al., 2020). Vestibular (e.g., Rodriguez & Crane 2020), but also tactile (Churan et al., 2017; Harris et al., 2017) and auditory (von Hopffgarten and Bremmer, 2011) signals have also been shown to contribute to the perception of self-motion.

The interplay of signals from different sensory modalities in heading perception is typically investigated by combining visual optic flow stimuli with cues from other sources. While probing combined visual-vestibular self-motion processing has been subject of a large body of literature (e.g. Harris et al., 2000; Hummel et al., 2016; Angelaki, 2014; for a review see e.g. Fetsch et al., 2012), investigation of the interaction of visual and tactile information in heading perception has received comparatively little attention. Seno and colleagues (2011) demonstrated that an air flow towards the face of observers facilitates the impression of self-motion (vection) when presented concurrently with optic flow simulating forward self-motion. Air flow combined with visually simulated backward self-motion did not facilitate vection, nor did airflow alone. In our own previous work, we could show that adding congruent tactile air flow (across participants' foreheads) to visual optical flow significantly improved the precision of reproduced travelled distances (Churan et al., 2017), even though stimuli were not integrated in a statistically optimal fashion in terms of a Bayesian framework. Also, tactile flow across the fingers can induce a strong sensation of self-motion. Harris and colleagues (2017) presented their subjects with real oscillatory sideways self-motion (vestibular stimulation) and tactile flow across the participants' fingers, which could be presented either congruently or incongruently by varying the phase and speed of the tactile stimulus relative to the visual stimulus. Remarkably, results provided clear evidence for tactile flow to dominate perceived self-motion. In these previous studies, the tactile stimulus, when presented congruently with visual or vestibular self-motion stimuli, allowed to increase the immersiveness of self-motion, i.e., vection. Here, on the contrary, we aimed to determine if visually perceived heading is affected by a behaviorally irrelevant tactile flow stimulus. Visually, we simulated self-motion across a ground-plane in various directions. Tactile flow was delivered by nozzles around the participant's head. Subjects had to report the visual heading direction. A potential influence of the tactile flow on visual heading direction was examined by varying the angle between the visually simulated self-motion direction and the tactile flow.

2.3. Methods

2.3.1. Subjects

Ten subjects participated in this study (7 male; mean age = 26.3 years, ranging from 23 to 31 years), all with normal or corrected-to-normal vision. All subjects provided written informed consent prior to the start of an experiment and remained naive to the purpose of the study during the experiment but were offered disclosure thereafter. Testing sessions took place on two separate days. Testing on each day lasted approx. 2.5 hours. Subjects were compensated for their participation (8€ per hour). The experiment was approved by the local ethics committee and conformed to the Declaration of Helsinki.

2.3.2. Apparatus

Visual stimuli were designed with MATLAB R2019a (The MathWorks, Natick, MA) and the psychophysics toolbox (Brainard, 1997; Kleiner et al., 2007) running on a Windows PC (XP 32 Bit, Dell Technologies, Round Rock, Texas, USA). Visual stimuli were back-projected on a transparent screen by a video projector (Christie M 4.1 DS+6K-M SXGA), at a frame rate of 120 Hz and a resolution of 1,152 × 864 pixels at 70 cm viewing distance, thereby covering the central 81° by 66° of the visual field. Subjects, with their head stabilized by a chin rest, gave their response via mouse click. During stimulus presentation, they had to fixate a central target. We recorded eye position monocularly with an EyeLink 1000 (SR Research, Canada). Trials in which a blink occurred were discarded. This also applied to trials in which deviation of the eye position exceeded a $\pm 3°\ by\ \pm\ 3°$control window centered around the fixation target. These trials were aborted and repeated later during the course of the experiment.

2.3.3. Visual Stimulus

Self-motion was simulated as forward movement with a constant speed of 7 m/s across a virtual 2D ground plane of max. 2000 white (luminance 100 cd/m2) random dots on a black (luminance <0.1 cd/m2) background. The size and position of each dot changed regarding their position relative to the observer with each frame. Coherence of dot motion was 100%. The maximum lifetime of each dot was limited to prevent subjects from orienting themselves on a single dot's trajectory. After a maximum of 250 ms, each single dot disappeared and re-appeared at a new random location.

2.3.4. Tactile Stimulus

The tactile setup is shown in Fig. 1. Airflow from one of seven nozzles simulated the tactile component of self-motion. All nozzles were arranged with a distance of 3 cm to the subject's forehead and with 1.7 cm distance in-between them, which corresponds to an angular distance of 8 degrees. Precise positioning of the nozzles was ensured by a solid plastic spacer enclosing the nozzles tips. Small grids were mounted in front of the nozzle tips to slightly expand the air flow and by this, generating a more natural feeling of a wind breeze resulting e.g., from self-motion. Nozzles were installed on a plastic panel which was fixed centrally on top at the headband of soundproof earmuffs (3M 1436 3M Ear Defender). The plastic panel also carried one supply hose and seven solenoid valves (AMV-MNS-24-01, BMT, Frankfurt, Germany). The weight of the apparatus (1350 g) on the subject's head was sprung by a foam cushion which was placed under the headband of the soundproof earmuffs. Air flow with a speed of approx. 6.2 m/s was provided by a gas cylinder with a dynamic pressure of approx. 1 bar. Solenoid valves for opening and closing the air supply were controlled by a data acquisition box (DAQ Type: USB-1208FS, Measurement Computing Corporation, Norton, USA) that was connected to the stimulus computer via an USB port and accessed via MATLAB. Calibration of the visuo-tactile stimulus system guaranteed to present the onset and offset of visual and tactile stimuli within approx. 7 ms. Subjects wore protective goggles to protect their eyes from the air flow. To prevent distraction from the noise caused by the air flow and to ensure that participants could not identify the tactile stimulus direction by the nozzles' sounds, subjects wore in-ear plugs. Additionally, pink noise was delivered via over-ear headphones (Panasonic RPHS46EK) which subjects wore under the soundproof earmuffs. Pink noise (95 dB SPL) was delivered only during stimulus presentation, thereby covering the noise produced by the opening of the valves and the air stream (72 dB SPL).

Figure 1. Experimental Setup. Seven head-mounted nozzles provided air flow with a static pressure of 1 bar. The apparatus was controlled by a data acquisition box and mounted on top of soundproof earmuffs.

2.3.5. Procedure

Testing on each of the two days lasted approx. 2.5 hours. On day one, subjects completed either the visual-only or the tactile-only discrimination task for the determining the discrimination thresholds for unimodal self-motion stimuli. This task was followed by five (of ten) blocks of the bimodal heading perception task, with two blocks of trials each probing visual-only or tactile-only heading perception randomly interspersed. On day two, subjects completed first the discrimination task in the remaining sensory modality and solved the remaining unimodal and bimodal heading perception tasks. In a final experiment on day two, subjects had to rate perceived vection (i.e., vividness of perceived self-motion, see below for details) in the unimodal and bimodal sensory conditions.

2.3.6. Heading discrimination

The subject's ability to discriminate forward headings was tested in both modalities, vision and somatosensation, separately. Subjects always compared a test heading direction

(visual: 0°, +/-2°, +/-4°, +/-6°, +/-8°; tactile: 0°, +/-8°, +/-16°) to the standard heading of straight-ahead (0°) with the standard heading being always presented first, followed by the test heading. Both stimuli were presented for 250 ms, with ten trials for each test direction, and directions presented in pseudorandomized order. After presentation of the test stimulus, subjects had to indicate if it was perceived to the left or to the right with respect to the standard stimulus by pressing one of two arrow keys on the keyboard. To avoid possible interactions between the measurements in the visual and the tactile modality, the two measurements were performed on different days and the order was balanced across subjects.

2.3.7. Heading perception

In the visual modality, self-motion was simulated in nine possible directions, ranging from -16° to +16° in four-degree steps. Here, 0° means straight-forward self-motion and negative/positive values indicate directions forward and to the left/right. In the tactile modality, forward motion was simulated in seven possible directions ranging from -24° to 24° in eight-degree steps. In the bimodal task, participants were presented with nine possible visual headings to prevent them from anticipating a specific range of headings and consequently adjusting their responses to a limited range of headings. Tactile headings have been chosen to cover a wide range of offsets relative to visual headings with offsets to both sides of a given heading direction. The combination of nine visual and seven tactile headings resulted in sixty-three visuo-tactile stimulus conditions. Each trial simulated self-motion for 500 ms and 16 trials were performed per condition, resulting in a total of (9+7+63) *16 = 1264 trials per subject (for sequence of trials, see below). After stimulus presentation, a moveable green dot (7 x 7 pixels) was presented on the screen and the subject's task was to estimate perceived heading by placing this dot with the mouse pointer at the appropriate position on a continuous line, displayed horizontally across the screen ("horizon"). For each trial, the green dot was initially located at a random position on the horizontal line. Response time was not restricted. In the visual and the bimodal blocks of trials, the participant's task was to indicate the "visually perceived" heading, in the tactile-only blocks of trials it was the "perceived" heading direction. Participants fixated a red fixation point located centrally on the screen during all parts of the experiment. If fixation was successfully detected, the trial started automatically. Figure 2 shows the sequence of a unimodal visual trial.

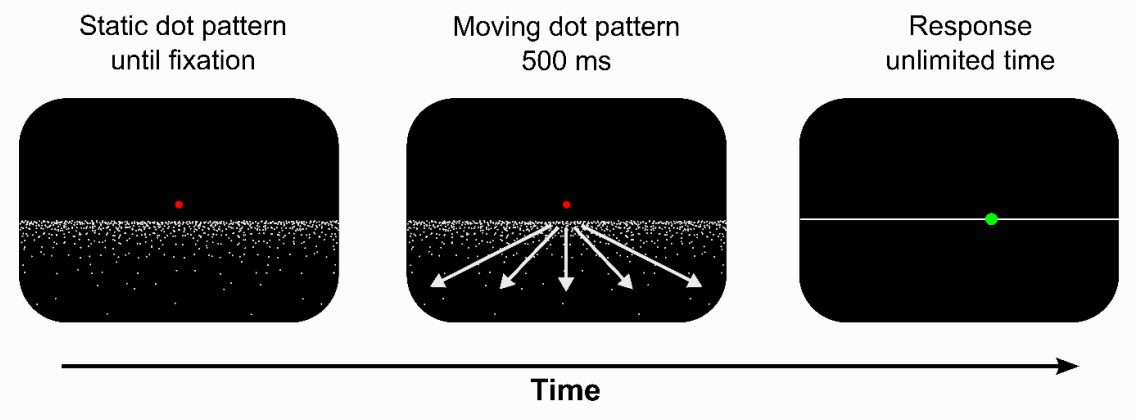

Figure 2. Sequence of a visual-only trial in the heading perception task. A static dot pattern was presented until stable fixation of the central fixation point was achieved. Then, dots started moving for 500 ms, thereby simulating a forward self-motion in one of nine directions. White arrows in the second panel indicate the moving direction of the dots (simulating straight-ahead heading). Then the dots vanished from the screen and participants indicated perceived heading by placing a dot (green) with the mouse pointer at the appropriate position.

2.3.8. Vection

To quantify the immersiveness of self-motion (vection) as induced by the visual, tactile, or bimodal stimulation, subjects evaluated perceived vection on a 1-10 Likert-scale (Weech et al., 2018) where a value of 1 represents “no impression of self-motion” and a value of 10 represents “very strong impression of self-motion”. In this experiment, each trial presented visual-only or tactile only stimuli simulating straight-ahead (0°) self-motion for 3 seconds. In the bimodal condition, visually simulated self-motion directed straight-ahead was paired in a given trial with one of seven directions of the tactile flow (ranging from -24° to +24°, in steps of 8°). Trials of each condition were presented twice in randomized order (unimodal visual: 2, unimodal tactile: 2, bimodal: 2 * 7 = 14 trials). Eight of ten subjects completed this task.

2.3.9. Data Processing

For all analyses, a p value of 0.05 or smaller indicated statistical significance. For repeated measurements, we calculated analyses of variance (ANOVA). Greenhouse-Geisser correction was applied to p values in case of violated sphericity assumption (Mauchly test $p < .05$). Effect sizes will be reported by eta squared.

2.3.10. Fitting of psychometric functions

Cumulative Gaussian functions were fitted to subjects' responses in the heading discrimination task using the psignifit 3.0 toolbox (Fründ et al., 2011). The cumulative Gaussian functions were used to derive the point of subjective equality (PSE) as the point at which the heading was selected as being rightward from straight-ahead 50% of the time. Measures of the just noticeable difference (JND) were obtained from standard deviations of the fitted Gaussian functions.

2.3.11. Influence of tactile flow on visual heading perception

In a final step, we aimed to determine a potential modulatory influence of the task irrelevant tactile flow on visual heading perception. To this end, the condition in which visual and tactile were directed in the same direction (congruent) served as reference. We did not expect any differences between the effects of tactile flow to the left or to the right of the visually simulated (incongruent conditions). Therefore, we determined the effect of the absolute angular separation α between visual and tactile flow. This approach is illustrated in Figure 3. Here, in the experimental conditions A, B, and C, the angular separation α between visual and tactile flow was always the same. Accordingly, results of visual heading perception in all three conditions would be averaged (D). Importantly, this approach allowed us to interpret the modulatory effect of tactile flow as being directed towards or away from it.

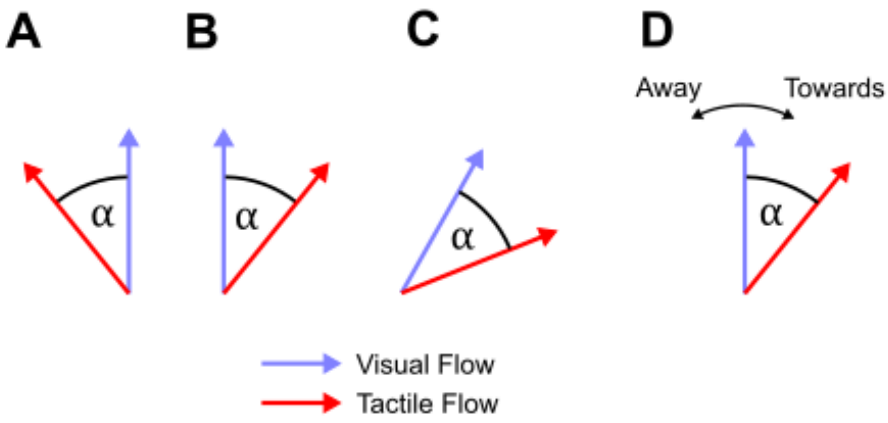

Figure 3. Effect of the absolute angular separation between visual and tactile flow in bimodal trials. A, B and C show examples of possible offsets between visual (blue arrow) and tactile (red arrow) flow in the bimodal condition. In A and B, visual heading is straight-ahead (as if seen from above), while tactile flow is 16° (alpha) to the left or right of the visual heading.

In C, tactile flow is also 16° to the right of visual heading, which itself, however, is 8° to the right. Importantly, the absolute angular difference between tactile and visual flow is always 16°. We did not expect any differences between the effects of tactile flow to the left or to the right of the visually simulated heading. Accordingly, in our data analysis, visual heading performance was averaged over identical angular differences alpha, regardless of the sign of alpha, i.e., whether tactile flow was to the left or right of the visual flow. This approach allowed us to quantify effects of tactile stimulation on visual heading perception as being directed away from or towards tactile flow (D).

2.4. Results

2.4.1. Vection

To investigate how the information from the two modalities (and their spatial congruency) contribute to the vividness of self-motion perception (vection), subjects judged their vection on a Likert-scale (1 = “no impression of self-motion”, 10 = “strong impression of self-motion”). Figure 4 shows the mean ratings across eight subjects. A Friedman-Test for repeated measurements revealed a significant difference between conditions ($p < 0.001$, $X^2 = 46.459$). Stimuli in the bimodal condition induced stronger sensation of self-motion compared to unimodal conditions. Across bimodal heading stimuli, a coherent presentation of the visual and the tactile stimulus (both straight-ahead) produced the strongest impression of self-motion. In comparison, experienced vection was rated lowest for the conditions with the most peripheral tactile flow (0/-24, 0/24) (One-way ANOVA, FGG (1.56) = 9.9, $p < .01$, $\eta^2GG = .593$). Experienced vection between tactile heading offsets 24 degree towards the left and 24 degrees towards the right from visual heading did not differ significantly (Paired t-Test, t(7) = 0.761, $p = 0.47$).

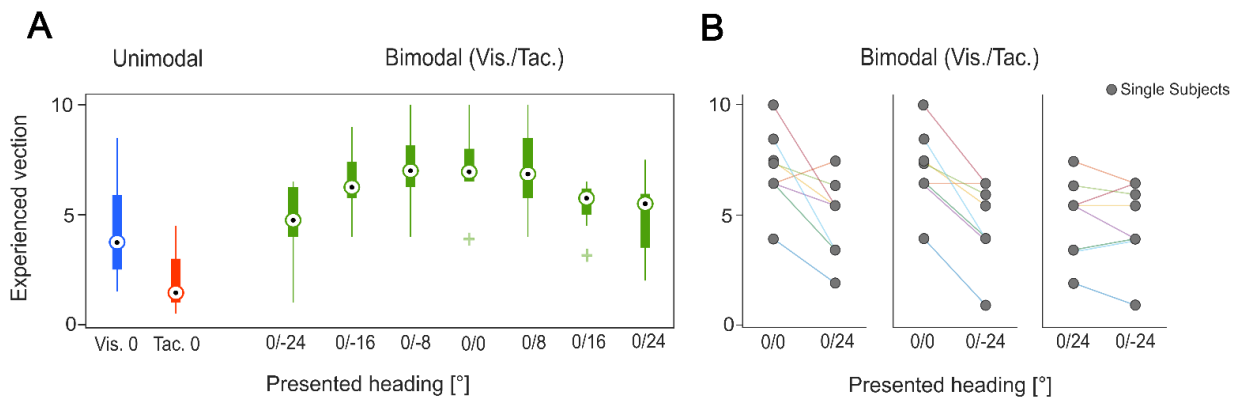

Figure 4. Boxplots for experienced vection of self-motion in the visual-only, tactile-only and bimodal conditions. Perceived vection was rated on a Likert scale (1 = "no impression of self-motion", 10 = "strong impression of vection") (ordinate). A: The central, black dots indicate the median and the bottom and top edges of the boxes the 25th and 75th percentiles, respectively. The most extreme data points are indicated by the vertical lines. In the bimodal condition, the offset between visual (always straight-ahead) and tactile self-motion direction are indicated at the bottom. B: Experienced vection ratings of each subject are compared between congruent (0/0) and incongruent (0/-24 and 0/24) conditions (left and middle panel) or between both incongruent conditions (right panel). Values were significantly different between the congruent (0/0) and both incongruent conditions (0/-24 and 0/24), but not different between the two incongruent conditions.

2.4.2. Unimodal heading discrimination

In a first step, we collected behavioral data from ten subjects performing a heading discrimination task. In the following, figures show averaged data across participants, unless stated otherwise. Subjects compared a test stimulus (visual: 0°, +/-2°, +/-4°, +/-6°, +/-8°; tactile: 0°, +/-8°, +/-16° headings) to a standard stimulus (0° heading, i.e., straight-ahead) by means of a two-alternative forced choice task (2AFC). Psychometric functions in Figure 5 illustrate the proportion of rightward answers (positive values indicate rightward, negative values leftward answers) obtained in the visual (blue curve) and tactile condition (red curve), respectively.

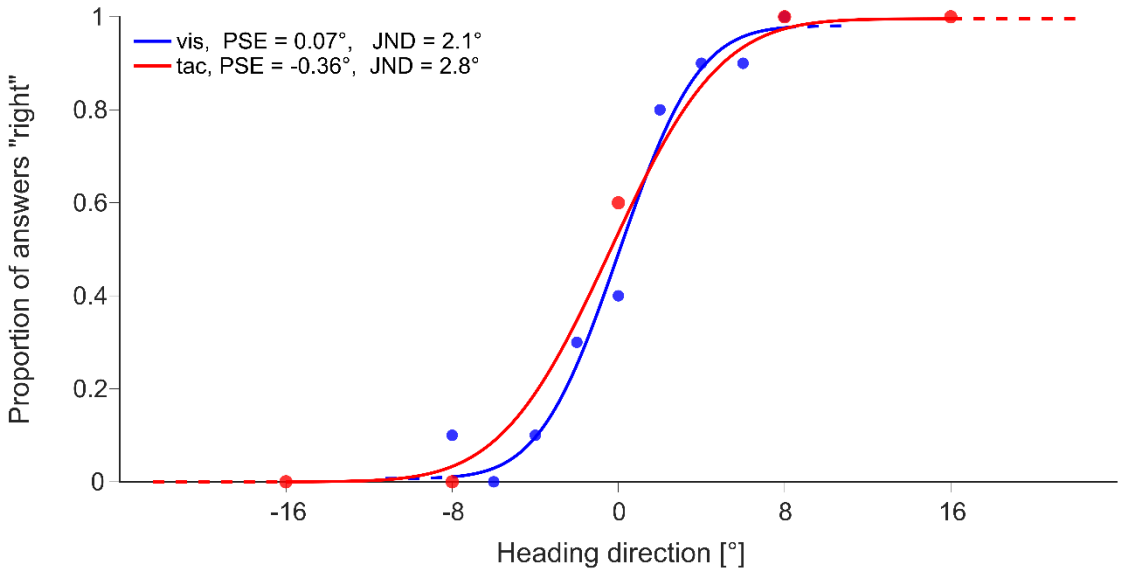

Figure 5. Psychometric functions for straight-ahead [0°] self-motion in uni-sensory conditions. Blue and red symbols depict data from the visual-only and tactile-only condition, respectively. Solid lines show the cumulative gaussian fits. Test stimuli (tactile-only: 0°, +/-8°, +/-16° & visual-only: +/-2°, +/-4°, +/-6°, +/-8°) were compared to straight-ahead (0°).

PSE values in the unimodal conditions were both close to zero and not significantly different (visual: M = 0.05°; tactile: M = -0.36; paired samples t-test, p = .37 T = .94). JNDs were 2.1° (visual) and 2.8° (tactile) and did not differ significantly either (paired samples t-test, p = .15, T = -1.59). While the exact numerical values as derived from the tactile domain must be considered with some care (see Discussion), overall, perception was similar for visual and tactile stimuli.

2.4.3. Unimodal heading perception

In a second step, we probed unimodal heading perception. Here, subjects reported perceived heading direction after being provided with visual (optic flow) or tactile (air flow) stimuli in seperate blocks of trials. Figure 6 shows perceived heading (ordinate) as a function of real heading (abscissa) for both modalities and corresponding linear regressions (y = mx + b; with y: perceived heading; x: real heading; m: slope, and b: intercept or accuracy) fitted to the data. Here, we only considered headings which could be presented experimentally in both sensory modalities (0°, +/-8°, and +/-16°). Intercept values were both close to 0 (visual: b_{visual} = -0.06; tactile: $b_{tactile}$ = 0.37), and a paired sample t-test indicated no statistically significant difference (p = 0.24, T= 1.25). Slope coefficients m differed significantly between conditions (paired samples t-test, p < .01, T = 4.01) with larger slope coefficients for the visual (m_{visual} = 0.69) as compared to the tactile condition ($m_{tactile}$ = 0.32), thus suggesting a significant difference in the centripetal bias between conditions, being stronger for tactile as compared to visual heading.

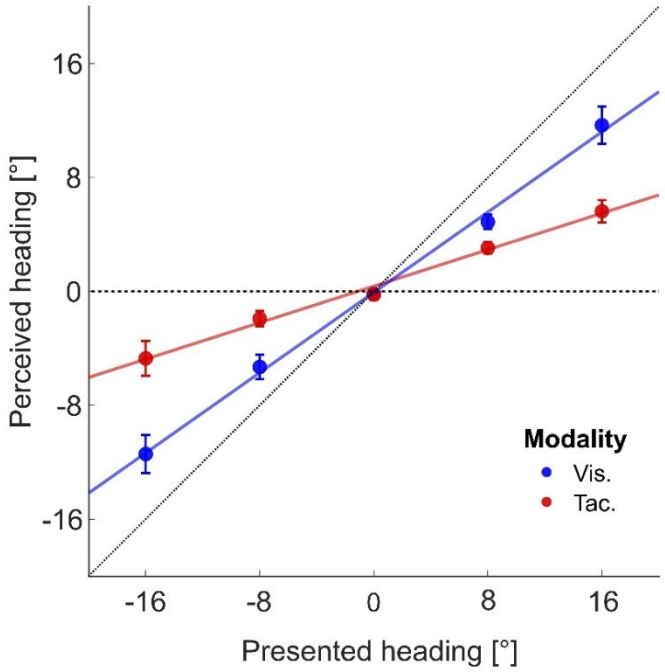

Figure 6. Data and fits for perceived as a function of presented heading direction [°] for identical visual and tactile headings. Colored lines indicate a linear regression fit for the visual-only (blue line) and tactile-only (red line) condition for identical headings between both modalities (0°, +/- 8°, +/-16°). The oblique dashed line (identity) represents veridical perception. Error bars represent standard errors over participants.

2.4.4. Bimodal heading perception

In bimodal trials, subjects were presented a tactile (air flow) and a visual stimulus (optic flow) simultaneously, either simulating the same heading (congruent condition) or with an offset angle interposed in-between (ranging from 4° to 40° in steps of 4°, Incongruent condition). Importantly, in this condition, the tactile stimulus was behaviorally irrelevant: Participants were asked to report the **visually** perceived heading (VPH) by placing a mouse pointer at the appropriate position on a continuous, horizontal line, after stimulus presentation.

Here, we were interested in the modulatory influence of tactile flow on visually perceived heading (VPH). To this end, we first computed the heading error, i.e., the difference between visually presented heading and VPH. In Figure 7, each panel shows for the group of participants the average modulatory influence of the tactile flow on this heading error for a given visually simulated self-motion direction.

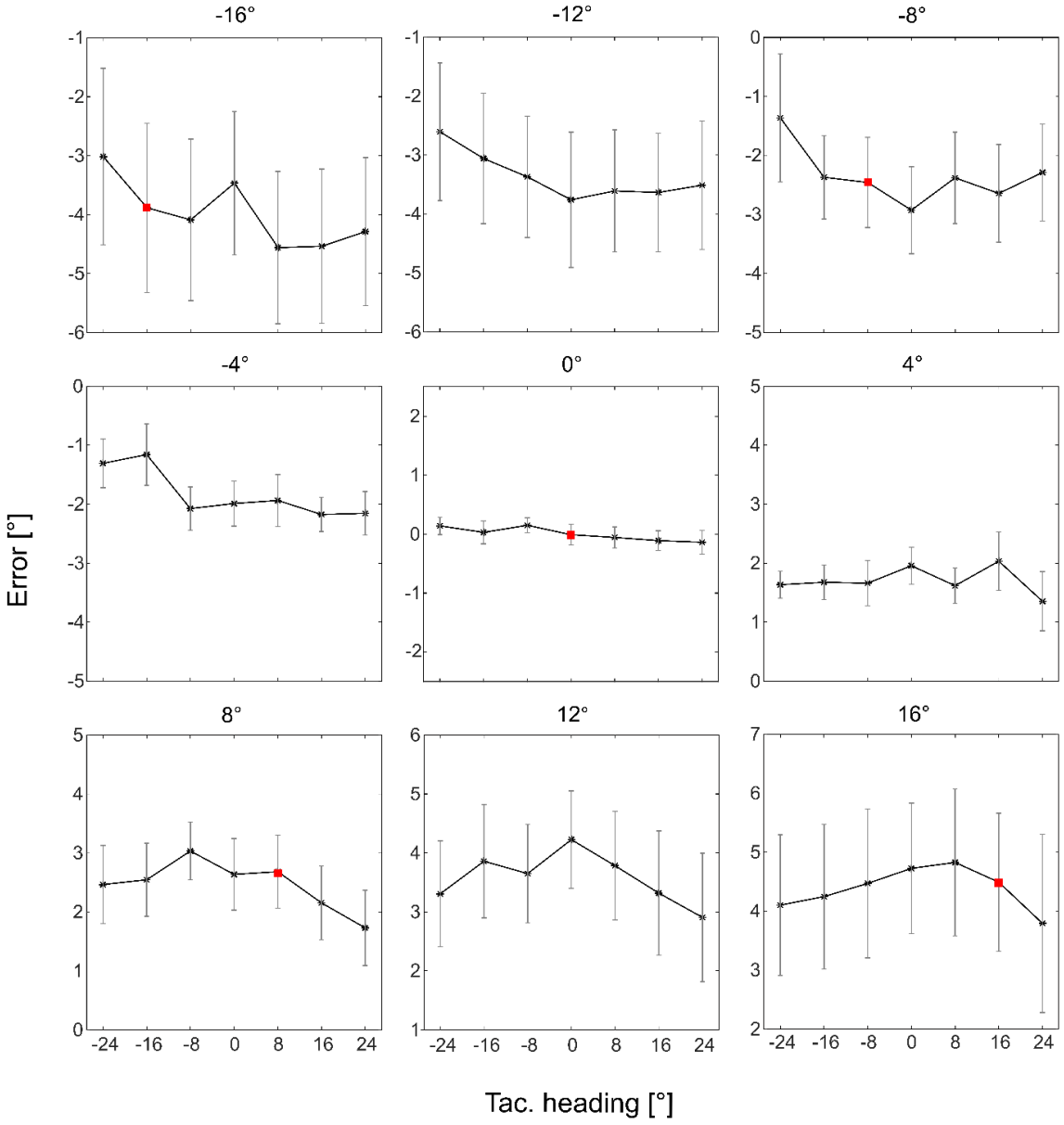

Figure 7. Tactile modulation of visual heading error. Each panel shows for a given heading (indicated above each panel) the heading error, i.e., the difference between visually presented heading and visually perceived heading (VPH) as a function of tactile heading direction. Red crosses indicate congruent visuo-tactile heading conditions. Errorbars represent standard errors over participants.

To investigate the effect of the behaviorally irrelevant tactile stimulus on heading perception independent of the absolute visual heading, data from the incongruent conditions were normalized with respect to the congruent condition (see Methods for details). Figure 8

shows the modulatory influence as a function of the angular separation of visual and tactile flow. On the ordinate, negative values indicate a modulation of visuall perceived heading **away** from the tactile flow while positive values indicate a modulation of visually perceived heading **towards** the tactile flow.

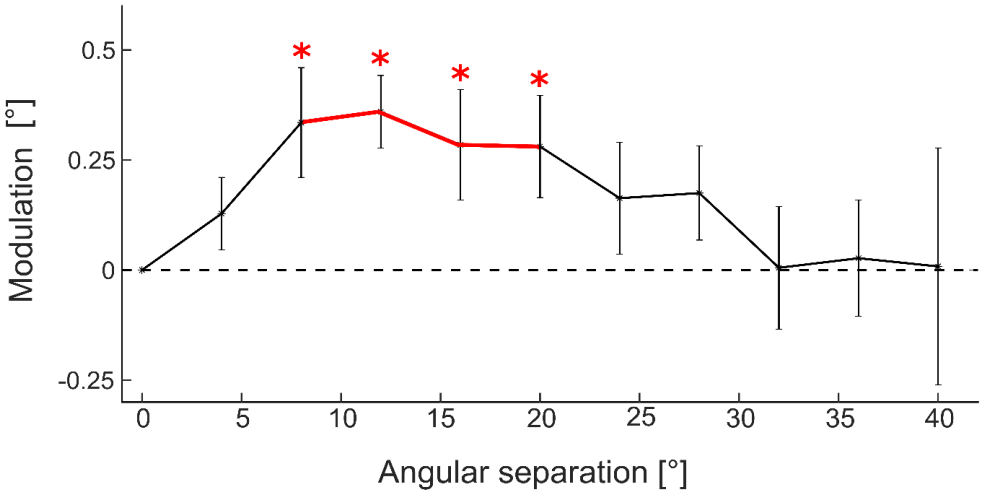

Figure 8. Modulation of visually perceived heading by tactilely presented heading as a function of collapsed, absolute visuo-tactile offsets angles. Data was point reflected at 0° and combined for greater statistical power. Errorbars represent standard errors over participants. One sample t-tests: * = p < .05.

The modulatory effect differed across angular separations between visual and tactile flow. We found small influences for offset angles up to about 30°, peaking at roughly 12°, which were statistically significant for angular separations between 8° and 20° (one sample t-tests, $p < .05$).

2.5. Discussion

In this study, we have tested the role of behaviorally irrelevant tactile flow for visual heading perception. We found a small, but significant modulatory influence. Importantly, this modulatory influence was tuned, reaching a peak for an angular separation of about 12°, and did not extend beyond a critical angular separation of both self-motion directions of about 30°.

2.5.1 Unimodal heading perception

In our study, participants first completed a 2AFC-task which served to examine how reliable participants can judge their self-motion direction based solely on visual or tactile flow. JNDs for visual and tactile stimuli were in the same range and not significantly different. It must be noted, however, that due to our experimental setup, the computation of the JND for the tactile domain should be considered with care. Already for the stimulus directions next to straight-ahead (+/- 8°), discrimination performance saturated, i.e., response rates were either 0% (rightward choices for headings left from straight ahead) or 100% (rightward choices for heading right from straight-ahead). Given the spatial resolution of the probed headings (stimulus spacing of 8°), the resulting tactile JND should be considered as an upper bound.

In general, perceived headings were compressed towards straight-ahead in both sensory modalities (centripetal bias). Undershoots of perceived visual heading have been shown before (e.g., Bremmer et al., 2017; Lich and Bremmer, 2014). On the contrary, overshoots have also been documented (Crane, 2012; Cuturi and MacNeilage, 2013). This raises the question about the cause for such seemingly contradictory results. We assume the exact experimental setup and conditions to be crucial. In Bremmer et al. (2017), stimuli were presented on a large tangent screen, simulating self-motion across a ground plane, and lasted for only 40 ms. Subjects had to indicate their perceived heading by a ruler stimulus with random numbers presented after stimulus presentation. Albeit the stimuli being different (3D cloud of random dots vs. 2D ground plane) and presented via different means (head-mounted display), in the study by Lich and Bremmer (2014), the response task was identical (ruler stimulus). On the contrary, in the studies by Crane (2012) and Cuturi and MacNeilage (2013), which both used 3D cloud of random dot stimuli, participants had to indicate their perceived heading with a response dial. Accordingly, in both studies, participants indicated their perceived heading from a bird's eye perspective (allocentric frame of reference), while they perceived their self-motion in an egocentric frame of reference. In contrast, in our current study, as well as in the two previous studies (Bremmer et al., 2017; Lich and Bremmer, 2012), participants perceived and responded in an egocentric frame of reference. We suggest that the change in reference frame might cause the switch from an under- to an overshoot of perceived heading around straight ahead. As an alternative explanation, the different biases might also be related to a general center-screen bias as reported early on by Warren and Kurtz (1992). Hence, further studies are required to resolve this issue.

Like for the visual domain, we found an even more pronounced undershoot of perceived heading or centripetal bias also in the tactile domain. To our best knowledge, no comparable data have been obtained before. One possible explanation for the centripetal bias might be the response format as already discussed above. When subjects used a (mouse) pointer to indicate heading, perceived heading was limited by the size of the screen (D'Avossa and Kersten, 1996; Li et al., 2002). Since we used a large presentation screen covering the central 81° x 66° of the subject's visual field, it appears unlikely this option to have caused the observed effects. A potentially more important factor is the range of presented heading directions. From headings as presented in previous trials, subjects might have inferred that potential headings were limited to a rather limited range, adapting their responses accordingly (Crane, 2012; De Winkel et al., 2015). This, however, does not explain differences of central biases between visual and tactile stimuli. Accordingly, more experiments are needed to answer this open question.

2.5.2. Visual heading perception in the unimodal and bimodal condition

Participants had to report their perceived visual heading in the pure visual and in the bimodal condition. Accordingly, the tactile flow stimulus was behaviorally irrelevant in the bimodal condition. We could show a small, but significant effect on visual heading perception, though. This finding is somewhat similar to results by Butz and colleagues (2010). These authors presented a group of dots arranged in form of a hexagon. After 160ms, the hexagon was rotated, either by half the angle of the separation of the dots, or by the full angle. In the latter case, the resulting motion is ambiguous (Lakatos and Shepard, 1997). Six such frames were presented, resulting in coherent clockwise (CW) or counterclockwise (CCW) rotation, or by an ambiguous rotation. Rotations of the tactile stimulus, presented to the palm or the back of the hand of the participants, shifted the perceived direction of visual rotation (CW vs CCW). The shift direction also depended on whether the – behaviorally irrelevant - tactile stimulus was presented to the palm or the back of the hand. While our experiment was quite different from that of Butz and colleagues, both studies show that also behaviorally irrelevant tactile stimuli can modulate perception of visual (self-)motion.

The importance of tactile stimulation for self-motion perception is further underlined by studies with behaviorally relevant tactile stimuli. As shown by Harris and colleagues (2017), in such case, tactile stimulation can even override a visual percept of self-motion. In their

study, the authors presented subjects with real oscillatory sideways self-motion (vestibular stimulation) and tactile flow across the participants' fingers. This tactile stimulation could be presented either congruently or incongruently by varying the phase and speed of the tactile stimulus relative to the visual stimulus. Remarkably, results provided clear evidence for tactile flow to dominate perceived self-motion. These and the above discussed findings strongly suggest that tactile flow is more tightly linked to self-motion perception than previously thought.

2.5.3. Neural mechanisms of tactile influences on visually perceived heading

It is well known that visual heading perception is most accurate for self-motion around straight-ahead (Cuturi and MacNeilage, 2013; Sun et al., 2020). Neurophysiological recordings in the animal model of human multisensory perception, i.e., the awake behaving macaque monkey, have shown that response properties of neurons in the medial-superior temporal area (area MST) and the ventral intraparietal area (area VIP) can account for this behavioral effect (e.g., Gu et al., 2010; Bremmer et al., 2017). Preferred directions of self-motion are non-uniformly distributed in both areas, with more neurons preferring sideways motion. Accordingly, straight-ahead self-motion overlaps with the part of the tuning curves of these neurons with the steepest slope. Hence, small changes in heading direction cause large changes in firing rate, thereby causing a robust and accurate heading perception. Our findings are in line with these previous results.

It is also known from neurophysiological studies in non-human primates that neurons in area VIP respond not only to visually simulated self-motion (Bremmer et al., 2002a; Chen et al., 2011), but also to tactile flow, typically resulting from self-motion (Bremmer et al., 2002b; Guipponi et al., 2015). Importantly, a functional equivalent of macaque area VIP had been identified in human posterior parietal cortex, i.e., hVIP, suggesting similar processing of multisensory self-motion information in humans and monkeys (Bremmer et al., 2001; Field et al., 2020). Neurons in macaque area VIP have been shown to respond in an action congruent manner, i.e., neurons preferring visually simulated forward self-motion typically also prefer tactile flow which would result from forward self-motion. Furthermore, visual, and tactile receptive fields tend to overlap spatially (Duhamel et al., 1998; Bremmer et al., 2002b; Avillac et al., 2004; 2005; Sereno and Huang, 2006). A small subset of bimodal VIP neurons has been shown to react to incongruent visual and tactile stimulation as well (Avillac et al., 2007). It had

been suggested that such differential encodings could be used to dissociate self- from object motion (Bremmer et al., 2002b). These previous finding might point towards area hVIP being involved in the observed perceptual effects.

Other studies have tested the spatial profile of surround suppression in demanding visual tasks (e.g., Hopf et al., 2006). These authors found that visual input was suppressed in an area surrounding the target and then recovering at more distant locations. While the exact shape and size of such a suppressive, torus-like region is not known for heading stimuli, it could be that it matches the region for which we observed the strongest effect of the tactile distractor stimuli. This then would allow the tactile distractor to impose its strongest effect on visual heading perception.

2.5.4 Limitation of our study

A limitation of our approach was the way tactile flow was provided. When asked to judge perceived vividness of the delivered heading stimuli, participants indicated the immersiveness of self-motion delivered by tactile flow as lowest across all conditions. Due to a diameter of the nozzles of 3 mm, the tactile flow might have covered a too small part of the forehead to induce a “natural” impression of self-motion. However, vividness-judgements of bimodally provided heading stimuli simulating congruent heading (straight-ahead) revealed higher scores (stronger impression of vividness) than stimuli simulating incongruent headings. Accordingly, tactile flow contributed significantly to the percept of vection. Further studies could aim for tactile flow with a wider range of applicable airstream in order to provide a more “naturalistic” impression of self-motion.

3. STUDY 2

The study has been published as:

Rosenblum, L., Kreß, A., Schwenk, J. C., & Bremmer, F. (2022). Visuo-tactile heading perception. *Journal of Neurophysiology, 128*(5), 1355-1364. https://doi.org/10.1152/jn.00231.2022

3.1. Abstract

Self-motion through an environment induces various sensory signals, i.e., visual, vestibular, auditory, or tactile. Numerous studies have investigated the role of visual and vestibular stimulation for the perception of self-motion direction (heading). Here, we investigated the rarely considered interaction of visual and tactile stimuli in heading perception. Participants were presented optic flow simulating forward self-motion across a horizontal ground plane (visual) or airflow towards the participants' forehead (tactile), or both. In separate blocks of trials, participants indicated perceived heading from unimodal visual, tactile, or bimodal sensory signals. In bimodal trials, presented headings were either spatially congruent or incongruent with a maximum offset between visual and tactile heading of 30°. To investigate the reference frame in which visuo-tactile heading is encoded, we varied head and eye orientation during presentation of the stimuli. Visual and tactile stimuli were designed to achieve comparable heading accuracies between modalities. Nevertheless, in bimodal trials, heading perception was dominated by the visual stimulus. A change of head orientation had no significant effect on perceived heading, while, surprisingly, a change in eye orientation affected tactile heading perception. Overall, we conclude that tactile flow is more important to heading perception than previously thought.

3.2. Introduction

Successful navigation through an environment requires the accurate estimation of one's traveled distance (path integration) and direction of self-motion (heading). Previous studies have documented the role of visual (Bremmer & Lappe, 1999), vestibular (Berthoz et al., 1995), auditory (Von Hopffgarten & Bremmer, 2011), and tactile (Churan et al., 2017; Harrison et al., 2021) information for the processing of traveled distance. Studies on heading perception have mainly focused on visual (e.g., Lappe et al., 1999) or vestibular (e.g., Crane, 2012) stimulation or the interaction of both modalities (e.g. Cuturi & MacNeilage, 2013; Rodriguez & Crane, 2021). In case of directionally congruent visuo-vestibular stimulation, information from both modalities is typically integrated to form a unified perception of heading (Butler et al., 2015; Crane, 2015). The role of tactile information for heading perception has only rarely been investigated. Murata and colleagues (2014) could show that perception of self-motion can be driven solely by airflow towards the participants' body. In combination with contextual-related visual stimuli, airflow has been shown to facilitate vection, i.e., the perception of self-motion (Yahata et al., 2021). In the context of heading, Feng and Lindeman (2016) have demonstrated that directional wind can be used as an orientational cue in a spatial orientation task. Finally, in a recent study, we were able to show that tactile heading stimuli (airflow), despite being behaviorally irrelevant, were capable of biasing visually perceived heading. In that study, visual and tactile flow could either be spatially congruent or incongruent (Rosenblum et al., 2022). Results showed a small but significant attraction towards the tactile flow (distractor), which peaked for an angular separation of 10° between visual and tactile self-motion direction.

In our current study, we tested unimodal (visual or tactile) and bimodal (visuo-tactile) heading perception. In the visual modality, self-motion was simulated as forward motion across a 2D ground plane (optic flow). In the tactile modality, self-motion stimuli were delivered by airflow towards the forehead. In separate blocks of trials, participants indicated perceived heading from unimodal visual, unimodal tactile, or bimodal heading information. In bimodal trials, signals from both modalities were presented simultaneously, presenting either congruent heading or headings with an angular separation between visual and tactile heading. Additionally, to estimate the reference frame of visual, tactile and bimodal heading perception, stimuli were presented in different sessions with varying eye and head orientation.

3.3. Methods

3.3.1. Participants

A total of 15 subjects (7 female, all right-handed) participated in the experiment. Mean age was 25 ± 5 years (mean ± SD, range 20 - 34). All participants had normal or corrected-to-normal vision. The experiment was conducted following the Declaration of Helsinki and was approved by the local ethics committee. All participants provided written informed consent before the start of the experiment and remained naive to the purpose of the study during the experiment but were offered disclosure thereafter. Experimental sessions took place on six separate days. Testing on each day lasted approx. 1.5 hours. Participants were compensated for their participation (8€ per hour).

3.3.2. Apparatus

Visual stimuli were designed with MATLAB R2019a (The MathWorks, Natick, MA) and the psychophysics toolbox (Brainard, 1997) running on a Windows PC (Win 10 64-bit, Dell Technologies, Round Rock, Texas, USA). Visual stimuli were back-projected on a transparent screen by a video projector (Christie M 4.1 DS+6K-M SXGA), at a frame rate of 120 Hz and a resolution of 1152 × 864 pixels, at 65 cm viewing distance, thereby covering the central 81° by 33° of the visual field. Participants, whose head was stabilized by a chin rest, gave their response via mouse click.

3.3.3. Visual Stimulus

Self-motion was simulated as forward movement in one of seven directions with constant speed across a virtual 2D ground plane of 70 white (luminance 100 cd/m2) random dots on a black (luminance <0.1 cd/m2) background. Dot size and the position of each dot changed dependent on their position relative to the observer with each frame. The maximal lifetime of each dot was limited to prevent participants from orienting on a single dot's trajectory. After a maximum of 250 ms, a dot disappeared and reappeared at a new random location. To achieve comparable heading performance (similar accuracy) in the visual and tactile modality, dot motion coherency was set to 50%, i.e., half of the presented dots moved in random directions with all motion trajectories simulating forward motion.

3.3.4. Tactile Stimulus

Airflow was provided from one of nine commercially available hairdryers (CLATRONIC HT 3393, Clatronic, Kempen, Germany) (with the heating system removed). Dryers were installed above and around the participants' head on a holder with a half-circle shape with a 6 cm distance in-between the hairdryers, which corresponds to an angular separation of 10 degrees, and an angle of inclination of 30 degrees towards the participants' forehead. To make sure that presented heading as induced by airflow across the participants' forehead could not have been identified by vision of the dryers' rotating motors, participants were provided with sight protection (matt black cape) mounted on top of protective goggles covering space above 10 ° of the upper visual field. Airflow was provided with a speed of approx. 8.5 m/s. The hairdryers were operated by an ARDUINO MEGA 2560 Rev3 (Arduino, Somerville, Massachusetts, USA) connected to the stimulus computer via a USB port and controlled by the 'MATLAB Support Package for Arduino Hardware' (https://www.mathworks.com/matlabcentral/fileexchange/47522-matlab-support-package-for-arduino-hardware). The power supply was delivered by three Adafruit Motor Shields v2.3 (Adafruit, New York, USA). Calibration of the visuo-tactile stimulus system guaranteed presentation onset and offset of visual and tactile stimuli within max. 15 ms. To cancel noise caused by the dryer's motor rotation (75 dB SPL), participants wore in-ear plugs (EAR PD01002, Axisis GmbH, Düsseldorf, Germany). Additionally, white noise (95 dB SPL) was delivered via noise-canceling over-ear headphones (Bose QuietComfort 35 II, Bose GmbH, Friedrichsdorf, Germany).

3.3.5. Procedure

Self-motion was simulated visual-only (optic flow), tactile-only (tactile flow), or bimodally in separate blocks of trials. In unimodal visual trials (Uni Vis), stimuli simulated heading directions ranging from -20° to +20° in 10° steps. In unimodal tactile trials (Uni Tac), directions of airflow ranged from -40° to +40° in 10° steps (Figure 1). In both cases, negative values indicated headings to the left and positive values heading to the right from straight-ahead (0°). Each trial simulated self-motion for 500 ms. Participants conducted 30 trials per heading in both unimodal sets of trials. Figure 1A shows all possible headings of both modalities. In bimodal blocks of trials, each visual heading (-20° to +20° in 10° steps) was

simultaneously presented with one of seven tactile headings, either being directionally congruent (no offset between visual and tactile heading) or incongruent with an offset of up to ± 30°. Visual headings of +20° and -20° were combined with only six tactile headings due to the limited range of tactile flow directions (±40°). This resulted in a total of 5 x 7 – 2 = 33 visuo-tactile stimulus combinations. Each combination was presented 20 times, resulting in a total of 660 trials. After stimulus presentation, participants had to indicate "perceived heading" by placing a mouse-controlled, green probe at the appropriate position on a horizontal line spanning the full width of the screen. The initial position of this probe was randomized across trials. Participants fixated a red fixation point on the screen during all parts of a trial. Response time was unlimited, and the next trial started automatically after the response was made.

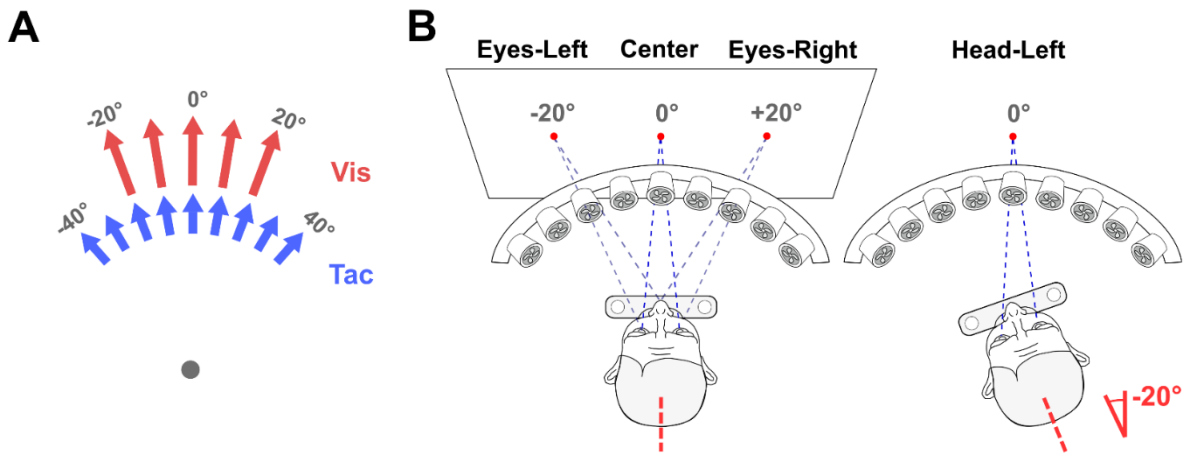

Figure 1. Experimental conditions and setup. A. In the visual modality, self-motion stimuli (optic flow) simulated five possible heading directions (-20° to 20° in 10° steps). In the tactile modality, self-motion stimuli (airflow) simulated nine possible headings (-40° to 40° in 10° steps). 0° corresponds to straight-ahead self-motion, negative values indicate motion to the left and positive values motion to the right from straight-ahead. Self-motion was presented visual-only (Uni Vis), tactile-only (Uni Tac) or bimodally. The Grey dot indicates the participants' head position. B. In blocks of trials, Uni Vis, Uni Tac, and Bimodal heading stimuli were presented in four different conditions, in which head and eye orientations were varied. In the Center condition, participants fixated centrally with the head oriented towards straight-ahead (0°). In the Head-Left condition, participants fixated centrally with the head on the chin rest rotated 20° towards the left. Head orientation in each condition is shown by the dashed red line. In the Eyes-Left condition, the fixation point was at -20°, i.e., towards the left, with the head centrally aligned. In the Eyes-Right condition, the fixation point was at +20°, i.e.,

towards the right, with the head centrally aligned. Relative sizes and distances between the tactile stimulation apparatus, participant and screen are drawn not to scale.

Uni Vis, Uni Tac, and bimodal blocks of trials were presented in four different combinations of head and eye orientation (Fig. 1*B*): *Center* condition: Participants' head and eyes centrally aligned, oriented towards straight-ahead (Fixation 0°, Head 0°). *Head-Left* condition: Head rotated 20° towards the left while eyes fixated centrally (Fixation 0°, Head -20°). Appropriate rotation of the chin rest allowed for stabilizing head orientation in this condition. *Eyes-Left* condition: Fixation -20° towards the left from straight-ahead (fixation point location -20°) with head orientation straight-ahead (Fixation -20°, Head 0°). These conditions were completed by all participants (N=15). To probe for the spatial symmetry of potential effects, seven participants were also tested in the *Eyes-Right* condition: Fixation +20° towards the right from straight-ahead (fixation point location +20°) with head orientation straight-ahead (Fixation +20°, Head 0°). In all conditions, participant's torso was aligned with the center of the setup and oriented towards straight-ahead. The combination of Uni Vis, Uni Tac, and bimodal trials with the three head/eye settings tested in all participants (Center, Head-Left, Eyes-Left) resulted in nine experimental conditions, tested on six separate days. Each bimodal block of trials was tested on a separate day, always followed by corresponding unimodal blocks of trials on the next day. For seven participants, additional testing of the Eyes-Right condition resulted in two additional sessions on two separate days. Corresponding unimodal visual and unimodal tactile blocks of trials of one condition were always tested on the same day. The order (Uni Vis – Uni Tac. Vs. Uni Tac – Uni Vis) was balanced across participants. In a given block of trials, heading directions were presented in pseudo-randomized order. The order of the conditions (Center, Head-Left, Eyes-Left, Eyes-Right) was balanced across participants.

Because of its size and position in front of the participant, the tactile stimulation apparatus prohibited the use of an eye-tracker during the experiment. However, we verified visually that fixation behavior was comparable between central and shifted conditions (Head-Left, Eyes-Left, Eyes-Right) in a subset of participants without the tactile stimulation apparatus in place.

3.3.6. Data Processing

For all analyses, a *p*-value of 0.05 or smaller indicated statistical significance. For repeated measurements analysis of variance (ANOVA), Greenhouse-Geisser correction was applied to *p* values in case of violated sphericity assumption (Mauchly test $p < .05$). Effect sizes are reported by eta squared.

3.3.7. Multisensory integration

For each participant, we calculated for the bimodal task and directionally congruent visual and tactile self-motion stimuli the standard deviations of perceived headings. In case of optimal integration of heading stimuli in a Bayesian sense, responses for bimodal stimuli should show smaller standard deviations (i.e., a higher precision) as compared to the smallest standard deviations (highest precisions) of the responses to both unimodal stimuli (Ernst & Banks, 2002). Predicted bimodal standard deviations (σ_{biOpt}^2) were calculated from the unimodal standard deviations (σ_{vis} for visual and σ_{tac} for tactile stimuli):

$$\sigma_{biOpt} = \sqrt{\frac{(\sigma_{vis}^2 * \sigma_{tac}^2)}{(\sigma_{vis}^2 + \sigma_{tac}^2)}} \qquad (1)$$

3.3.8. Impact of single modality stimuli to bimodal heading perception

To investigate the impact of visual and tactile stimuli on bimodal heading perception, perceived headings of bimodal trials were entered into the following multiple regression model:

$$z = m_{vis}*x + m_{tac}*y + m_{vis^2}*x^2 + m_{tac^2}*y^2 + m_{int}*x*y + b \qquad (2)$$

Here, for each participant, perceived heading in bimodal trials (z) was modeled as a function of perceived heading during pure visual (x) and tactile (y) stimulation, comprising linear (x, y), interaction (x*y) and quadratic (x2, y2) terms, and an intercept (b). To identify the optimal model for explaining perceived headings of each condition, parameters of the multiple regression model were removed successively, evaluating at each step whether the further model reduction was justified using the Bayesian Information Criterion (BIC) (Raftery, 2016). The BIC

depends on the model residuals (RSS) and the number of free parameters (k) entered in the model with smaller BIC values indicating higher model fits.

$$\mathrm{BIC} = n \ln\left(\frac{RSS}{n}\right) + k \ln(n) \qquad (3)$$

With k: number of parameters estimated by the model, n: number of data points (sample size), RSS: residual sum of squares of the model.

3.4. Results

3.4.1. Unimodal heading perception

In unimodal trials, participants reported perceived heading for visual-only (optic flow) or tactile-only (airflow) stimuli in four conditions, varying in head/eye orientation (*Center, Head-Left, Eyes-Left, Eyes-Right*). Figure 2 shows representative data from a single participant for the Center condition (Panels *A*-*B*) and group data averaged across participants for all four conditions (Panels *C*–*J*). Mean perceived heading (ordinate) is shown as a function of presented heading (abscissa) for unimodal visual (upper row, data shown in red) and unimodal tactile trials (lower row, data shown in blue). Here, for the tactile modality, for comparison reasons, we only considered headings that had also been presented in the visual modality (-20° to +20° in steps of 10°). The diagonal dashed lines indicate veridical heading performance. We fitted data with linear regression functions: y = *m*x + *b*, with y: perceived heading; x: presented heading; m: slope, *b*: intercept. Concerning the slope m, a value around m=1.0 would indicate close to veridical performance (assuming an intercept b close to 0.0), while values of m<1.0 or m>1.0 would indicate a shift of perceived heading towards (centripetal bias) or away from (centrifugal bias) straight-ahead, respectively.

Single participant data: For the single participant (*A*-*B*), performance in the visual and tactile condition were rather similar, as indicated by similar slopes in the Uni Vis (m_{vis} = 0.41) and Uni Tac (m_{tac} = 0.37) conditions. This similarity was intended to allow for testing for a Bayesian-integration based prediction of the performance in the bimodal condition (see Methods for details). In both modalities, intercept values were close to zero (b_{vis} = 0.06 and b_{tac} = -0.08; both linear regressions $p < .001$).

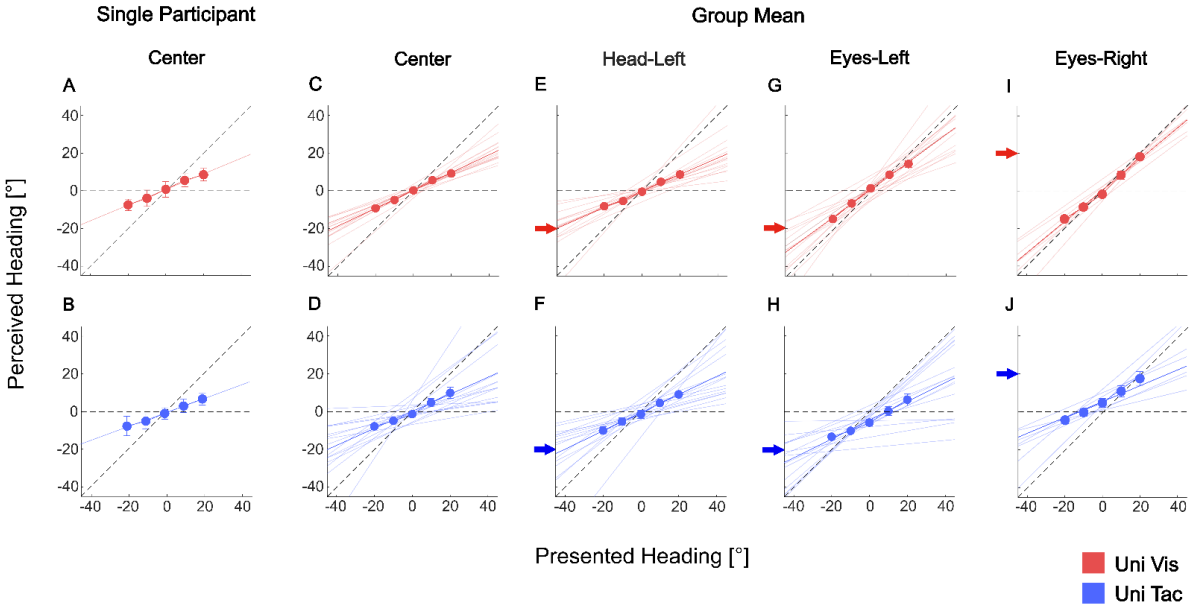

Figure 2. Data and fitted linear regression models for perceived heading in unimodal trials. The top row (red) shows data for the Uni Vis condition, the bottom row (blue) shows data for the Uni Tac condition. ***A-B.*** Perceived heading (ordinate) as a function of presented heading (abscissa) of one participant averaged over trials in the *Center* condition. Error bars represent standard deviation over trials. Solid lines show linear regressions fitted to the perceived heading. ***C-D.*** Mean perceived heading averaged over participants for the Center condition. Light red and blue lines represent linear regression fits to data of single participants. ***E-F.*** Mean perceived heading averaged over participants for the Head-Left condition. ***G-H.*** Mean perceived heading averaged over participants for the Eyes-Left condition. ***I-J.*** Mean perceived heading averaged over participants for the Eyes-Right condition. Error bars represent standard errors over participants, but in most cases were smaller than the symbol size. In all cases, arrows on the ordinate either mark head or eye position in that condition.

Group data: The colored symbols in panels *C-J* show the mean (+/- standard error) across participants of perceived heading for both modalities and all four conditions. The solid thick colored lines show the linear regression fit to these average values. The thin colored lines depict the fit to the single participant data. In the Head-Left, Eyes-Left, and Eyes-Right conditions, colored arrows on the y-axis indicate the respective head or eye position. Linear regressions were statistically significant ($p < .001$) in all conditions. Slopes of the linear regression fits as derived from Uni Vis (*C, E, G, I*) and Uni Tac (*D, E, F, J*) data did not differ significantly between both modalities ($m_{vis\_Center} = 0.49$, $m_{tac\_Center} = 0.49$, $m_{vis\_Head\text{-}Left} = 0.43$, $m_{tac\_Head\text{-}Left} = 0.53$, $m_{vis\_Eyes\text{-}Left} = 0.7$, $m_{tac\_Eyes\text{-}Left} = 0.4$, $m_{vis\_Eyes\text{-}Right} = 0.83$, $m_{tac\_Eyes\text{-}Right} = 0.54$; all $t < 2.6$ and

all $p > .0125$ (= 0.05/4) with Bonferroni correction for multiple comparisons). To probe the spatial symmetry of a potential effect of an eye orientation away from straight-ahead, a sub-sample of participants also completed the Eyes-Right condition (N=7). Slopes in the Eyes-Left and Eyes-Right condition were not significantly different, neither for the Uni Vis ($m_{\text{Eyes-Left}}$ = 0.7, $m_{\text{Eyes-Right}}$ = 0.83, paired t-Test, $t(6) = -1.26$, $p = .255$) nor the Uni Tac ($m_{\text{Eyes-Left}}$ = 0.4, $m_{\text{Eyes-Right}}$ = 0.54, paired t-Test, $t(6) = -0.95$, $p = .38$) trials. In Uni Vis trials, slopes of all four conditions were comparable with one exception: Average heading performance in the Eyes-Left condition showed the steepest slope of the regression ($F(3,18) = 15.691$, $p < .001$, $\eta^2 = .723$). In Uni Tac trials, slopes were comparable, i.e. not significantly different between all four conditions ($F_{GG}(1.248, 7.489) = 0.552$, $p = .518$, $\eta^2_{GG} = .084$).

Intercept values (*b*) in all four conditions (Center, Head-Left, Eyes-Left, and Eyes-Right) and both modalities (visual and tactile) did not differ significantly from zero (all $p > .627$, mean intercept values over all modalities/conditions: 0.08) with one exception: Mean intercept values of -3.8° ($p < .01$) in Uni Tac trials in the Eyes-Left condition (*H*) and 5.3° ($p < .01$) in the Eyes-Right condition (*J*) indicated that average perceived heading in this conditions was shifted towards the eye-orientation.

3.4.2. Bimodal heading perception

In bimodal trials, a tactile (airflow) and a visual (optic flow) self-motion stimulus were presented simultaneously, either directionally congruent or incongruent with an offset of max. 30°. Figure 3 shows mean perceived heading as function of the directional offset between visual and tactile heading stimuli for the four experimental conditions. In each panel, differently colored symbols and lines depict the results for a given visual heading. Colored arrows on the ordinate indicate visually presented headings. If perceived heading in the bimodal condition was independent from the tactile stimulus, all colored lines were flat (slope = 0.0). Likewise, diagonal lines with slope = 1.0 would indicate a strict correlation between tactile information and perceived bimodal heading.

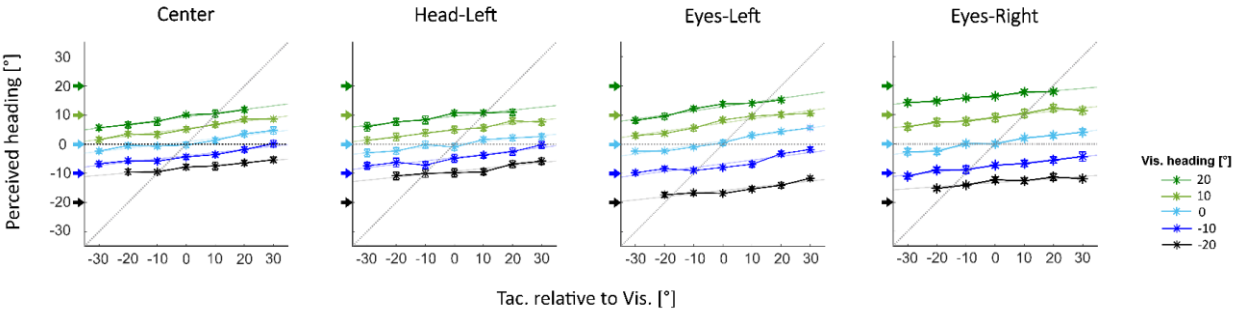

Figure 3. Heading estimation in bimodal trials. In bimodal trials, visual and tactile heading stimuli either simulated congruent headings or had an offset of max. 30° between them. Mean perceived headings (ordinate) are shown for each visual heading separately (colored lines) as a function of tactile headings relative to visual heading (abscissa). Colored arrows indicate visually presented headings. Error bars represent standard errors over participants.

Slopes of $m > 0$ of single regression lines (representing each visually presented heading) indicate that stimuli from both modalities were used for heading estimation in all conditions (all $p < .001$). Slopes of single linear regression did not differ between all four conditions ($F(3, 18) = 0.43$, $p = .734$, $\eta^2 = .067$) and intercept values (average spacing between regression lines) were comparable between all four conditions ($F(3, 18) = 1.863$, $p = .172$, $\eta^2 = .237$). Perceived headings in the Center condition (mean slope: 0.11, average spacing between regression lines: 3.6°) and in the Head-Left trials showed a similar overall pattern: mean slope: 0.11, average spacing between regression lines: 3.9°. Given that the different visual heading stimuli varied by 10° each, an average spacing of only 3.6° between regression lines (together with a mean intercept of about 0°) is indicative of a centripetal bias. Quantitatively, in line with the data from Uni Vis trials, heading performance showed highest accuracy (i.e., a reduced centripetal bias) in the Eyes-Left condition, as indicated by slightly larger slopes (mean slope 0.13) and wider spacings between regression lines (average spacing between regression lines: 6.3°). In a subsample of participants, an Eyes-Right condition was also measured (mean slope 0.1). Again, spacings between regression lines (average spacing between regression lines: 7.4°) indicated higher accuracy compared to the Center and Head-Left condition.

To probe for multisensory integration, for each participant, we calculated the standard deviations of perceived headings for congruent headings in Uni Vis, Uni Tac, and bimodal trials (-20° to 20° in 10° steps). Next, we derived from unimodal standard deviations corresponding values that would have been expected for bimodal trials (S_{biOpt}) if stimulus

integration was Bayes-optimal. Here, lower standard deviations (i.e., higher precisions) in bimodal as compared to unimodal trials would indicate optimal stimulus integration. Average heading performance in none of the four conditions showed such optimal stimulus integration: Observed mean standard deviations in the Center condition (S_{bi} = 6.7°), the Head-Left condition (S_{bi} = 8.4°) and the Eyes-Left condition (S_{bi} = 5.5°) were significantly larger (i.e. lower precision) compared to predicted standard deviations (Center: S_{biOpt} = 4.2°; Head-Left: S_{biOpt} = 4.6°; Eyes-Left: S_{biOpt} = 3.5°) ($F(1, 14) = 46.66$, $p < .001$, $\eta^2 = .77$). The same applies to heading performance in the Eyes-Right condition that was completed by a subsample of participants. Also here, observed mean standard deviation (S_{bi} = 4.4°) was significantly larger compared to the predicted standard deviation (S_{biOpt} = 3.3°) ($F(1, 6) = 18.5$, $p < .05$, $\eta^2 = .76$).

Although heading stimuli from both modalities were evidently not integrated optimally (in a Bayesian sense), it is apparent from Figure 4 that sensory stimuli of both modalities were considered by the participants for their heading judgments. To quantify the contribution (or weight) of information from both modalities in bimodal heading perception, perceived headings from unimodal trials (x: vis, y: tac) were entered as regressors into a multiple regression with bimodal perceived heading as the dependent variable (z) for each participant. In all conditions, the full model (as depicted in Equation 2, Methods) was successively compared to models without quadratic terms, without the interaction term, and without quadratic and interaction terms (see Methods for details). In all conditions, an interaction term, quadratic terms, or both, did not improve model fits compared to the purely linear model. In other words: bimodal heading perception in all conditions were best explained by a linear combination of perceived heading in purely visual and tactile trials. Coefficients obtained for this model for each of the conditions are listed in table 1.

Table 1. Mean coefficients derived from the linear regression model. Perceived headings of bimodal trials (z) were predicted by perceived heading from unimodal visual (x) and unimodal tactile trials (y) following a 2D linear regression model ($z = m_{vis}*x + m_{tac}*y + b$) for each of the 33 bimodal conditions separately with: b: Intercept, m_{vis}: Mean coefficient for regressor unimodal visual perceived heading, m_{tac}: Mean coefficient for regressor unimodal visual perceived heading, R^2: Mean goodness of fit

	N	m_{vis}	m_{tac}	b	R^2
Center	15	0.68	0.33	0.39	0.9
Head-Left	15	0.88	0.3	0.41	0.88
Eyes-Left	15	0.79	0.33	0.8	0.95
Eyes-Right	7	0.72	0.28	0.01	0.95

Figure 4*A* shows the 2D linear regression plane for data of one participant tested in the Center condition. Perceived heading in bimodal trials (z-axis) could be predicted (light blue plane) by a linear combination of perceived heading in Uni Vis (x-axis) and Uni Tac (y-axis) trials (Blue dots. R^2 = 0.94).

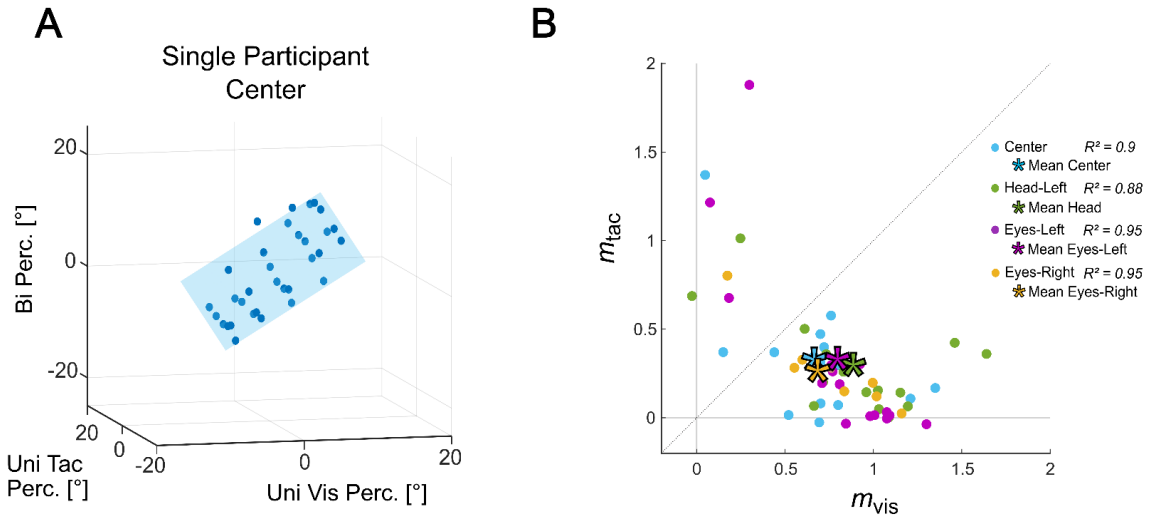

Figure 4. Modeling bimodal heading perception. A. Perceived headings in bimodal trials (z-axis) were modeled utilizing 2D linear regression, with x = perceived vis heading and y = perceived tactile heading. **B**. Gradients of the 2D linear regression for the four experimental conditions. Data points represent gradients, i.e., slopes in x (vis) and y (tac) direction, of regression planes from individual participants and conditions (Center: blue, Head-Left: green, Eyes-Left: purple, Eyes-Right: yellow). Means over participants are represented by asterisks. Most data points were below the diagonal ($m_{vis} > m_{tac}$), indicating a stronger weight of visual as compared to tactile information.

Figure 4*B* shows the distribution of the gradients, i.e., slopes in x (visual) and y (tactile) direction, of the 2D regression planes for all four experimental conditions (Center: Blue, Head-Left: Green, Eyes-Left: Purple, Eyes-Right: Yellow). Along a single axis, a value of 1.0 would indicate the same absolute weight as in the unimodal condition. Values smaller than 1.0 would be indicative of a reduced weight. Values larger than 1.0 would indicate a boosted weight of that sensory modality in the bimodal condition. In all conditions, mean values were

significantly smaller than 1.0: $m_{Vis,Center}$ = 0.684; $m_{Vis,Eyes\_Right}$ = 0.762; $m_{Tac,Center}$ = 0.329; $m_{Tac,Head\_Left}$ = 0.295; $m_{Tac,Eyes\_Left}$ = 0.334; $m_{Tac,Eyes\_Right}$ = 0.272; (all $p < .00625$, Bonferroni corrected for multiple comparisons), with the exception of the Head-Left ($m_{Vis,Head\text{-}Left}$ = 0.8884) and the Eyes-Right ($m_{Vis,\ Eyes\text{-}Right}$ = 0.7620) condition ($p > .11$) in Uni Vis trials. Most participants showed higher slopes (higher relative weights) for the visual than for the tactile regressor (see Table 1), indicating that the visual modality contributed more strongly to heading judgements in bimodal trials than the tactile modality. While some participants based their responses completely on visual stimuli and disregarded tactile stimuli (zero on the y-axis), most relied on stimuli from both modalities in all conditions. Interestingly, two participants (Subj. No. 4 and Subj. No. 6) based their responses more strongly on tactile compared to visual stimuli (data points above the diagonal). Goodness of fit (R^2) analyses of fitted linear regression models showed overall high values ($R^2 > 0.87$) and were comparable between the three conditions that were completed by all participants (Center, Head-Left and Eyes-Left condition, $F_{GG}(1.418, 19.847) = 3.875$, $p = .052$, $\eta^2_{GG} = .21$).

3.4.3. Influence of head- and eye-position on heading perception

While self-motion through an environment occurs in body-centered coordinates, visual information is sensed in eye-centered coordinates, and tactile flow on the head is registered in head-centered coordinates. By varying eye and head orientation for otherwise identical stimulation, we aimed to quantify the influence of the position of the sensors (eye, head) on heading perception. For unisensory conditions, we already showed (Figure 3) that only for tactile stimuli, the orientation of the eyes away from straight-ahead had a significant influence: given a shift of the eyes of 20°, average perceived tactile heading was shifted by 3.8° (19%) and 5.3° (26.5%) for shifts to the left and right, respectively.

Figure 5 shows bimodal data. Figure 5A-D depicts mean perceived bimodal heading (z-axis) as a function of perceived heading in Uni Vis trials (x-axis) and Uni Tac trials (y-axis) and corresponding linear regression fits. In panel *A*, the grey planes above and below the Center plane (blue) indicate theoretical shifts in perceived heading for the Head/Eyes-Left, and the Eyes-Right condition, if bimodal perception was Head/Eye centered, respectively. In all conditions (Panels *B-D),* mean perceived heading was not shifted towards head-/ or eye-position as compared to the Center condition. This is also shown in panels E and F, which

show the differences of intercepts (E) and slopes (F), between the Head/Eyes-Left and Eyes-Right conditions and the Center condition. Difference-values for the intercept (mean Head-Left = 0.03, mean Eyes-Left = 0.61, mean Eyes-Right = -0.66) did not differ significantly from zero (one-sample t-Test, all $p > .531$) and there was no significant difference between conditions ($F(1.422, 2) = .123$, $p = .876$, $\eta^2 = .02$).

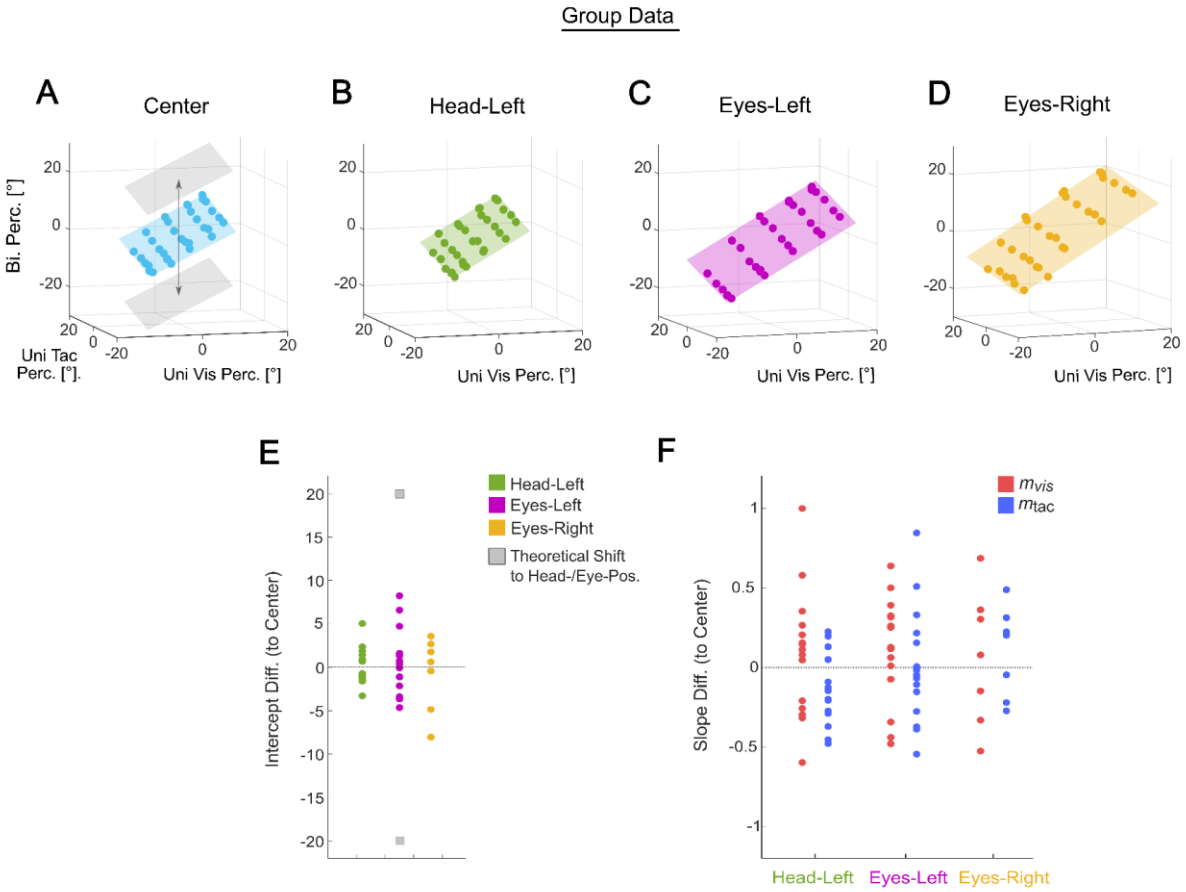

Figure 5. Mean bimodal heading perception as modeled based on unimodal heading perception for all conditions and comparison between fit parameters. Mean perceived headings in bimodal trials (z-axis) were modeled based on perceived heading from unimodal visual (x-axis) and unimodal tactile (y-axis) trials. ***A.*** Transparent grey planes indicate expected shift of perceived heading towards eccentric head- or eye-position relative to the Center condition (blue plane), if perception was strictly head- or eye-centered. ***B.*** Mean perceived headings in bimodal trials in the Head-Left, ***C.*** Eye-Left and ***D.*** Eyes-Right condition. ***E.*** Difference of intercept values of each condition and the Center condition for each participant. ***F***. Difference in slope values (unimodal visual (Red) and unimodal tactile (Blue)) between each condition (x-axis) and the Center condition. Single points represent data from individual participants.

Likewise, difference values for the slopes did not differ significantly from zero (one-sample t-Test, all $p > .21$) and were comparable between modalities ($F(1,6) = .272$, $p = .621$, $\eta^2 = .043$) and conditions ($F(2,12) = .725$, $p = .504$, $\eta^2 = .108$). In sum, there was no influence of head- and eye-position on perceived bimodal heading, pointing towards a body (or world) centered perception.

3.5. Discussion

In this study we have investigated and compared unimodal visual, unimodal tactile and bimodal (visuo-tactile) heading perception. By varying head and eye orientation we aimed to determine the reference frame of heading perception.

3.5.1. Unimodal heading perception

In the Center condition, heading stimuli were designed to produce comparable performance accuracies between Uni Vis and Uni Tac trials. Given the experimental apparatus, this was achieved by lowering the coherence of the moving visual stimuli to about 50%. Perceived headings were biased towards straight-ahead in both modalities (i.e., centripetal bias). The same holds true for heading performance in the Head-Left condition. Interestingly, heading performance for Uni Vis trials in the Eyes-Left and Eyes-Right conditions revealed a reduced centripetal bias, while it was comparable between all conditions for Uni Tac trials. The bias of perceived heading towards straight-ahead is in line with results from the literature (Bremmer et al., 2017; D'Avossa & Kersten, 1996; Rosenblum et al., 2022; Sun et al., 2020; Warren & Kurtz, 1992; but see also Cuturi & MacNeilage (2013) who found priors to the side (± 90°)) and consistent with Bayesian accounts which have proposed a prior for straight ahead as the most common heading direction (MacKay, 2003; Sun et al., 2020). Another possible explanation might be that participants learned the range of presented headings (likely during the first trials), leading them to adapt their responses to a limited range on the screen (Crane, 2012; De Winkel et al., 2015). Remarkably, we found a reduced centripetal bias (in screen coordinates) of perceived headings in the Uni Vis trials in the Eyes-Left/Right conditions. While this, in principle, could have been caused by an overall attraction of perceived heading towards the eye, we found no evidence for an eye-centered visual heading perception (see below). Hence, we speculate that heading perception with

eccentric gaze might have been perceptually more demanding, leading eventually to an overall better performance.

3.5.2. Bimodal heading perception

In bimodal trials, visual and tactile self-motion stimuli were presented simultaneously, simulating either congruent or incongruent headings with varying angular separation of max. 30° between them. Visuo-tactile heading stimuli were presented in four conditions varying in head- and eye-orientation (*Center, Head-Left, Eyes-Left, Eyes-Right*). Perceived heading in all conditions was biased towards (body/world-centered) straight-ahead (i.e., centripetal bias). Like for the Uni Vis data, the centripetal bias was reduced in Eyes-Left/Right conditions.

Our analysis of response variance revealed that heading stimuli from the visual and tactile modality were not integrated optimally in a Bayesian sense (Alais & Burr, 2004). One possible explanation might be that stimuli of both modalities were inferred to correspond to different sources. Bayesian models of causal inference predict optimal stimulus integration as a function of spatial proximity between stimuli (Acerbi et al., 2018; De Winkel et al., 2017; Jones et al., 2019). However, in our task, participants could have learned already during the first trials that visual and tactile stimuli could present incongruent headings with a large spatial offset between them.

Participants were instructed to “indicate perceived heading” without being asked to focus on one modality in particular. Yet, participants relied more on visual information, a result in line with previous work on multisensory integration (Battaglia et al., 2003; Meijer et al., 2019). Nevertheless, also tactile stimuli were clearly considered for heading perception. In sum, Bayes-non-optimal multisensory integration as found in our current study was also reported in previous work (Krala et al., 2019; Meijer et al., 2019; Rahnev & Denison, 2018; Stengard & Van Den Berg, 2019) and can also be found in case tactile stimuli are not task-relevant (Rosenblum et al., 2022).

We also found inter-individual differences. While most participants based their heading estimates predominantly on the visual stimuli in all conditions, two participants relied more strongly on tactile stimuli in all conditions. A similar dominance of tactile over visual stimuli has recently been shown by Harris and colleagues (2017).

In our present study, we have tested perception only. Hence, we can only speculate concerning the underlying neural processing. Numerous imaging studies in human observers and neurophysiological studies in the macaque monkey, i.e., the prime animal model of human vision, have documented responsiveness for visual self-motion stimuli in various brain regions (for reviews, see: Britten, 2008; Noel & Angelaki, 2022). Among these, the only area also showing responses to tactile stimuli is the macaque ventral intraparietal area (area VIP. Duhamel et al., 1998; Avillac et al., 2005). Importantly, neurons with visual and tactile responses have spatially overlapping visual and tactile receptive fields and reveal directionally congruent self-motion responses (Bremmer et al., 2002). Importantly, a functional equivalent of macaque area VIP (hVIP) has also been shown in humans by mean of fMRI (Bremmer et al., 2001). Hence, we speculate that neural processing in area hVIP could underly the observed perceptual effects.

3.5.3. Influence of head- and eye-position on heading perception

We have found no influence of head position or eye orientation on visual heading perception. This was somewhat surprising given previous work providing some evidence for an eye centered processing of visual self-motion information (Monkeys: Chen et al., 2014; Fetsch et al., 2007. Humans: Crane, 2017). A possible explanation might be the stimulus design. While Crane employed a 2AFC task, we asked our participants to indicate perceived self-motion direction. Perhaps even more important: Crane (2017) also tested the influence of the proportion of visual stimuli in the display showing coherent motion. A reduction in motion coherence induced a shift from eye-centered towards screen (or body or world) centered. Hence, it might have been the coherence (roughly 50%) of the moving dots in our displays which might have contributed towards a body (or world) centered perception of heading. Given that we have not varied body position, our data do not allow to dissociate between a body- and a world centered heading perception.

Unexpectedly, tactile heading perception was modulated by varying eye position. Heading was shifted by 20-25% of the underlying shift in eye position. This is remarkable given that tactile information is initially encoded in a body centered frame of reference (tactile RFs on the skin), and eye-position independent responses have been shown for macaque area VIP (Avillac et al., 2005). We speculate that for eye position away from straight-ahead, participants

were less sure about the tactile stimulation and focused more on where the eye was directed. More experiments, however, would be necessary to better understand the observed effects.

3.5.4. Study limitations

A limitation of our approach is the response format, which forced participants to transfer tactile perception into a visual frame of reference. Future studies could aim for a different, for example verbal response format (as employed by e.g., Harrar & Harris, 2009; Pritchett & Harris, 2011).

Another limitation, leading to higher accuracies for the Eyes-Left/Right condition might be the size of the screen. When participants fixated 20° to the left/right from straight-ahead, screen boundaries might have provided external landmarks. However, the influence of this was likely small, given that screen size was 81° in total, i.e., extending 40° to both sides from the midline.

3.5.5. Conclusion

This study demonstrates that tactile as well as visual stimuli are used for heading estimation in a heading estimation task. For a combination of stimuli from both modalities, simulating either congruent heading or with an offset of max. 30° between stimuli, participants took both sensory signals into account but relied more strongly on visual stimuli. In bimodal trials, varying head- and eye-position had no significant effect on perceived heading. Only in unimodal tactile trials, heading perception was shifted towards eye-position, but not head-position. Since body-position relative to the world has been not manipulated in this study, we cannot dissociate between a body- or world-centered frame of reference. Overall, it can be concluded that tactile flow is more important to heading perception than previously thought.

4. STUDY 3

The study has been published as:

Rosenblum, L., Kreß, A., Arikan, B.E., Straube, B., Bremmer, F. (2023). Neural correlates of visual and tactile path integration and their task related modulation. *Sci Rep 13*(9913) https://doi.org/10.1038/s41598-023-36797-8

4.1. Abstract

Self-motion induces sensory signals that allow to determine travel distance (path integration). For veridical path integration, one must distinguish self-generated from externally induced sensory signals. Predictive coding has been suggested to attenuate self-induced sensory responses, while task relevance can reverse the attenuating effect of prediction. But how is self-motion processing affected by prediction and task demands, and do effects generalize across senses? In this fMRI study, we investigated visual and tactile self-motion processing and its modulation by task demands. Visual stimuli simulated forward self-motion across a ground plane. Tactile self-motion stimuli were delivered by airflow across the subjects' forehead. In one task, subjects replicated a previously observed distance (Reproduction/Active; high behavioral demand) of passive self-displacement (Reproduction/Passive). In a second task, subjects travelled a self-chosen distance (Self/Active; low behavioral demand) which was recorded and played back to them (Self/Passive). For both tasks and sensory modalities, Active as compared to Passive trials showed enhancement in early visual areas and suppression in higher order areas of the inferior parietal lobule (IPL). Contrasting high and low demanding active trials yielded supramodal enhancement in the anterior insula. Suppression in the IPL suggests this area to be a comparator of sensory self-motion signals and predictions thereof.

4.2. Introduction

Self-motion through an environment induces various sensory signals that allow for the estimation of parameters such as traveled distance, direction (heading), and speed. The visual pattern induced by self-motion is called optic flow (Lappe et al., 1999a; Matthis et al., 2022). Path integration describes the ability to estimate the traveled distance (and angular direction) of one's self-motion with respect to a reference point. The integration of optic flow over time

allows the moving observer to determine the distance that has been traveled (Alefantis et al., 2022; Bremmer & Lappe, 1999). For the tactile modality, a previous behavioral study has shown that the estimation of traveled distance is feasible by the integration of tactile flow over time in a distance replication task (Churan et al., 2017).

Neural correlates of path-integration have been mainly studied in the visual modality. Key cortical regions for visual self-motion processing are areas hMST (Dukelow et al., 2001; Schmitt et al., 2020), hVIP (Bremmer et al., 2001; Wall & Smith, 2008), hCSv (Smith, 2021) and hV6 (Sabrina Pitzalis et al., 2020). But also auditory self-motion cues (pitch scaling with speed) can be used to reproduce traveled distance (Von Hopffgarten & Bremmer, 2011). Based on this result, in a follow-up fMRI study employing visual and auditory self-motion stimuli, we have shown that the active reproduction compared to the passive encoding of a travel distance leads to enhanced BOLD activity in early sensory (visual and auditory) cortices. In addition, we found suppressed BOLD response in higher-order areas such as the angular gyrus (Krala et al., 2019). The finding of enhanced BOLD response in early cortical areas was somewhat surprising given that the predictive coding framework hypothesizes the attenuation of neural responses for self-generated (i.e., predicted) signals (but see also (Morillon et al., 2019; Reznik, 2021) for cases of response enhancement). We suggested that enhanced BOLD response in early sensory cortices might have been driven by engagement of attentional and working memory resources during the on-line comparison of traveled and target distance to solve the task of reproduction. In this sense, attention operates as a top-down mechanism that increases the precision of perceptual inference (Ferrari & Noppeney, 2021; Schröger et al., 2015; Smout et al., 2019), and optimizes the correctness of prediction errors by reversing the effect of prediction (Auksztulewicz & Friston, 2015; Hsu et al., 2014; Jiang et al., 2013). We proposed that in that context, behavioral task demands led to an enhanced BOLD response in early cortices while BOLD activation was suppressed in higher-level areas reflecting conformity of predictions and information about traveled distance (Arnold et al., 2014; Kok et al., 2012). However, in our previous study, behavioral task demand was not manipulated as an experimental factor.

In the present study, we investigated the neural correlates of tactile and visual self-motion processing in a path-integration task using human fMRI. We aimed to further examine how the perception of traveled distance is influenced by task-demands by manipulating it as an experimental factor. Subjects solved a path integration task using either visual or tactile

flow. High behavioral demand was induced by a Reproduction (Repro) task, where subjects actively replicated (Active; *high* monitoring demand) a previously observed self-displacement (Passive; *high* encoding demand). As a low demanding task, we introduced the Self task (Self), where subjects first traveled a self-chosen distance (Active; *low* monitoring demand) which was recorded and then played back to them, without a further task (Passive; *low* encoding demand). In Active trials of the Repro task (= Repro/*Act*), behavioral demand was expected to be higher compared to Active trials of the Self task (= Self/*Act*) given that subjects had to maintain a target distance in register and evaluate and compare traveled distance online to be able to successfully solve the task. Following our previous study on visual and auditory path-integration (Krala et al., 2019), we expected to find enhanced BOLD response in early sensory areas and suppressed BOLD response in higher-order areas for Active as compared to Passive trials. Likewise, given the higher behavioral demand, we expected to find stronger BOLD activation in Repro/Act trials as compared to Self/*Act* trials.

4.3. Results

4.3.1. Behavioral Results

For the Repro task where subjects actively reproduced a previously observed travel distance, we quantified the accuracy of replicated distance by computing the resulting 'Error' (Reproduced distance - Presented distance). Subjects were presented with two different target distances and always traveled at a constant speed. Here, the short distance of 1 in arbitrary units (a.u.) corresponds to a travel duration of 1 sec and a long distance of 1.5 a.u. to a travel duration of 1.5 sec. Errors were investigated for both presented distances in both modalities (Vis & Tac) separately. Fig. 1A (left panel) shows the Errors (ordinate) for both target distances and both modalities (gray dots depict single subject data, while colored asterisks depict the mean). Positive values on the y-axis correspond to an overestimation of travel distances (overshoot) and negative values to an underestimation of travel distances (undershoot). While subjects' responses revealed overall a slight undershoot for short distances (*Mean* Vis_{Short}: -0.02 a.u.s, *Mean* Tac_{Short}: -0.03 a.u.s.), long distances were overestimated by most subjects (*Mean* Vis_{Long}: 0.06 a.u.s; *Mean* Tac_{Long}: 0.1 a.u.s) [RM ANOVA, $F(1, 20) = 16.558$, $p < .001$, $\eta^2 = .453$, main effect "Distance"]. Accuracy did not differ significantly between both modalities [RM ANOVA, $F(1, 20) = 0.835$, $p = .372$, $\eta^2 = .04$, main effect "Modality"] indicating comparable performance between conditions. After the experiment, subjects were asked to indicate their

reproduction strategy in an open response format. Counting and memorizing a rhythm as reproduction strategies was reported by most of the subjects.

In the Self task, subjects traveled self-chosen distances that were recorded and played back to them. Fig. 1B shows mean traveled distances [a.u.] for the Vis and Tac trials separately (ordinate). Bars show the subject mean of the self-produced distances and dots depicting single subject data. The overall produced distances were slightly but significantly longer in the visual (*Mean* = 1.1 a.u.s, *SD* = 0.2 a.u.s) as compared to the tactile modality (*Mean* = 1.0 a.u.s, *SD* = 0.19 a.u.s) (paired samples t-test: $t(20) = 3.194$, $p < .01$). Traveled distances correlated between the visual and tactile modality across subjects, i.e., participants who traveled shorter (longer) distances in the visual modality also tended to travel shorter (longer) distances in the tactile modality (Sig. Pearson's corr. 0.734, $p < .001$).

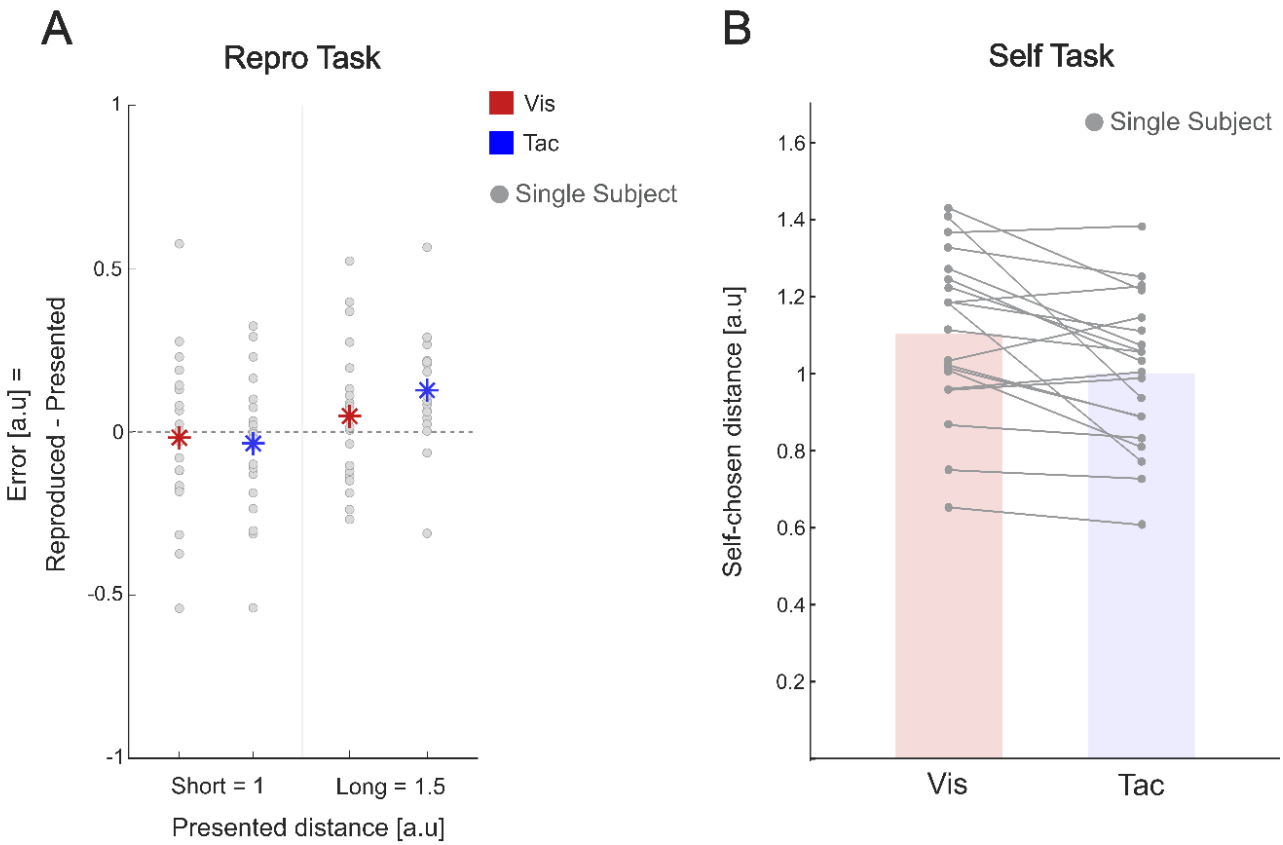

Figure 1. A. Accuracy of reproduced distances in the Repro task. Mean Error, defined as reproduced distances (Repro/Act) minus presented distance (Repro/Pas), as a function of target distance (short and long). Asterisks represent mean across all subjects for the visual (red) and tactile (blue) conditions and single grey dots represent single subject data. Positive values indicate that subjects overshot the target distance, and vice versa. ***B*. Mean traveled distances**

in the Self task. Mean self-chosen traveled distances are shown on the y-axis for the visual (red bar) and tactile (blue bar) modalities. Like in A, dots represent single subject data, and lines connect data points from the same subjects.

4.3.2 Imaging Results

4.3.2.1. Neural correlates of path-integration

To investigate the overall effect of sensory modality on BOLD activation during distance encoding, we conducted F-tests over visual and tactile trials irrespective of task condition (main effect against baseline). Given the nature of our self-motion stimuli, we expected to find a significant BOLD response in early visual cortex and in areas sensitive for visual self-motion stimuli and in early and higher somatosensory cortices for tactile stimuli, respectively. In particular, we expected to find a BOLD response in the ventral intraparietal area (hVIP) for both stimulus modalities given the multimodal response properties of area hVIP (e.g., Bremmer et al., 2001; Field et al., 2020). Figure 2 displays the clusters for main effects of each modality (Vis = red, Tac = blue) and Table 1 reports the activation peaks in significant clusters. For visual trials, we observed significant activation in bilateral striate (V1) and extrastriate visual areas (V2, V3, MT-complex) and bilateral area hVIP (Bremmer et al., 2001). Visual areas that have been found to encode different aspects of self-motion were investigated based on peak coordinates derived from previous studies. Specifically, we probed area V6 (Pitzalis et al., 2010), cingulate sulcus visual area (CSv) (Di Marco et al., 2021), and the MST+ region (Pitzalis et al., 2013). For effects of interest depicted in Fig. 2, we have identified significant activation in bilateral areas V6 and MST+ on the peak-level only.

For tactile trials, we found significant activations in the left primary and secondary somatosensory cortices (S1, S2), bilateral anterior insular cortex (AIC), and left area hVIP. On the uncorr. level (not shown in Fig. 2), we also found significant activation for right area hVIP, ([*x, y, z* = 34, -56, 46], k_E = 140, $p_{unorr.}$ < .01) and for right area S1 ([*x, y, z* = 46, -32, 46], k_E = 86, $p_{unorr.}$ < .01).

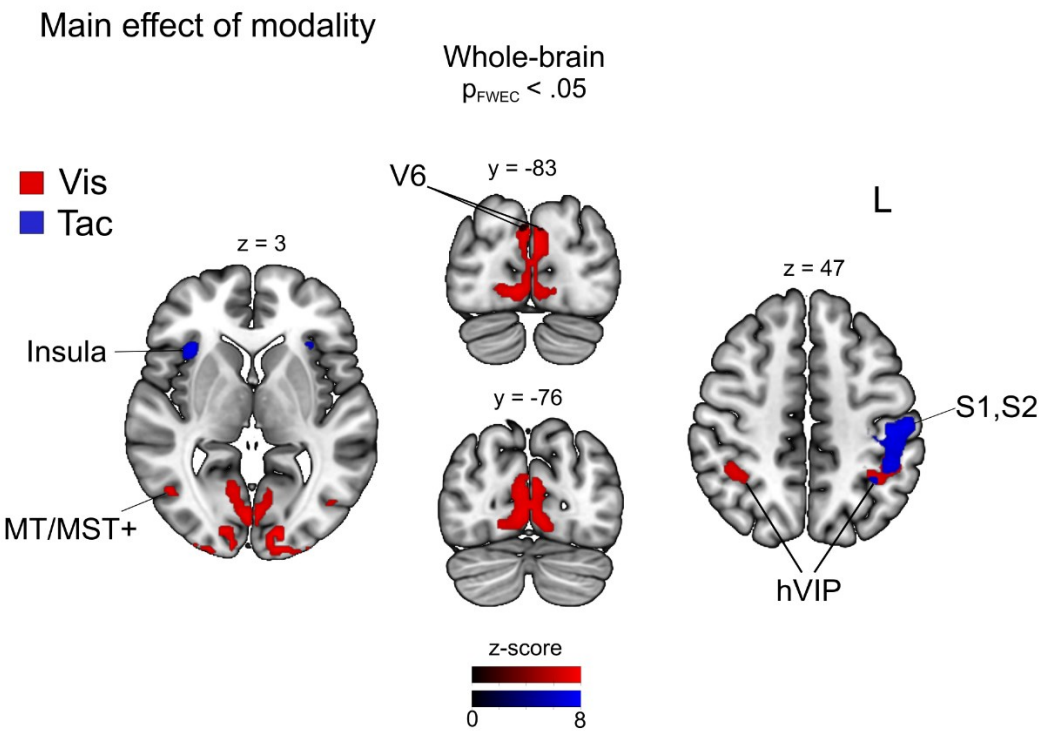

Figure 2. Neural responses induced by visual (red) and tactile (blue) self-motion stimuli. Clusters showing a significant main effect for visual and tactile self-motion encoding, respectively, across all tasks. Whole-brain results show BOLD responses in early and higher-order visual areas for visual optic flow stimuli and responses in early and higher-order somatosensory areas for tactile flow simulating forward self-motion, significant at pFWE < .05.

Table 1. Anatomical locations of cluster activations for main effects of the visual and tactile modality, respectively. Coordinates are listed in MNI space. p = .05 FEW

				Coordinates (peak of sign, cluster, MNI)				
	Anatomical Label	Cluster extent (Anatomy toolbox)	Side	x	y	z	*z* value	k_E
Vis	Occipital pole	V1, V2, V3	R	30	-94	-6	> 8	1802
		V1, V2, V3	L	-32	-94	-8	> 8	409
	Lateral occipital cortex	V5	R	44	-62	2	6.32	22
			L	-42	-70	2	6.11	13
	IPS	hVIP	R	40	-44	46	5.41	85
			L	-34	-50	46	6.21	214
Tac	Parietal lobe	Postcentral gyrus	L	-44	-18	58	7.18	420
	Parietal lobe	Postcentral gyrus	L	-46	-42	48	5.47	5
	Parietal Operculum	hVIP, SII	L	-44	-42	48	5.74	117
	Insular Cortex	Operculum	L	-32	16	10	6.64	110
		Operculum	R	32	18	8	6.34	133
	Supramarginal Gyrus	IPL	R	56	-38	18	5.94	22
			L	-42	-34	20	5.38	15

4.3.2.2. Modulatory effect of behavioral demand

In the Repro task, contrasting Act against Pas trials (*Act > Pas*) for the visual modality yielded significant bilateral clusters in early visual sensory cortices. Surprisingly, for the tactile modality, this contrast also showed significant bilateral clusters in early visual sensory cortices. Figure 3 (top row) shows significant activation clusters for this contrast in each modality (Vis = red, Tac = blue) as well as corresponding mean beta estimates for peak voxels. White lines demarcate overlapping activation in both conditions. A conjunction analysis over both modalities (Repro/*Act* > Repro/*Pas* visual ∩ Repro/*Act* > Repro/*Pas* tactile) showed significant bilateral activations in early visual cortices (Figure 3, right column. Conjunction = Green). For unimodal visual trials and the conjunction analyses, we found large significant clusters that contained multiple anatomical regions. We reviewed the significant clusters by entering the corresponding contrast to the Anatomy Toolbox and by applying a V3A mask (Nau, Schindler, et al., 2018) and found small, but significant activations of bilateral area V3A.

To identify possible suppression effects in Act relative to Pas trials, we calculated the contrast (*Pas > Act*) (Fig. 3, bottom row). For visual trials, we observed significant clusters in higher-order visual areas (e.g., V3, MT/V5, hVIP) and the inferior parietal lobe (IPL). For the tactile modality, the (*Pas > Act*) contrast showed significant bilateral clusters in higher-order visual areas located in the lateral occipital cortex (LOC) and the left IPL. A conjunction analysis over both modalities (Repro/*Pas* > Repro/*Act* visual ∩ Repro/*Pas* > Repro/*Act* tactile) showed significant bilateral clusters in V3 and the IPL. Table 2 reports all identified cluster peaks of the contrasts derived from the Repro task.

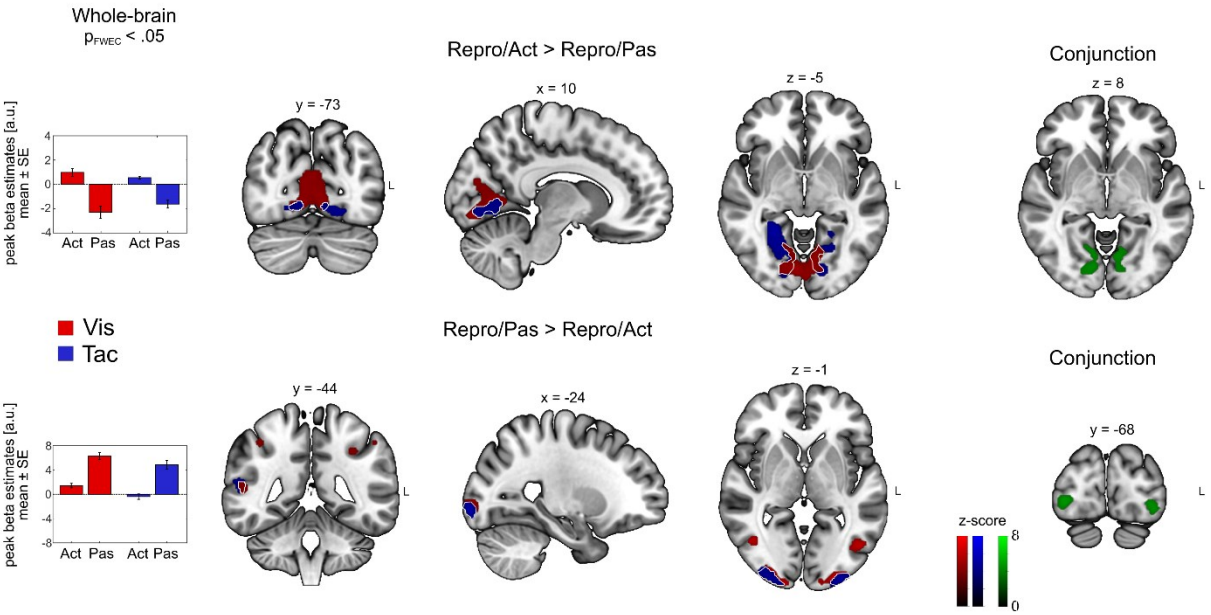

Figure 3. Modulatory effect of behavioral demand. Whole-brain results showing BOLD enhancement (upper row) and BOLD suppression (bottom row) during the reproduction of target distances compared to passively encoding distances for visual (shown in red) and tactile (shown in blue) stimuli. Commonly enhanced or suppressed regions across visual and tactile stimuli are demarcated by a white line. Bar graphs show mean beta estimates across subjects (±*SE*) for the corresponding peak voxel. Clusters derived from a conjunction analysis across both modalities are shown on the right (green). Cluster-forming threshold for all maps was $p_{FWE} < 0.05$.

Table 2. Anatomical locations of cluster activations for contrasts of interest in the Repro task. Coordinates are listed in MNI space. Initial search threshold was $p < .001$, only regions passing the $p_{FWE} < .05$ at the cluster level are shown.

				Coordinates (peak of sign, cluster, MNI)						
	Anatomical Label	Cluster extent (Anatomy toolbox)	Side	x	y	z	k_E	*z* value	p_{FWE} voxel	p_{FWE} cluster
Repro/Act > Repro/Pas										
Vis	Lingual	V1, V2, V3A	R	2	-78	2	5882	6.38	< .001	< .001
Tac	Lingual	V1, V2, V3	R	26	-48	-4	7209	6.85	< .001	< .001
Conj	Lingual	V1, V2, V3A	R	12	-62	0	3975	5.49	= .001	< .001
Repro/Pas > Repro/Act										
Vis	Occipital Mid	hOc4lp	L	-30	-96	-6	2156	> 8	< .001	< .001
	Occipital Inf	hOc3v	R	30	-94	-6	702	7.57	< .001	< .001
	Temporal Mid	MT/V5	R	44	-62	6	3336	5.91	< .001	< .001
	Precentral	Area 6d3	L	-28	-6	54	2191	5.32	< .010	< .001
	Parietal Inf	IPS	L	-32	-42	40	2586	5.17	< .010	< .001
	Frontal Inf Oper	Pars Opercularis	R	54	10	18	749	4.39	= .112	< .001
Tac	Occipital Mid	hOc4lp	L	-30	-96	-6	1723	> 8	< .001	< .001
	Occipital Inf	hOc3v	R	30	-94	-6	408	7.27	< .001	< .010
	Temporal Sup	IPL	R	54	-42	14	2323	5.43	= .001	< .001
	Angular	IPS	L		-36	-66	40	447	4.42	< .010
	Temporal Sup	IPL	L	-56	-38	22	247	4.23	= .201	< .050
	Precuneus	SPL	L	-4	-62	62	430	3.94	= .469	< .010
Conj	Occipital Mid	hOc4lp	L	-30	-96	-6	1258	> 8	< .001	< .001
	Occipital Inf	hOc3v	R	30	-94	-6	388	7.27	< .001	< .010
	Temporal Sup	IPL	R	52	-42	12	1160	5.33	< .010	< .001
	Parietal Inf	IPS	L	-30	-48	44	331	4.15	= .255	< .050

Table 3. Anatomical locations of cluster activations for contrasts of interest in the Self task and the comparison between Repro/Act and Self/Act trials. Coordinates are listed in MNI space. Initial search threshold was $p < .001$, only regions passing the $p_{FWE} < .05$ at the cluster level are shown.

				Coordinates (peak of sign, cluster, MNI)						
	Anatomical Label	Cluster extent (Anatomy toolbox)	Side	x	y	z	k_E	*z* value	p_{FWE} voxel	p_{FWE} cluster
Self/Act > Self/Pas										
Vis	Calcarine	V1, V2	L	-16	-96	-6	891	5.52	< .010	< .001
	Calcarine	V1, V2	R	16	-94	-2	719	5.22	< .010	< .001
Tac	Precuneus	SPL	R	8	-72	52	519	4.76	= .057	< .010
	Precentral	Area 6d1	L	-32	-20	70	398	4.69	= .071	< .010
	Calcarine	V1, V2	R	16	-94	-4	891	4.64	= .086	< .001
	Calcarine	V1, V2	L	-14	-94	-8	1235	4.53	= .123	< .001
Conj	Calcarine	V1, V2	R	16	-94	-4	286	4.46	= .086	< .050
	Calcarine	V1, V2	L	-14	-94	-8	476	3.67	= .123	< .010
Self/Pas > Self/Act										
Vis	Angular	IPL	L	-56	-62	30	1817	5.47	= .001	< .001
	Frontal Sup II	Area p32	L	-14	54	26	1247	4.23	= .202	< .001
	Temporal Mid	IPL	R	46	-50	18	620	4.2	= .223	= .001
Tac	Angular	IPL	L	-58	-60	30	522	4.4	= .111	< .010
Conj	Angular	IPL	L	-58	-60	30	522	4.4	= .111	< .010
Repro/Act > Self/Act										
Vis	Insula	OP8	L	-34	20	14	428	4.45	= .091	< .010
	Insula	OP8	R	32	16	10	511	4.3	= .160	< .010
Tac	Supp Motor Area	preSMA	L	-6	-2	58	376	4.43	= .099	< .001
	Insula	Area Id7	R	36	24	0	648	4.38	= .119	< .010
	Precentral L	Area 4p	L	-32	-20	50	340	4.34	= .136	< .050
	Frontal Inf Oper	Area 44	L	-56	8	24	522	4.34	= .137	< .010

In the Self Task, contrasting Act against Pas trials (*Act > Pas*) for the visual and tactile modality yielded bilateral significant clusters in early visual and somatosensory cortices, respectively (Fig. 4, upper row). These clusters also showed significant activation in a conjunction analysis over both modalities (Self/*Act* > Self/*Pas* visual ∩ Self/*Act* > Self/*Pas* tactile). For the tactile modality we additionally found enhanced activation in the left premotor cortex and

the right precuneus. Contrasting the passive against the active condition (*Pas* > *Act*) resulted in a significant cluster in the IPL for both visual and tactile trials (bottom row). A conjunction analysis across both modalities (Self/*Pas* > Self/*Act* visual ∩ Self/*Pas* > Self/*Act* tactile) identified significant activation in the angular gyrus (Fig. 4, lower row). Table 3 reports significant cluster peaks of the contrasts derived from the Self task.

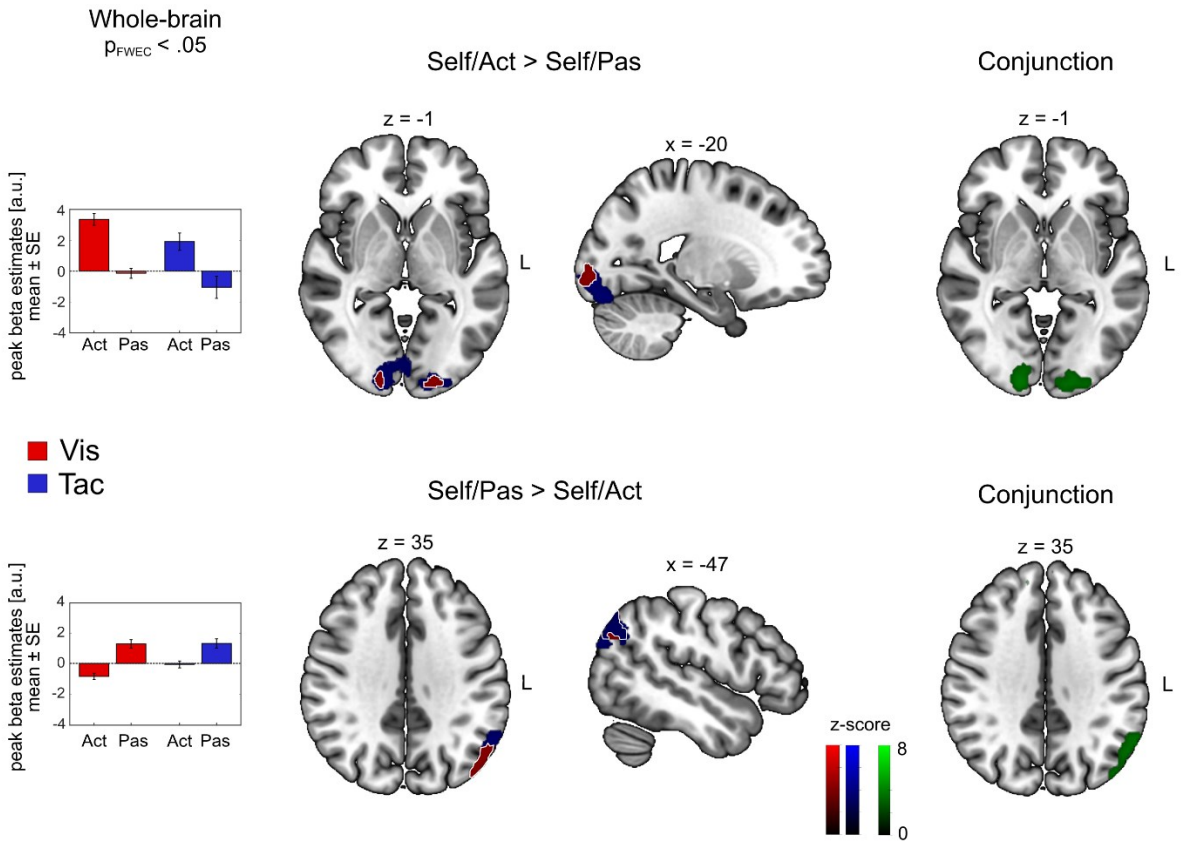

Figure 4. Modulatory effect of behavioral demand. Whole-brain results showing BOLD enhancement (upper row) and BOLD suppression (bottom row) during the travel of self-chosen distances compared to passively observing replayed distances for visual (red) and tactile (blue) trials. Commonly enhanced or suppressed regions across visual and tactile trials are demarcated by white lines. Bar graphs show mean beta estimates across subjects (±*SE*) for the corresponding peak voxel. Clusters derived from a conjunction analysis across both modalities are shown on the right (green). Coordinates are listed in MNI space. Initial search threshold was $p < .001$, only regions passing the $p_{FWE} < .05$ at the cluster level are shown.

Activation of visual cortices in tactile trials in both, the Repro and the Self task, might have occurred because subjects imagined visual stimuli to solve the path-integration task in purely tactile trials. We investigated this observation further by means of a connectivity analysis (see below, section 'Connectivity analysis').

We investigated potential differences in BOLD response between the active reproduction of distances (Repro/Act, *high* monitoring demand) and the active production of self-chosen distances (Self/Act, low monitoring demand) by contrasting trials of both tasks (Repro/*Act* > Self/*Act*). For both modalities, we found significant clusters in the anterior insular cortex (Fig. 5). Beta estimates derived from the cluster peaks suggest enhanced BOLD response during active reproduction and suppressed BOLD response during the travel of self-chosen distances for both sensory modalities, indicating a modulatory effect of behavioral demand. Enhanced activation induced by both modalities was found in different subdivisions of the anterior insular cortex (AIC). Further significant clusters for the tactile modality were located in the motor cortex (primary motor cortex and pre-supplementary motor area). Table 3 shows the coordinates of peak clusters. The reverse contrast (Self/*Act* > Repro/*Act*) did not result in any significant clusters. There was no overlap in brain regions relevant for enhancement within the Repro conditions and across task conditions (Repro/*Act* > Repro/*Pas* ∩ Repro/*Act* > Self/*Act*).

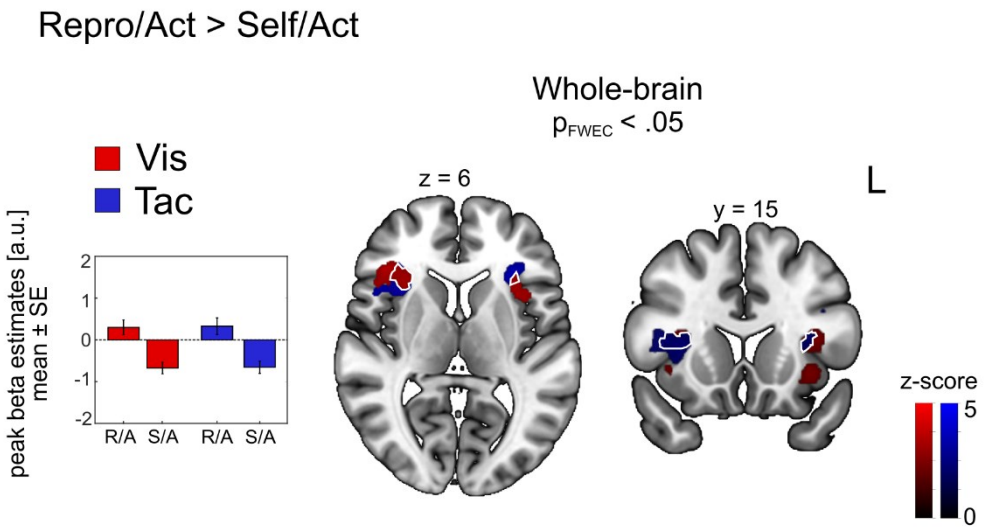

Figure 5. Comparison of BOLD contrast in Act trials between the Repro and the Self task. Whole-brain results show BOLD enhancement during the active reproduction compared to the production of self-chosen distances for visual (red) and tactile (blue) stimuli. Commonly enhanced regions across visual and tactile trials are demarcated by white lines. Bar graphs show mean beta estimates across subjects (±*SE*) for the corresponding peak voxel. Cluster-forming threshold was $p < 0.001$ uncorrected, with clusters significant at $p_{FWEc} < 0.05$ shown.

Both tasks have also been presented in a bimodal condition where visual and tactile stimuli presented congruent distances. The bimodal condition should have led to an increase in perceived vection by coupling visual and tactile self-motion cues. However, we have also analyzed bimodal trials with respect to our contrast of interests (Results shown in Supplementary Figure S1 and Supplementary Table S1). We also tested for multimodality effects (Bi > Sum(Vis,Tac)) in all contrasts of interest. However, none revealed significant activation. Thus, in our study, bimodal encoding appears to be a sum of both modalities. For the comparison between Act trials of both tasks ('Repro/*Act* > Self/*Act'* and vice versa) we did not find significant activation.

4.3.2.3. Connectivity Analysis

To further investigate the unexpected finding of activations in visual cortex during tactile trials in both the Repro and the Self task, we conducted a PPI analysis (i.e., Psychophysiological Interactions) using the CONN toolbox (https://web.conn-toolbox.org/). We performed a whole-brain seed-based functional connectivity analysis by using a seed region derived from contrasting all tactile with all visual trials irrespective of the task [*Tac > Vis*; Seed region: Right Parietal Operculum; [*x, y, z]* = -50, -34, 16]. On the first level, Eigenvariates extracted from the seed region created PPI regressors for all conditions of interest (Repro/*Act*, Repro/*Pas*, Self/*Act*, Self/*Pas* and the MC condition). Then we performed a whole-brain analysis to identify areas in which functional connectivity with our seed region was modulated by the type of task(-demand). Seed-based analysis results were subject to a family-wise error correction for multiple comparisons following the Gaussian Random field theory for the parametric test (Worsley et al., 1996). Figure 6 depicts the results of the connectivity analysis with corresponding beta values for the peak voxel for each effect of interest separately.

On the whole-brain level, a significant F-test identified that connectivity between the seed region (blue cluster) and the occipital pole (yellow cluster differed significantly between task conditions (Left: V1, V2; [*x, y, z*] = 46, -32, 20, $Z = 4.21$, $k_E = 212$, $p_{FWE}c < .05$). To identify task condition dependent differences, we performed post-hoc t-tests on beta estimates derived from single task conditions. Positive beta estimates suggest connectivity between the seed region (tactile processing area) and visual areas during the passive encoding (Repro/*Pas*) and passive observation of traveled distances (Self/*Pas*). Compared to passive trials, the active reproduction of distances revealed higher beta estimates. However, the motor conditions revealed highest beta estimates and Post-hoc t-tests showed that beta estimates between

Repro/*Act* and MC trials ($t(20) = -0.943$, $p = .357$) and between Self/*Act* and MC trials ($t(20) = 0.94$, $p = .358$) did not differ significantly.

To test for laterality, we have also entered the right frontal operculum as a seed region ([*x, y, z*] = 46, -32, 20) into a PPI analyses. The seed region was defined based on the most significant right hemispheric peak cluster derived from the *Tac > Vis* contrast. The right frontal operculum showed significant connectivity to the bilateral calcarine cortex (V1, [*x, y, z* = 10, -78, 0], $p_{FEW} < .05$).

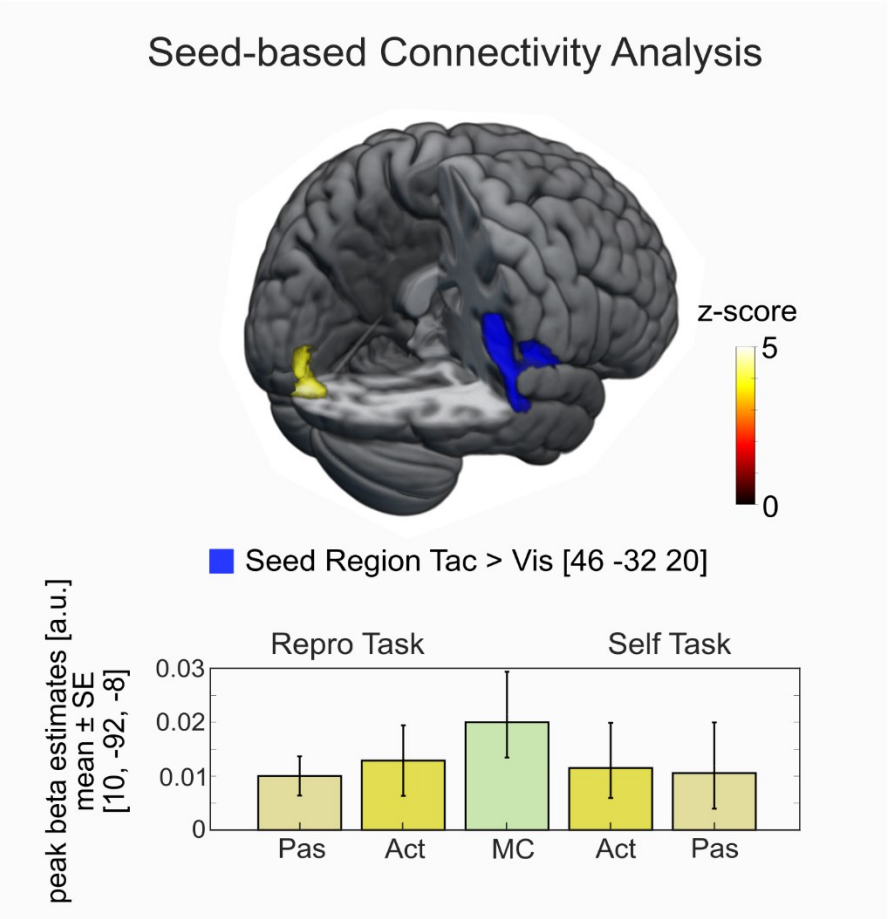

Figure 6. PPI whole-brain analysis depicting significant connectivity between the (tactile) seed region and visual areas as identified by a F-test. The tactile Seed region in the right Parietal Operculum (MNI= -50, -34, 16), derived from enhanced activation in all tactile compared to all visual trials irrespective of the task, showed significant connectivity with early sensory areas (Occipital Pole; MNI= 10, -92, -8) for both, Act and Pas trials in both tasks (Repro, Self). Threshold: $p_{FWE} < .05$. Bar graphs show mean beta estimates across subjects (±*SE*) for the corresponding peak voxel.

4.4. Discussion

We investigated the neural correlates of visual and tactile distance encoding (path integration) during (simulated) self-motion. We employed two types of path-integration tasks differing in behavioral demands during active distance re-/production. For both tasks and for both sensory modalities (visual, tactile) we found an enhancement (Act>Pas) in early visual areas and suppression (Pas>Act) in higher order areas of the inferior parietal lobule (IPL). Suppression in areas of the IPL suggests this area to be a comparator of predictions and incoming self-motion signals. Task demand (Act: Repro>Self) was related to enhanced BOLD response in the anterior insular cortex across modalities. We conclude that the effect of action on sensory processing is, first, supramodal and, second, more complex than previously assumed as it is dependent on task demand and the signal processing stage.

In the Repro task (high demand), subjects were presented with two different target distances that had to be reproduced. The accuracy of distance reproduction did not differ between the visual and the tactile modality. While the short target distance was replicated rather accurately, the longer target distance was often overestimated (i.e., subjects drove a longer distance than presented). Previous studies on the reproduction of traveled distance have shown accurate reproduction performance for self-motion stimuli from the visual (e.g. Frenz & Lappe, 2005) and auditory modality (e.g., Von Hopffgarten & Bremmer, 2011). Overestimation of travel distances might have occurred because our tasks required a comparison of the already traveled distance with the remaining distance until the target distance is reached (Lappe et al., 2007; Redlick et al., 2001). Overall, our results show that also tactile self-motion stimuli allow for the estimation of travel distance.

In line with our previous study (Krala et al., 2019), for the visual modality, we found BOLD enhancement in early visual cortical areas and BOLD suppression in higher-order areas located in the IPL for Active compared to Passive trials. For the successful reproduction of a previously observed target distance, it is necessary to first encode the target distance and to maintain it in the working memory to be able to recall it during reproduction. Hence, this task induces a high behavioral demand. BOLD enhancement in Repro/*Act* compared to Repro/*Pas* is in line with our hypothesis.

Surprisingly, we found a comparable pattern of BOLD responses in visual cortices for the tactile modality. Here, active reproduction yielded enhanced BOLD response not only in somatosensory cortical areas (SI and SII), but also in early visual cortex and suppressed BOLD

response in higher-order visual areas that largely matched the BOLD responses in the visual modality. Additionally, area V3A showed enhanced BOLD response during tactilely based active distance reproduction. Previous studies in humans (Tootell et al., 1997) and non-human primates (Nakhla et al., 2021) demonstrated neural selectivity for visual motion of area V3A (However, see also Orban et al., (2003)) who showed stronger motion sensitivity in human area V3A than monkey area V3A). A role for the processing of tactile motion so far has not been described. A conjunction analysis between contrasts of interest for visual and tactile stimulation emphasized the similarities of distance processing in the visual and the tactile modality by displaying V1 and V3a as joint regions of enhanced BOLD activation for Act compared to Pas trials and IPL as a common region for suppressed BOLD response. Our results might suggest a supramodal processing self-motion cues in V1, V3A and IPL during the Repro task. As an alternative, activation of areas V1 and V3A could also have resulted from imagery of the visual self-motion stimulus (Kovács et al., 2008; Mertz et al., 2000). Previous work has shown that visual imagery can activate similar (if not identical) regions as real visual self-motion stimuli (Kovács et al., 2008). More recent work has revealed layer specific differences between visual stimulation and imagery in early visual cortex (Iamshchinina et al., 2021). Yet, our approach did not allow for such fine grain detailed analysis. Hence, our observed BOLD activation might be also, at least in part, related to visual imagery. Likewise, action patterns are thought to be stored in memory in form of (movement) models (see e.g., Bartlett, 1932; Schmidt, 1975). Action imagery has also found to be represented in motoric memory (Annett, 1996). In that sense, neural activation in our study might be attributable to the imagination of inducing self-motion through one's own action. Along this line, studies by Rieger and colleagues demonstrated similar activation patterns for the imagination and execution of a specific action (Bartlett, 1932; Iamshchinina et al., 2021; Rieger & Massen, 2014, for a review see: Schmidt, 1975). In summary, neural activation in our study might be due to imagery of self-motion and/or its control in cotical regions also responding visual self-motion information. Future studies will be necessary to disentangle both phenomena. Hence, to better understand the observed activation of early visual cortex by tactile stimuli, we conducted a connectivity analysis with a seed region derived from contrasting all tactile vs. all visual trials to achieve somatosensory activation clusters exclusively induced by tactile stimuli. This seed region was located in the right Parietal Operculum which has been shown to play a major role in somatosensory processing (de Haan et al., 2020; Sirigu & Desmurget, 2021). For tactile

trials, at the whole-brain level, the Parietal Operculum showed positive connectivity with the left early visual cortex (V1, V2) across conditions. These results suggest that subjects might have used visual distance representations (reflected in visual cortex activation) to guide their responses to tactile self-motion stimuli.

In both modalities, higher-order areas located in the IPL exhibited BOLD suppression during the active reproduction of target distances. The IPL comprises the angular gyrus (AG), supramarginal gyrus (SMG), and the lateral intraparietal sulcus (lPS). The AG is thought, among others, to be involved in attention allocation towards task-relevant information (Singh-Curry & Husain, 2009; Studer et al., 2014) and retrieved memories (Cabeza et al., 2008). Human studies on path integration have described the AG to be involved in the encoding of heading stimuli (Indovina et al., 2016) and travel distance (Chrastil et al., 2015). Importantly, the AG has also been described to play a role in the encoding and recall of specific paths which is also in line with the specific task presented in the Active trials of our experiment (Boccia et al., 2016). Since we found suppressed BOLD response of the AG across both modalities, our findings suggest a supramodal involvement of the AG in the encoding of target distances. This is also supported by previous studies describing activation of the AG by visuo-tactile stimuli [e.g., (van Kemenade et al., 2017)]. The SMG has also been demonstrated to be engaged in the allocation of attention towards memory contents (Ciaramelli et al., 2008). These areas may initiate attentional control towards the stimulus (Arnold et al., 2014) and maintain the target distance in visual short-term memory (Bettencourt & Xu, 2015; Derbie & Dejenie, 2022).

Hippocampal and parahippocampal formation are involved in navigational tasks including path integration (see e.g., Ekstrom & Ranganath, 2018). Hence, activation of the hippocampus and/or hippocampal formation would have been plausible. Yet, we did not find such activation. We can only speculate why this was the case. First, our task involved a virtual scenery with a ground plane composed of random dots with a limited lifetime. Trials were short and no landmarks were available. Hence, it appears unclear if e.g., place cells were established in this short-lived experimental context. Second, our task was comparably easy, i.e., a single forward translation that had to be reproduced. Everyday navigational or homing tasks typically comprise translations and rotations, often with the task to return to the starting point, involving most likely grid cell activation, which might have been absent here. Overall, active and passive tasks were presented from an egocentric perspective. Other than allocentric encoding, found in the hippocampal and parahippocampal formation, egocentric encoding

is found in parietal cortex (Rolls, 2020). Overall, the task design (short trials, random dots with limited lifetime, no landmarks, forward translation, egocentric perspective) might have contributed to the lack of hippocampal activation.

The predictive coding framework states that neural processing succeeds to distinguish self-generated from externally induced motion signals by attenuating the responses to self-generated information. In that sense, bottom-up and top-down signals interact synergistically to ensure consistent predictions at different processing levels. Predictions are defined as top-down signals that can facilitate perception and enable appropriate reactions by employing information from prediction error signals i.e., discrepancies between top-down predictions and actual incoming bottom-up sensory evidence (Friston & Kiebel, 2009; Nichols et al., 2005), but also see (Teufel & Fletcher, 2020) who have shown that predictive information is also embedded in bottom-up processing).The fact that areas along the IPL showed suppressed BOLD activation in both modalities suggests a supramodal engagement of this region. This idea is also in line with previous findings indicating a common mechanism for processing of prediction errors in the auditory and visual modality (Krala et al., 2019; Straube et al., 2017; van Kemenade et al., 2017). Our study extends these findings by showing supramodal prediction processing in the IPL across the visual and tactile modality.

In the Self task, the production of self-chosen distances introduced lower behavioral demand compared to the Repro task since participants were free to travel without the need to memorize and recall a given target distance. The only requirement was to stay within a certain distance limit that participants had been previously trained to maintain. Here we found a comparable pattern to our above-described results. Comparable to the Repro task, a conjunction analysis between visual and tactile trials revealed enhancement in V1 and suppression in IPL as joint areas in the processing of visual and tactile self-displacement. Suppressed BOLD activity in the IPL suggests sensory attenuation of self-generated stimuli, reflecting conformity of predictions as stated by the predictive coding framework (e.g., Uhlmann et al., 2020). For both modalities, contrasting active trials with a higher behavioral demand (Repro task) with trials with a lower behavioral demanding (Self task) yielded enhanced activation in bilateral AIC, indicating a supramodal engagement of the insula in solving behaviorally demanding tasks. Hence, our findings complement previous studies that found modulation of visuo-auditory AIC activation by task demands (Bushara et al., 2001) and stimulus salience (Benoit et al., 2010).

The insula, a key region in the encoding of interoceptive signaling (Fermin et al., 2022) and agency (Arikan et al., 2019) has also been shown to play a major role in the experience of time (Vicario et al., 2020; Wittmann et al., 2010). In our study, the participant's task was to replicate the traveled distance, not travel duration. We took several measures to ensure that subjects re/-produced distances and not durations by introducing the task specifically as a distance re/-production task. We introduced the scenario of bike riding where airflow emerges against the forehead as a function of travel direction and speed. However, responses of subjects after the experiment regarding their strategies indicated that most subjects transformed encoded distances into rhythms or paces. Most answers included 'counting' during self-motion in a broader sense. This indicates that the specific encoding and production of distances with a specific length might have been solved also by judging the passage of time by engaging structures like the insula. However, task instruction focused participants on the travel distance and similar optic flow and tactile flow stimuli have been shown to provide sufficient information for distance encoding (Bremmer & Lappe, 1999; Churan et al., 2017). Furthermore, in a similar behavioral visual-auditory distance reproduction task (Von Hopffgarten & Bremmer, 2011), control experiments, which excluded solving the task by relying on temporal parameters, unequivocally showed that participants could solve the task by processing visual (and auditory) self-motion signals. Nevertheless, participants might still have relied, at least in part, on temporal information. Indeed, temporal processing is ubiquitous in everyday life and covers roughly twelve orders of magnitude. We can perceive differences in the order of microseconds when localizing sound (Blauert, 1996). At the same time, the circadian clock modulates visual processing (Dacey et al., 2005). Remarkable, the neural basis of the encoding of time in the range of hundreds of milliseconds to seconds if far from being understood (Finnerty et al., 2015). At the subcortical level, the basal ganglia and the cerebellum have been implicated in temporal processing, while at the level of the cortex a whole network of regions is involved, including visual cortex (Mauk & Buonomano, 2004; Merchant et al., 2013). So, while we suggest that the observed effects were related to self-motion processing (Von Hopffgarten & Bremmer, 2011), further studies are required that specifically aim to disentangle self-motion and temporal processing.

The insula has also been identified to play a role in vection (Kleinschmidt et al., 2002). In their study, Kleinschmidt and colleagues observed insular deactivation during perceived circular self-motion. Accordingly, in our study, when contrasting Repro/*Act* with Self/*Act* trials,

lower beta estimates for Self/*Act* trials indicated lower while positive beta values for Repro/*Act* trials indicated higher activation. This activation in Repro/*Act* trials would be in line with our hypothesized BOLD enhancement due to high behavioral demand in Repro/*Act* compared to Self/*Act* trials. Importantly, the insula showed enhanced activation for both, visual and tactile trials, suggesting a supramodal mechanism of distance encoding. However, given the nature of our task, also temporal aspects might have contributed to AIC activation.

In our task, bimodal trials have been introduced to couple visual and tactile vection perception and have been not of interest in this study. However, we also have analyzed the bimodal trials according to our contrasts of interest (Supplementary Figure 1). Our previous observations in the unimodal conditions also apply to the bimodal condition. More precisely, for both, the Repro and the Self task, Act relative to Pas trials showed BOLD enhancement of early visual cortices and suppression in higher order visual areas (Supplementary Table 1). In both tasks, visual areas are more strongly engaged into the task solving which is evident from enhanced BOLD response in visual cortices in bimodal trials, where tactile information is also present. This suggests that subject mainly relied on the visual information for solving both path-integration tasks. We also tested for multimodality effects in all contrasts of interest by investigating for an advantage of bimodal trials over the sum of both unimodal conditions. However, we did not find significant activation for any of the contrasts of interest. Thus, in our study, bimodal encoding appears to be a sum of both modalities.

To conclude, we have demonstrated that while self-motion signals resulted in enhanced BOLD responses in early sensory areas, this pattern was extended by insular activation if behavioral demand was high. In line with the predictive coding framework (Friston, 2005; Mumford, 1992), we found attenuated BOLD contrast in the IPL, reflecting conformity of predictions (i.e., less prediction errors) and information about traveled distance. Notably, tactile path-integration was accompanied by activation of visual areas, possibly due to visual imagery.

4.5. Methods

4.5.1. Participants

Twenty-three healthy, right-handed (Edinburgh Handedness Inventory, (Oldfield, 1971) subjects participated in the study (10 females; mean age 28 years; range 20 - 57 years, all normal or corrected-to-normal vision) after providing written informed consent. Exclusion

criteria included left-handedness, history of mental disorders, frequent alcohol or drug consumption or consumption on the day of the experiment. All subjects participated in one pretesting (behavioral pre-training) and one scanner session (on separate days). Participants received reimbursement (10€/h) after each session and were naive to the purpose of the study. Data from two participants were excluded from further analysis because of excessive head motion. In one subject, a single run out of four had to be excluded because of technical failure. All procedures used in this study were approved by the local ethics committee of the Faculty of Psychology at Philipps-University Marburg and conformed to the Declaration of Helsinki, except for pre-registration (World Medical Association; 2013).

4.5.2 Stimuli & Apparatus

Visual stimuli were programmed using MATLAB R2019a (The MathWorks, Natick, MA) and Psychtoolbox (Brainard, 1997). Stimuli were presented on a computer screen (LG 42 LM345, LG Electronics, Seoul, South Korea, refresh rate 60 Hz) using Octave (6.1). Participants viewed the screen via an angled mirror which covered a field of view of 21.7° (hor.) × 12.3° (vert.). Visual stimuli simulated straight-ahead self-motion across a ground plane of 2000 white random dots (luminance: 89 cd/m^2, on a dark background: <0.1 cd/m^2) with unlimited lifetime, simulating self-motion with a speed of appr. 16.2 m/s. During self-motion, ground plane dots increased continuously in size when getting (virtually) closer to the observer (diameter ranged from 0.46° to 1.15°).

Tactile flow was controlled by a data acquisition system (DAQ, USB-1208FS, Measurement Computing, Sicklerville, NJ) using filtered air from a compressor (Güde Airpower 480/10/90, Wolpertshausen, Germany) which was located in a separate control room during the experiment. The DAQ was run by the Data Acquisition Toolbox for MATLAB (https://de.mathworks.com/products/data-acquisition.html). A nozzle attached to the inner side of the headcoil, controlled by a magnetic valve (BMT, Type AMV-MNS-24-01 (24 VDC/2W), London U.K.) served to provide tactile flow across the subjects' forehead with a speed of 1.7 m/s (Fig 7A). A thin net for air diffusion in front of the air outlet created a natural feeling of airflow. Airflow leaving the compressor was filtered and down-regulated by a pressure relief device (D-MIN-10, LUX-Tools, Wermelskirchen, Germany) before arriving at the subject's forehead (1 bar). Visual and tactile stimuli were presented with a maximum offset of 30 ms. Correct timing of airflow was constantly checked using a flow meter (Serie FCH-m-PP-LC, BIO-TECH, Vilshofen,

Germany) during the whole experiment. In all conditions, participants were instructed to fixate a central target on the projection screen throughout each trial (target form specified in: Thaler et al. (Thaler et al., 2013); outer circle: 1,1° field of view, inner target: 0.28° field of view). Previous fMRI measurements with an identical visual stimulus under video-oculography (Krala et al., 2019) and our own pilot recordings with the tactile stimulation outside the scanner and using an eye tracker established that subjects can maintain fixation over the length of time chosen for the runs (see below).

In the active condition (see below), simulated self-motion was controlled using a commercially available gamepad that was customized to the MRI environment 8see Krala et al., 2019; Trees et al., 2014). By forward deflection of the left analog stick of the gamepad, subjects traveled straight ahead with a constant speed. The gamepad was placed on the subjects' upper thigh and fixed using Velcro tape. Subjects wore earplugs and MRI compatible noise-canceling headphones (Optime 1, MR confon GmbH, Magdeburg, Germany) during the whole experiment.

4.5.3. Procedure

For the experiment, we introduced the scenario of bike riding and explained the analogy of airstream perceived due to air resistance of the skin against air flow. In separate trials, straight-ahead self-motion was simulated visually or tactilely. Subjects were also presented with bimodal trials where visual and tactile stimuli were presented simultaneously. However, in this manuscript we focus on unimodal distance encoding and its neural correlates only.

In both sensory conditions, each subject completed two tasks: The Reproduction task (*Repro*, higher behavioral demand) and the Self task (*Self*, lower behavioral demand). Both tasks were presented in serial order over a total of 4 consecutive runs. Task order was counterbalanced across subjects. Figure 7B illustrates the structure of trials. In both tasks, each trial consisted of an active (*Act*) part and a passive (*Pas*) part. Trials of different sensory modalities were presented in pseudorandomized order. Intertrial interval and Interstimulus interval (ISI) were randomized, ranging from 2 to 5 secs.

In the *Repro* task, each trial started with the Pas part where subjects had to passively observe a traveled distance. Travel speed was always constant. To vary travel distances and to prevent subjects from learning a target distance, half of the trials involved a short distance (travel duration: 1 sec), while the other half involved a long distance (travel duration: 1.5 sec).

Each Pas part was followed by an Act part in which the subjects replicated the previously observed travel distance by joystick deflection. They were allowed to drive a distance with a maximal duration of 3 secs (twice the maximum duration in the passive displacement) until the trial ended. In the *Repro* task, we expected behavioral demand to be high given the task of continuous comparison of actively steered and passively displayed target distance. Figure 7C shows the time course of a visual (top row) and a tactile (buttom row) trial of the Repro task. After the experiment, subjects were asked to report their replication strategy, in case they had applied any.

In the *Self* task, subjects first traveled a self-chosen distance via joystick deflection in the Act part which was recorded and played back to them in the subsequent Pas part. Subjects drove at a constant speed and could travel a self-chosen distance. In a behavioral pretesting outside the scanner, subjects were trained to produce self-displacements within the range of the target distances from the Repro task. Subjects were allowed to drive a distance twice the target distance at maximum until the trial ended. When subjects overshot the target distance by more than twice the target distance, the trial ended and was counted as invalid. In the Self task, we expected behavioral demand to be lower compared to the Repro task, given that no specific predefined distance had to be reproduced.

To account for brain activation associated with the joystick deflection, we presented a motor control task (MC) after every third trial. In each MC trial, a green fixation cross was presented on the screen center with a red dot above. The red dot disappeared within a random interval between 1250 ms to 2250 ms. Participants were instructed to deflect the analog stick as long as the red dot was absent. After 1000 or 1500 ms, the red dot reappeared, and participants released the joystick.

Six trials per modality were presented on each run, resulting in a total of 18 trials per run plus 8 motor control trials. In total, subjects conducted 104 trials over 4 runs, with each run lasting approximately 11 min.

Before scanning, participants were invited to a behavioral training session outside the scanner to familiarize themselves with the equipment and the task. Each subject conducted two blocks (18 trials per block) of the Repro- and two blocks (18 trials per block) of the Self task, each *en bloc*, plus 8 motor control trials per block.

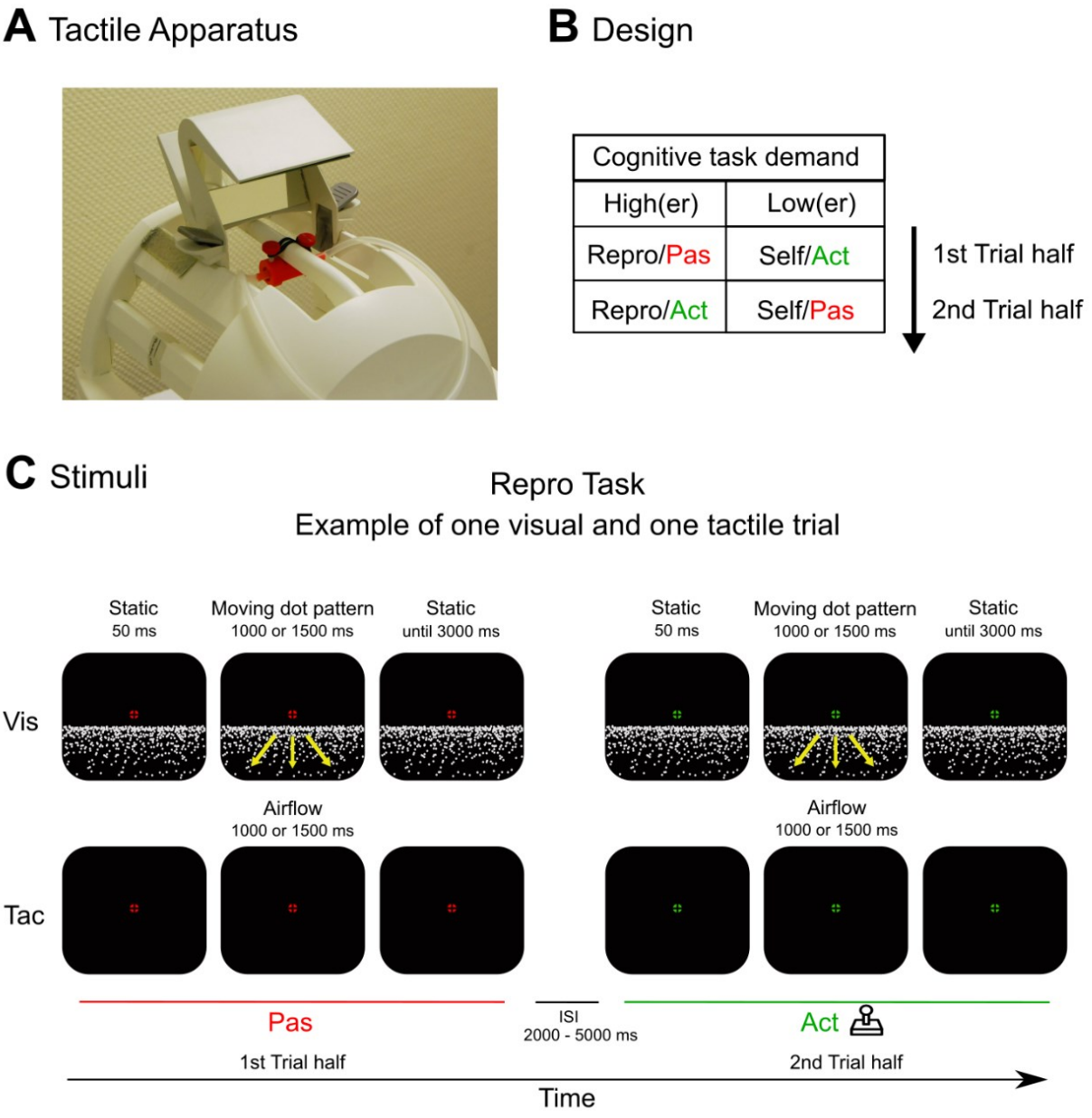

Figure 7*A*. Tactile airflow simulating forward self-motion was provided over the subjects' fore-head. A nozzle with a thin net in front of the air outlet was attached to the inner side of the head-coil and controlled by a magnetic valve. The air outlet was adjustable in tilt angle and in position on the head-coil towards the subjects' head to ensure similar airflow position and direction for each subject. Position of the air outlet was aligned regarding subject positioning in the head coil. ***B*. Experimental Design** Subjects conducted two tasks, each task in a block: The *Repro* task (higher behavioral demand) and the *Self* task (lower behavioral demand). In both tasks, a given trial always consisted of an active (Act) part and a passive (Pas) part. *Repro* task: Subjects passively observed a travel distance (Pas) which they actively reproduced (Act). *Self* task: Subjects traveled a self-chosen distance (Act) which was recorded and played back to them (Pas). ***C*. Example of a trial sequence of a Repro trial.** In the Pas part, a target distance was presented that had to be replicated in the Act part by joystick deflection. A jittered ISI of

2000ms – 5000ms was presented between Pas and Act parts. In Vis trials, subjects were presented with an optic flow pattern simulating forward self-motion across a ground plane. In Tac trials, subjects only saw the fixation cross and felt airflow simulating a self-motion.

4.5.4. fMRI acquisition parameters

Functional MRI data were acquired in a Siemens 3 Tesla MR Magnetom Trio Tim scanner (Siemens, Erlangen, Germany), using a 12-channel head coil. A gradient-echo EPI sequence was used (TR: 1450 ms, TE: 25 ms, flip angle: 70° (9), slice thickness: 4 (1) mm, gap: 15%, voxel size: 3 × 3 × 4.6 mm). For each run, 350 transversal functional images were acquired in descending order. Anatomical images were obtained using a T1-weighted MPRAGE sequence (TR: 1450 ms, TE: 2.26 ms, flip angle: 9°, slice thickness: 1 mm, gap: 50%, voxel size: 1 × 1 × 1.5 mm). To minimize head motion artifacts, participants' heads were stabilized with foam pads.

4.5.5. Behavioral Data Analysis

Analysis of behavioral data was performed using MATLAB 9.6 R2019a and SPSS (Version 23.0. Armonk, NY). For all analyses, a p-value of 0.05 or smaller determined statistical significance. For repeated measurements analyses of variance (ANOVA), Greenhouse-Geisser correction was applied to p values in case of violated sphericity assumption (Mauchly test $p < .05$). Effect sizes were reported by eta squared.

4.5.6. Functional Data Analysis

Preprocessing and statistical analyses of fMRI data were performed using Statistical Parametric Mapping Version 5 (SPM12, Wellcome Department of Imaging Neuroscience, University College London, U.K.) implemented in MATLAB R2019a. The AAL atlas (Tzourio-Mazoyer et al., 2002) and the SPM Anatomy Toolbox [(Eickhoff et al., 2005)] were used for anatomical reference of significant activations. Group-level images were visualized using MRIcroGL (Version 6, http://www.nitrc.org/projects/mricrogl/). Effect sizes were reported as mean beta estimates using the MarsBar toolbox for SPM12 (Release 0.45, http://marsbar.sourceforge.net; (Brett et al., 2002). Connectivity analysis was conducted using the CONN fMRI Connectivity Toolbox (http://web.mit.edu/swg/software.htm), implemented in SPM12.

4.5.7. Preprocessing

All scans were slice time-corrected (using the middle slice as the reference). For each run, functional images were realigned to the mean functional image of all runs. We excluded data of two participants from further analyses due to excessive head motion (translation > 3 mm). Each participant's anatomical scan was co-registered to their mean functional image and then segmented into tissue class images. The deformation field calculated in the segmentation step was used to spatially normalize the functional scans to a standard stereotaxic space based on the Montreal Neurological Institute (MNI), resampled to a voxel size of 2 mm × 2 mm × 2 mm. The volumes were then spatially smoothed using an isotropic 3D Gaussian smoothing kernel (8mm FWHM, (Friston et al., 1995). Functional data were analyzed using the general linear model (GLM). Low-frequency drifts were removed, employing a high-pass filter with a cutoff period of 128 s.

4.5.8. First-level analysis

Regressors of interest were modeled for each run of each participant. For Act trials, contrasts were defined to account for motor-related activity by considering BOLD responses of the Motor control (MC) task: Repro/*Act* > MC and Self/*Act* > MC. In the following, MC task corrected Act trials are referred to as 'Repro/*Act*' and 'Self/*Act*'. In the Repro task, trials of both target distances were combined into one regressor of interest. Eight conditions of interest were defined: Repro/*Pas*, Repro/*Act*, Self/*Pas*, Self/*Act*, for each of the two modalities (Vis, Tac). Six motion parameters as well as stimulus segments that had no motion information (static dot pattern) and periods between Active and Passive trials (ITI) were modeled as regressors of no interest. Trials in which participants overshot target distances by a factor of two were excluded (1.6 % of all trials).

4.5.9. Second-level analysis

First-level contrasts of interest were entered into second-level random-effects analysis using a flexible factorial design and containing subjects as a random factor. Using the above-mentioned conditions of interest, we examined BOLD responses associated with distance encoding in the perception of visually and tactilely simulated self-motion, respectively, with an F-test. We assessed modulations in BOLD responses as a function of different behavioral task

demand in the Repro and Self task by directional T-contrasts. For both, the Repro and the Self task, we examined BOLD enhancement effects for Act compared to Pas trials by using the T-contrasts [Repro/*Act* > Repro/*Pas*] and [Self/*Act* > Self/*Pas*]. BOLD suppression effects were assessed by the opposite contrasts [Repro/*Pas* > Repro/*Act*] and [Self/*Pas* > Self/*Act*]. All contrasts were calculated separately for the visual and the tactile modalities. To identify possible regions commonly activated during the presentation of visual and tactile modalities, we performed conjunction analyses (conjunction 0; minimum t statistic [(Nichols et al., 2005)]).

Corresponding contrasts were also investigated for the bimodal conditions and are in the Supplementary material. Bimodal data was also investigated for multimodality effects in all contrasts of interest by testing 'Bi > Sum(Vis,Tac)' (Response to combined stimulation must be greater than that from a summation of the both unimodal responses) for each contrast.

To investigate possible effects of behavioral demand, differences between Act trials of the Repro and the Self task were investigated by the contrasts [Repro/*Act* > Self/*Act*] and vice versa. We expected enhanced BOLD responses in sensory cortices for the Repro- as compared to the Self task given the higher attentional and working memory demands in the Repro task.

Group-level results were visualized by reporting normalized t-values (z-scores). F-tests were calculated at the whole brain level at $p < .05$ family-wise error (FWE) corrected at the cluster level. For directed T-tests informed by the F-tests, we applied the following criteria: BOLD responses at the whole-brain level were assessed for statistical significance using a threshold of $p_{FWEc} < .05$, corrected for multiple comparisons at the cluster level with an initial search threshold of $p < .001$ (Flandin & Friston, 2019; Friston et al., 1996).

Acknowledgments:

This study was funded by: Deutsche Forschungsgemeinschaft (DFG, German Research Foundation) – project number 222641018 – SFB/TRR 135 TP A2 (to FB) and A3 (to BS), the IRTG – The Brain in Action, and by the cluster project "The Adaptive Mind", funded by the Hessian Ministry for Science and the Arts (HMWK). BS is funded by the DFG (STR 1146/15-1 Grant Number 429442932, STR 1146/9-1/2, Grant Number 286893149).

4.6. Supplementary Information

In our study, bimodal trials simulated self-motion in the visual and tactile modality. In both modalities, stimuli presented congruent travel distance. We assessed all contrasts of interest that we have reported for the unimodal visual and unimodal tactile trials for the bimodal condition as well. Fig. S1 shows significant regions for all contrasts of interest and corresponding beta values. Significant clusters are listed in Table S1.

Supplementary Table S1

			Coordinates (peak of sign, cluster, MNI)				
Anatomical Label	Cluster extent (Anatomy toolbox)	Side	x	y	z	*z* value	k_E
Repro/Act > Repro/Pas							
Lingual	V1, V2, V3	L	-2	-82	16	6.48	2081
	V1, V2, V3	R	0	-80	6	6.28	409
Cingulate							
		R	22	-46	2	5.05	22
Lingual	V3A	R	28	-90	26	4.82	13
Repro/Pas > Repro/Act							
Occipital Mid	hOc4lp	L	-30	-96	-6	> 8	333
		R	30	-94	-6	7.45	324
Lateral Occipital Cortex	V5	L	-42	-66	4	6.22	120
		R	44	-62	6	5.91	676
Supramarginal Gyrus	IPL	L	-54	-50	44	5.16	57
Temporal Mid		L	-58	-54	2	4.83	10
Self/Act > Self/Pas							
Lingual	V1, V2, V3	L	-18	-94	-2	6.18	293
Self/Pas > Self/Act							
Parietal Inf	PGp	L	-44	-76	38	5.17	74

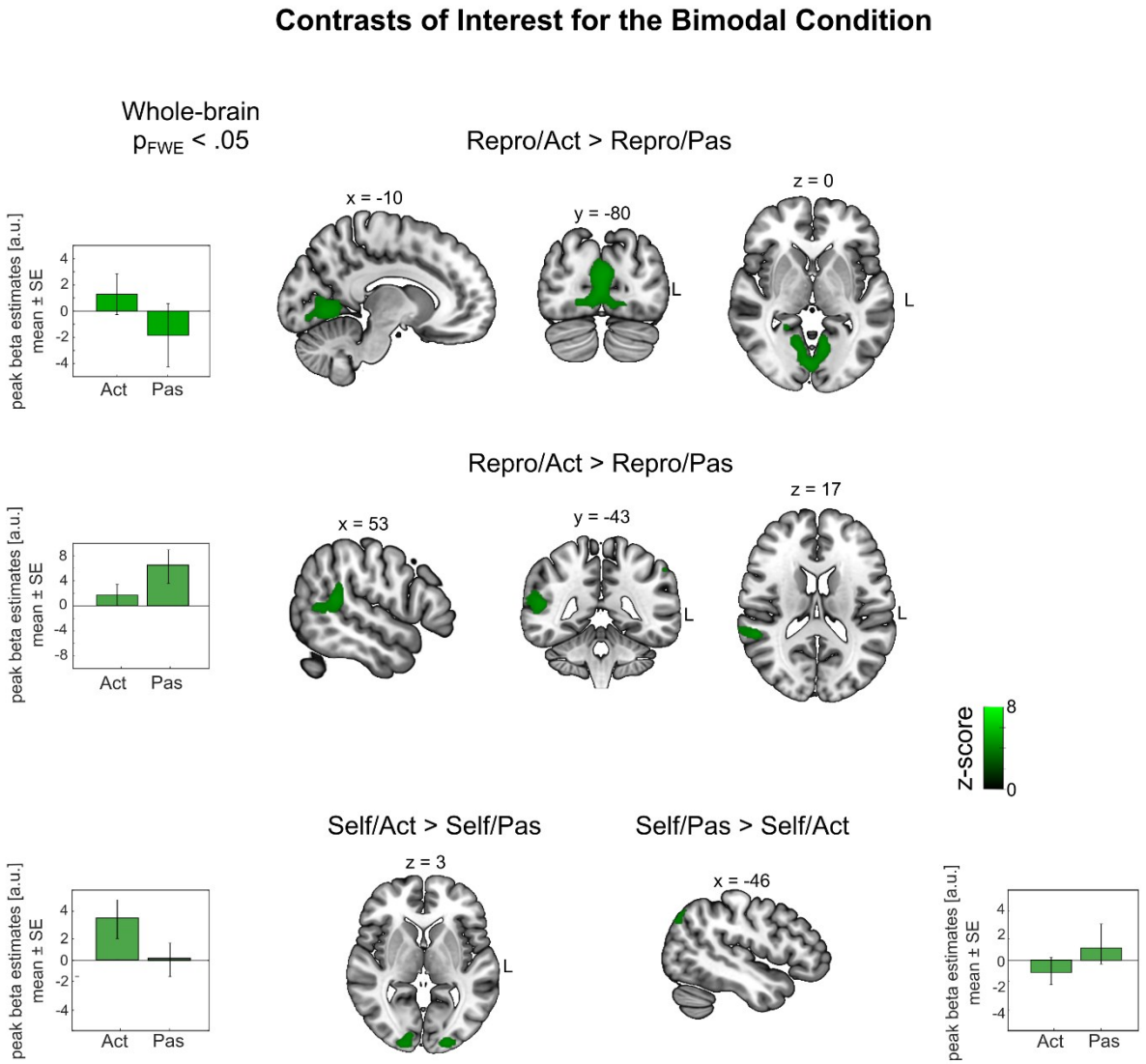

Figure S1. Modulatory effect of behavioral demand in the bimodal condition. Whole-brain results showing (i) BOLD enhancement and BOLD suppression for the Repro task (top and middle row) during the reproduction of target distances compared to passively encoding distances and (ii) for the Self task (bottom row) during the travel of self-chosen distances compared to passively observing replayed distances. Bar graphs show mean beta estimates across subjects (±*SE*) for the corresponding peak voxel. Coordinates are listed in MNI space. Cluster-forming threshold for all maps was p_{FWE} < .05.

5. DISCUSSION

In my thesis, I investigated key parameters of visual and tactile self-motion perception, namely heading and path integration. In two behavioral studies (study 1 & 2), I examined tactile heading perception and its interaction with visual heading perception. In one fMRI study (study 3), I investigated neural mechanisms of visuo-tactile based path integration. Up until now, self-motion has predominantly been studied in the visual and vestibular domains. My findings provide novel insights into tactile self-motion perception and its neural correlates.

In the following I will discuss heading perception from visual and tactile cues and biases in heading estimation. Furthermore, I will describe visuo-tactile integration in heading perception and discuss different integration models. Influences of eye- and head position on visuo-tactile heading perception and influence of reference frames on heading performance will be considered. In the context of path integration, neural correlates of visual and tactile distance encoding and its modulation by behavioral task demands will be discussed.

5.1. Heading perception

5.1.1 *Biases in heading perception*

I conducted two behavioral studies on visuo-tactile heading perception. In both studies, subjects indicated perceived heading from unimodal visual (optic flow) and unimodal tactile (tactile flow) heading stimuli in separate block of trials. In both studies, in bimodal trials, heading was simulated from the combination of stimuli from both modalities simulating either congruent or incongruent heading. In study 1, subjects indicated '*visually* perceived heading'. In study 2, subjects indicated 'perceived heading' (no focus on one modality). Across both studies and modalities, headings were perceived more towards straight-ahead than actually presented ('centripetal bias'). This 'centripetal bias' (also referred to as 'central bias') in heading perception has been described for the visual and vestibular modality by a large body of previous studies (e.g., Bremmer et al., 2017; Crane, 2012; D'Avossa & Kersten, 1996; Lich & Bremmer, 2014; Sun et al., 2020; Warren, 1995; Warren & Kurtz, 1992). One explanation that has been proposed is that the bias results from a strong prior in perceived heading towards straight-ahead as the most frequent heading direction during natural behavior (Sun et al., 2020). In contrast, other studies on visual and vestibular heading perception in humans have observed the opposite effect, i.e., a repulsion of perceived heading away from straight-ahead

('centrifugal bias'; Cuturi & MacNeilage, 2013). This apparent contradiction might arise from different experimental parameters employed between the studies. Studies investigating visual heading perception have applied optic flow stimuli differing in several parameters like motion coherence of the optic flow stimulus, duration of simulated self-motion or availability of depth information. Another heterogeneous factor between studies is the response format by which heading is indicated. In my studies, I have provided first evidence for comparable heading biases in the tactile modality.

For the visual modality, one important source for biases in perceived heading might lie in the perceived depth of the scene. In my studies, stimuli were presented on flat 2D screens simulating motion through a 3D environment which was achieved by introducing depth cues in the visual scene. Single dots the optic flow stimulus consisted of delivered depth information by expansion when travelling towards the observer (increasing in size when moving closer to the subject, i.e., the subjects moving forwards closer towards the FOE). Depth perception is obtained by disparity cues between both eyes. In humans, stereopsis supports reliable depth discriminations to a distance of up to 18 m between object and the observer (Allison et al., 2009). Disparity cues results from the two slightly different views of the world that humans and animals like owls, monkeys or cats receive from both eyes. Disparity in a visual scene can be simulated by viewing stimuli through head-mounted displays (Shibata, 2002) or 3D glasses (Glasses for displaying stereoscopic 3D images, see e.g. Wu et al., 2016). Overestimation of perceived heading (centrifugal bias) was mainly reported by studies using stereoscopic stimuli. For example, in the study by Cuturi & MacNeilage (2013) subjects viewed the optic flow stimuli through polarized glasses. In Crane (2012), disparity was rendered using red-green anaglyph glasses. Both studies reported overestimation of visually perceived heading. Conversely, optic flow stimuli in studies that found an underestimation of heading (centripetal bias) did not use stereoscopic stimulus presentation (Bremmer et al., 2017b; Li et al., 2002; Sun et al., 2020). This is also true for both my behavioral studies where subjects viewed stimuli without additional stereoscopical devices. However, De Winkel et al. (2015) also found a central bias of visually perceived heading although stimuli were presented stereoscopically using a dual-projector setup. Thus, depth cues as induced by horizontal disparity of the stimuli for the two eyes seem to be insufficient to explain these contradictory findings.

Another important factor that might influence the extent of biases in heading estimation is the motion coherence of the optic flow pattern. In my first behavioral study, motion

coherence was 100%, i.e., all dots forming the 2D plane simulated the same motion direction. In my second study, motion coherence was set to 50%, i.e., half of the dots simulated the same motion direction. This was done to match the accuracy of visual and tactile heading estimation. By manipulating optic flow motion coherence, accuracy under the visual condition was reduced to match tactile sensitivity. Increasing motion coherence (i.e., decreasing noise) is found to decrease the central bias (Sun et al., 2020). High noise in perceived heading increases the uncertainty of heading judgement and thus the reliance on strong priors, namely straight-ahead as the most common heading direction (MacKay, 2013). However, both my behavioral studies (study 1 & 2) were designed in order to create comparable central biases between modalities and across studies, thus suggesting that manipulated motion coherence in the second study is not the exclusive reason for the central bias found in that study.

One main difference between previously conducted heading studies that have found contradictory results regarding the nature of heading biases lies in the nature of the response format. For example, in Bremmer et al., (2017), subjects indicated perceived heading by choosing a number on a ruler covering the horizontal extent of the projection screen that appeared closest to their perceived heading direction with a random sequence of numbers. Thus, subjects reported heading direction from an egocentric perspective. In this study, visually perceived heading showed a bias towards straight-ahead ('centripetal bias'). In contrast, studies that found an overestimation of heading ('centrifugal bias') utilized an allocentric response format (e.g., from top view). For example, Cuturi & MacNeilage (2013) found heading to be biased away from straight-ahead. In their study, the transformation of self-motion perceived from an egocentric perspective into birds' eye view perspective during response might have enforced a transformation from an egocentric to an allocentric perspective. This assumption has been tested in a Bachelor thesis in our group (Beckert, 2022). In that study, subjects (N = 16) performed various heading judgment tasks. In one task, perceived heading was indicated from an optic flow stimulus presenting seven different heading directions across trials [±24°, ±16°, ±8°, 0° (= straight-ahead)]. The method of the subjects' report as another potential source of biases in heading estimation was investigated by varying the response format. In random trial order, self-motion stimuli were presented for two different durations (40 ms, 400 ms). The study compared two response formats varying in the subjects' perspective during the response: Response made from an egocentric point of view (i.e., "self-perspective"; egocentric frame of reference; following Bremmer et al., (2017), and from an allocentric point of

view (i.e., bird's eye view; allocentric reference frame, following Cuturi & MacNeilage, 2013). In half of the trials, subjects indicated perceived heading on a continuous line (egocentric response method). In the other half, subjects indicated perceived heading by placing an arrow on a 360° circle (allocentric response method). Results confirmed potential response biases due to shifts in response frames by showing a centripetal bias for the egocentric, and a centrifugal bias for the allocentric response method. Thus, the results support the theory of a coordinate transformation from an ego- to allocentric frame of reference as the source for a centrifugal bias while a centripetal bias is caused by a strong straight-ahead prior as the most reliable heading direction in the natural environment. Similar to the study by Beckert (2022), in my studies, perceived heading was indicated with the mouse cursor on a horizontal continuous line, spanning the “horizon”. Accordingly, in both studies, I found a central bias in heading estimation across both modalities.

Another difference between studies showing contradictory results is the presented self-motion duration. Studies that reported under- vs. overestimation of perceived heading differ in stimulus presentation duration. For example, studies reporting a central bias have all presented self-motion with a duration equal to or less than 500 ms (e.g., Bremmer et al., 2017: 40 ms; Sun et al., 2020: 500 ms; my behavioral studies: 500 ms). In comparison, studies that found overestimation of perceived heading presented stimuli with durations equal to or over 1000 ms (e.g., Cuturi & MacNeilage, 2013: 1000ms, Crane, 2012: 2000 ms). Notably, age has also been identified as a mediating factor. In Lich & Bremmer (2014), heading estimation of older subjects (mean age 67.8 years) showed a central bias for stimulus duration of 500 ms and 2000 ms while the performance of younger subjects (mean age 26.2 years) showed an undershoot only for stimulus duration of 500 ms, not 2000 ms). When information about temporal development of self-motion is missing, it is more difficult to generate a robust assumption about heading. This increases the uncertainty and the difficulty for heading estimation, favoring the emergence of a central bias (Layton & Fajen, 2016, see also Layton et al., 2012). In Beckert (2022), self-motion stimuli were presented for two different durations (40 ms vs. 400 ms). For both response methods, the results confirmed that the shorter stimulus duration led to an increased central bias in perceived heading. In my behavioral studies, self-motion stimuli in both modalities were presented for 500 ms. Accordingly, I have found heading estimation in both modalities to be compressed towards straight-ahead. These findings are in accordance with previous literature and support the hypothesis of stronger uncertainties for

shorter stimulus presentations, favoring biases based on straight-ahead priors in heading estimation (see Sun et al., 2020).

With my studies, I could further add to previous findings in the visual modality by providing first evidence for a central bias in tactile heading estimation. This suggests common heading encoding mechanism in both modalities. However, given the response format in my studies, it must be considered that tactile perceived heading was transformed into a visual coordinate system, by that, being subject to visual heading biases. This is also evident from findings of my second behavioral study where I investigated possible reference frames of heading perception in the visual and tactile domain. In that study, subjects indicated perceived heading in unimodal tactile, unimodal visual and bimodal trials in different blocks of trials with varying eye- and head position. Results indicated an effect of eye position on tactilely perceived heading.

5.1.2. *Reference frames*

Previous literature has reported different frames of reference in the encoding of stimuli from different sensory modalities. For example, for the encoding of visual stimuli, neurophysiological studies on macaque monkeys have proposed an eye-centered (retina-centered) frame of reference (Chen et al., 2013, 2014) or a continuum from eye to head coordinates (Duhamel et al., 1997) and a head-centered frame of reference of somatosensory encoding of facial stimuli (Avillac et al., 2005, 2007; Duhamel et al., 1997). In my study 2, in unimodal visual and bimodal trials, neither eye- nor head-position had an influence on perceived heading. Surprisingly, I found that (unimodal) tactile heading perception was biased by eyes-, and not by head position. A shift of eye position to the left (/right) shifted tactilely perceived heading up to 25% to the left (/right). Previous studies in humans hint towards an influence of eye-position on the perceived location of touch on the skin, suggesting that tactile reference frames are influenced by how attention is allocated during stimulus encoding and response localization (Harrar & Harris, 2010; Pritchett & Harris, 2011).

Extensive literature is conducted on the question of which reference frames (eye-centered, head-centered, body-part-centered) are used for specific tasks and how reference frames from different sensory modalities are integrated to form a unified percept. However, interpretation of the available findings is complicated by three main points: 1) The species: Recent literature reports behavioral results from humans (e.g., Moraresku & Vlcek, 2020) and

behavioral and neurophysiological studies on non-human primates; mainly macaque monkeys (e.g., Sasaki et al., 2020). 2) The type of tactile stimuli applied (Tactile flow; e.g., Feng & Lindeman, 2016; vs. vibrotactile stimuli, Harris et al., 2017). 3) The body region tactilely stimulated in the respective species. In humans, somatosensory reference frames have been studied in contexts other than self-motion. In accordance with neurophysiological studies on macaque monkeys, a study using vibrotactile stimuli towards the torso showed perceived touch location to be influenced by head-position (Ho & Spence, 2007). On the other hand, there are studies on human observers that have demonstrated that tactile perception on the limbs is indeed influenced by eye-position (e.g., Harrar & Harris, 2009). In my studies, perceived touch location had to be transformed into a visual coordinate for response. Thus, tactile location was forced into retina-centered coordinates (Harrar & Harris, 2010; Pritchett & Harris, 2011). There is also evidence for action-dependent transformation of tactile location into retina-centered coordinates (Harrar & Harris, 2010). Harris and colleagues (Harrar & Harris, 2009; Pritchett & Harris, 2011) employed verbal response formats that do not require transformation between different sensory reference frames. Hence, eye-position effects in my study were likely to arise by the response format.

5.1.3. *Visuo-tactile integration*

The fact that sensory information is arising from several modalities poses different challenges to the brain to form one coherent percept. Behavioral and neurophysiological studies point to multiple reference frames that are integrated across sensory modalities and weighted according to context (Chen et al., 2018; Sasaki et al., 2020) and attentional allocation (Chen et al., 2014).

I have investigated visuo-tactile interaction in the perception of heading in two behavioral studies. In both studies, bimodal trials presented either congruent headings or with an offset between heading stimuli of both modalities. In study 1, tactile flow was introduced as behaviorally irrelevant by asking subjects to indicate '*visually* perceived heading' in bimodal trials. In study 2, subjects indicated 'perceived heading' in bimodal trials, without a focus on one specific modality. In both studies, visual and tactile stimuli were not integrated in an optimal Bayesian fashion. The Bayesian framework defines how information from two sources is combined optimally. One prediction is that for stimulus integration, sources of information are weighted according to their variance (i.e., reliability) (Alais & Burr, 2019). The quotient is

characterized by smaller variance compared to both input sources alone (for reviews see Deneve & Pouget, 2004; French & DeAngelis, 2020; more specifically for a review in the context of self-motion perception, see Fetsch et al., 2010). In the context of heading perception, several recent studies have shown humans and non-human primates to behave as optimal observers in a Bayesian sense. However, all these studies were dedicated to visual-vestibular stimulus integration (human: Butler et al., 2015; Ramkhalawansingh et al., 2018; Saunders, 2014, monkeys: Angelaki et al., 2011; Gu et al., 2008). For tactile flow, one study by Churan et al. (2017) provided evidence for near optimal integration of visual optic flow and tactile flow for distance replication in a path integration task. Up until now, there had been no study investigating visuo-tactile heading perception. Thus, my studies provide new insights into visuo-tactile interaction in the perception of heading.

Aside from optimal integration, a large amount of research has described also non-optimal stimulus integration for visual-vestibular heading (human: Butler et al., 2010; De Winkel et al., 2010; Rodriguez & Crane, 2019; monkeys: Fetsch et al., 2009). In its simplest form, the Bayesian framework assumes a shared environmental source for incoming sensory signals, by this assuming integration of incoming information as the suitable processing operation. However, in the natural world, incoming sensory information can emerge from different sources and should not always be integrated. Several models take this into account by considering two separate sources (e.g., Bresciani et al., 2006; Shams et al., 2005). In study 1 and 2, visual and tactile heading stimuli might have been not integrated because participants quickly identified that both stimuli do not arise from the same source. This was the case for trials presenting congruent as well as incongruent visuo-tactile headings. Both, congruent and incongruent trials have been presented in randomized order over blocks, thus, revealing large offsets between visual and tactile heading stimuli already from the beginning of the bimodal blocks. Additionally, in study 1, this assumption was reinforced by the instruction that tactile flow was to be ignored. Notably, although tactile flow in that study was behaviorally irrelevant, it still influenced visually perceived heading, suggesting that subjects took tactile stimuli into account when estimating perceived heading.

During natural self-motion, the two most informative sources are the visual and the vestibular modality. Although encoding of incoming information on the retina is affected by constant eye-movements, visual and vestibular cues are most likely to coincide and are thus most likely integrated. This is also evident from studies that report optimal integration despite

spatial offsets between visual and vestibular headings (Butler et al., 2010; Fetsch et al., 2009). In my studies, subjects passively perceived simulated self-motion while sitting in a stationary environment. In the natural environment, tactile flow emerges from the observers' motion trough space but also from further, external sources (e.g., from object motion or from wind). For instance, environmental wind is prone to constantly changing weather conditions and can quickly change directions. All these stimuli add noise to the tactile flow perceived from self-motion through space. The integration – as well as segregation – of incoming sensory stimuli is important for the organism to ensure adequate interaction with the environment. This is also apparent from the previously described scenario: Tactile flow generated by self-motion should be considered for guidance while, at the same time, wind from external influences should be identified as such and factored out. Over the past decades, studies have increasingly been devoted to the question of how multisensory signals interact on the neural level to form one coherent percept. Several neurophysiology, imaging and electrophysiological studies on various species have addressed this question.

5.1.3.1. Neural correlates of visuo-tactile heading integration

In my studies (study 1 & 2) I could show that tactile flow had a small but significant influence on perceived heading in both cases, when it was behaviorally irrelevant (study 1) as well as behaviorally relevant (study 2). For multisensory integration to occur, spatial and temporal proximity of stimuli from different modalities have been identified as key features (Meredith & Stein, 1986). This is based on neurophysiological findings that identified neurons with overlapping receptive fields for different modalities. Several areas in the human and the non-human primates' brain have been identified as candidate areas for the integration of multisensory information based on their neuron's response properties.

In the context of self-motion, neurons in area VIP show properties that make them well suited for the encoding of multisensory stimuli. Area VIP neurons respond to stimulation from the visual (Bremmer et al., 2002a; Duhamel et al., 1998), tactile (Avillac et al., 2005, 2007; Duhamel et al., 1998), auditory (Bremmer et al., 2001; Schlack et al., 2005) and vestibular (Bremmer et al., 2002b; Chen et al., 2011; Schlack et al., 2002) modality. In humans, imaging studies have shown spatially overlapping representations for visual, auditory and tactile stimuli (Bremmer et al., 2001; Sereno & Huang, 2006) and for visual and vestibular stimuli (Aedo-Jury et al., 2020) in area hVIP. On a behavioral level, joint processing might be reflected in

optimal stimulus integration as stated by the Bayesian theorem. Although this was not the case in my studies, we still found interaction between the modalities. In study 1, visually perceived heading was influenced by behaviorally irrelevant tactile flow for offsets up to 30° between visual and tactile heading. Congruent bimodal stimulation is more likely to elicit a neurons' response, however, a small populations of area VIP neurons have been found to encode visual and tactile incongruent stimulation (Avillac et al., 2005; encoding of incongruent stimuli has been also described for neurons in other sensory areas; Kim et al., 2022; Nadler et al., 2013; Sasaki et al., 2017, 2019). Such neurons might play a role in the encoding of spatial conflicts between stimuli from different modalities. Differentiating between spatially and temporally interrelated cues might support the decision about whether stimuli emerge from the same source, providing a neural basis for casual inference (also see Kim et al., 2022). In the natural environment, features that appear in spatial proximity tend to arise from the same source and to be linked perceptually. Contrarily, spatially separated features tend to arise from different sources, making perceptual integration unlikely to appear (Avillac et al., 2007; Kubovy et al., 1998). Thus, in my study, the interaction of spatially incongruent visual and tactile headings with an offset of up to 30° might underlie a neural process to identify relation between stimuli according to joint origins. In the natural world, this might support that self-motion related signals can be differentiated from external noise (e.g., wind) to ensure that the organism does not get distracted by external stimuli. Signaling of incongruent stimuli might also serve to differentiate object from self-motion (see e.g., for monkey area MT neurons, Kim et al., 2022). For visual and vestibular perception, behavioral studies on human observers have reported integration of heading stimuli with large spatial offsets which allowed for optimal multisensory integration. Natural locomotion trough space is presumably mainly driven by visual and vestibular cues, which enhances visual-vestibular integration while tactile cues are prone to external events and are a less reliable cue for the estimation of self-motion parameters. Accordingly, bimodal visuo-tactile neurons of area VIP have been found to respond best to tactile stimuli in spatial proximity to visual stimuli while other neurons responded best to stimuli located at a greater distance (Colby et al., 1993). These findings suggest a role of area VIP in the encoding of peripersonal space which is defined as the space directly surrounding the observer (Bremmer et al., 2013; for a review see Cléry et al., 2015). Imaging studies on non-human primates provided evidence for the involvement of area VIP neurons in the encoding of visuo-tactile stimuli near the face (Cléry et al., 2017; Guipponi et al., 2015). For

human observers, a recent fMRI study also suggests area hVIP plays a significant role in the encoding of peripersonal space (Field et al., 2020).

5.2. Path integration

Path integration is a fundamental cognitive ability that has been demonstrated in many species. As an example, this process allows the organism to return to their home base on a direct path by constantly integrating navigational information from an outbound movement about travel speed, travel distance and changes in heading. Traveled distance can be accurately estimated or reproduced based on optic flow information from the visual modality only (Alefantis et al., 2022; Bremmer & Lappe, 1999; Churan et al., 2017; Frenz et al., 2007; Von Hopffgarten & Bremmer, 2011). In the tactile modality, path integration is mostly investigated by means of navigational tasks where animals or humans must return to a starting point (e.g. Chrastil et al., 2019; Harrison & Davis, 2023; Stangl et al., 2020). In the context of distance reproduction, tactile path integration has received only little attention. One previous study by Churan et al., (2017) investigated tactile flow for distance perception. Participants replicated traveled distances perceived from air flow provided by fans of hair dryers without heating system. In that study, congruent visual and tactile flow improved the precision of the subjects' reproduction performance. Neural correlates of visual path integration have been extensively investigated by neurophysiology studies in rodents and non-human primates as well as by fMRI in human observers. The aim of my study 3 was to investigate neural correlates of tactile path integration and to set it in relation to visual path integration by means of a distance reproduction task.

5.2.1 *Neural correlates of path integration*

In this study, participants conducted two different path integration tasks varying in behavioral task demands. Self-motion was simulated in the tactile modality by air flow towards the subjects' foreheads and in the visual modality by optic flow simulating translation over a 2D ground plane. To examine modality specific BOLD response to distance encoding, I have first investigated BOLD responses elicited by self-motion stimuli irrespective of task (Influence of task will be discussed in later section 7.7.3). For visual path integration, I have found BOLD responses of areas in line with previous imaging studies. Areas that contributed to

distance encoding were early visual cortices, such as V1 – V3 as well as motion specific areas like hMT and higher order cortices, notably area hVIP. For tactile self-motion encoding, early somatosensory areas like SI and higher order somatosensory areas such as SII and the Insula encoded path integration. One very recent study applying tactile flow towards the observers' face has reported similar findings (Nazarian et al., 2022). On a cellular level, SI and SII neurons have been reported to respond to motion-specific stimulus properties such as speed and direction of motion (SI: DiCarlo & Johnson, 2000; Pei et al., 2010; Ruiz et al., 1995; SII: Fitzgerald et al., 2006). In sum, the activation of early sensory specific cortices for visual and tactile self-motion stimuli, respectively, found in my study is in line with previous studies.

Both sensory systems differ in their responsiveness to different categories of stimuli. In the skin, mechanoreceptors respond to touch and stretching. In the eye, photoreceptors respond to light meeting the retina. However, in both, information about motion is conveyed by a spatiotemporal pattern of activation across sensory receptors. The brain regions encoding these signals have been found to employ comparable processing strategies. For example, early sensory areas devoted to vision and touch both show a topographic organization of receptive fields, retinotopy and somatotopy, respectively (Vision: e.g., Wandell et al., 2007; Tactile: e.g., Del Gratta et al., 2000). Furthermore, both cortices contain motion-sensitive neurons that represent information about motion direction (In primates; Visual: Albright, 1984; Hubel & Wiesel, 1968, Tactile: Pei & Bensmaia, 2014; see also: Pack & Bensmaia, 2015) and motion speed (Visual: for the macaque brain reviewed by Bradley & Goyal, 2008; see also Perrone & Thiele (2001) for monkey area MT, Tactile in humans and monkeys: Franzén & Lindblom, 1976;). Besides BOLD responses in sensory specific cortices, self-motion stimuli of both modalities elicited BOLD responses in early striate and extrastriate visual areas. For example, area V3A showed enhanced BOLD response across visual and tactile self-motion stimuli, indicating joint processing of self-motion signals in these areas across stimulus modalities. Previous imaging studies in human observers (Di Marco et al., 2021; Orban et al., 2003; Sunaert et al., 2000; Tootell et al., 1997) have described area V3A as a motion-sensitive visual region that encodes forwards translation (Di Marco et al., 2021; Huang et al., 2015). With my data I could demonstrate that area V3A is also engaged in the encoding of non-visual translational self-motion information. This might suggest crosstalk between sensory cortices during task solving of the path-integration task. I further examined this assumption by means of a connectivity analysis for a previously identified somatosensory cluster (compromising solely

somatosensory self-motion encoding) during task solving. I found for the tactile modality that the task of distance reproduction was accompanied by activation of visual areas. Active distance travelling compared to the passive observation of travel distances in the tactile modality engaged early visual cortices. Visual areas involved in tactile distance encoding were early visual areas, i.e., striate and early extrastriate cortex. This activation might be due to visual imagery of translation in purely tactile trials. This strongly suggests an interaction between visual and tactile sensory cortices in the encoding of self-motion signals. A similar encoding of tactile motion stimuli in visual areas has been shown before in human fMRI studies. For example, vibrotactile stimulation towards different parts of the body has been found to elicit BOLD responses in area MST (e.g., Beauchamp et al., 2007, 2009). For haptic shape recognition, Amedi et al., (2001) identified brain activity in the lateral occipital cortex. Along this line, the findings of my fMRI study add to the notion of multisensory processing in respective sensory-specific cortices (Driver & Noesselt, 2008; Sathian et al., 1997) by providing evidence for supramodal encoding of self-motion stimuli in visual cortices. Imagery (see Dunbar, 2004) might be one factor causing the engagement of visual areas. In the natural world, distance is practically not encoded over somatosensory information alone. Thus, in this specific task, tactile information encoding might have been supported by parallel imagination of traveled distance in the visual domain. This is also evident from the connectivity analysis showing significant functional coupling between the frontal operculum as tactile area and early visual areas during tactile distance encoding. Fitting with this, BOLD activation of visual cortices has been found in imaging studies on tactile shape perception (Lacey et al., 2010, 2011) and tactile discrimination (Sathian & Zangaladze, 2002).

Besides BOLD responses in sensory specific cortices, self-motion stimuli of both modalities elicited suppressed BOLD response in higher-order associative areas of the IPL, indicating joint processing across stimulus modalities. This is in line with previous imaging studies that have shown joint processing of visual and tactile stimuli as a function of overlapping receptive fields in area hVIP (Sereno & Huang, 2006). With this, my findings add to the existing literature by showing visuo-tactile self-motion encoding in area hVIP in the context for distance encoding.

5.2.1.1. Cognitive maps

Path integration is a navigation mechanism that involves maintaining the distance that an observer has traveled to estimate the current position in the environment. Another important navigation mechanism is 'cognitive mapping' (Tolman, 1948). Cognitive mapping represents a collection of path integration systems and describes how complex spatial information about the environment is stored over the long-term. Cognitive maps store spatial knowledge about relations between landmarks in the environment (Ericson & Warren, 2020), temporal associations between stimuli (Poucet, 1993) and other (also non-spatial) features of the environment (for a review see: Ekstrom & Ranganath, 2018). This allows the organism to infer general conclusions about the environment, by this allowing the system to efficiently adapt and react to new surroundings. It is also possible to navigate based completely on environmental landmarks, without the involvement of path integration (Gallistel, 1990). The first evidence for neural correlates of cognitive mapping was provided by neurophysiological studies in rats by O'Keefe and colleagues (O'Keefe et al., 1971; O'Keefe, 1976; O'Keefe & Nadel, 1979). A large body of neurophysiological studies in rodents described several groups of cells in cortical and subcortical structures engaged in the encoding of different navigational parameters (e.g., grid cells in the hippocampus (Wang et al., 2020), head directions cells in the thalamus (Shinder & Taube, 2019) and different cell populations in the medial and lateral orbitofrontal cortex (Bradfield & Hart, 2020). In the context of 'cognitive mapping', one well-studied candidate area is the hippocampus (for a review see: Zhu et al., 2023). Strong evidence for the role of hippocampal grid cells in navigation is provided by neurophysiological studies in rodents (Nielson et al., 2015) and non-human primates (Mao, 2023). A large body of studies using fMRI has also provided evidence for cognitive mapping in the human hippocampus (e.g. Garvert et al., 2021).

In my fMRI study, I was also expecting to find hippocampal activity due to the nature of the path integration task. However, similarly to the preceding study on path integration from our working group (Krala et al., 2019), I was not able to show significant hippocampal activation in any of the path-integration tasks. This might be due to the design of the paradigm. Firstly, the statistical power might have been too low to show slight activations of the hippocampal formation. Secondly, the visual and tactile stimuli did not provide spatial landmarks which would have allowed the participants to build a rich and unique representation of the presented environment. The artificial environment was composed of a ground plane

consisting of random dots, presented on a flat 2D screen. The simulated self-motion consisted of one simple straight-ahead translation. The construction and storage of spatial information in a long-term cognitive map was not necessary to solve the task at hand. Thus, in my study, the hippocampus was not necessarily engaged in the task solving process.

Importantly, in my task, self-motion through the artificial space was presented in an egocentric perspective. However, the hippocampal formation has been shown to encode a world-centered (allocentric) map of the surrounding environment (Bottini & Doeller, 2020; Nau et al., 2018). Conversely, recent studies have identified the parietal cortex to play a significant role in the encoding of egocentric spatial information, which is consistent with my findings of significant activation of the IPL in both path-integration tasks (Alexander et al., 2020; Rolls, 2020). The paradigm and stimulus design in my study might be the reason for absent significant hippocampus activation.

5.2.2. *Distance vs. duration encoding*

During locomotion, time and distance are proportional given a fixed traveling velocity. In study 3, subjects were specifically instructed to re-/produce self-motion *distances*. However, since traveling velocity was kept constant, the observed BOLD response patterns might also have reflected an involvement of duration encoding. Whether both dimensions are encoded in a shared or separate manner has been the subject of many investigations. Recent studies have employed different paradigms to disentangle the relationship between perceived spatial distance and duration (e.g., Cai & Connell, 2015, 2016; Von Hopffgarten & Bremmer, 2011).

Generally, spatial and temporal representations have been found to share common neural circuits (Bonato et al., 2012; Cai & Connell, 2015, 2016; Lambrechts et al., 2013; Riemer et al., 2022). On a behavioral level, representation of duration and space have been found to interfere with each other such that the temporal domain is affected by the spatial domain (e.g., Riemer et al., 2018, 2022). In these studies, information about motion speed was available, providing a link between both dimensions. Conversely, a proportional relationship between the temporal and spatial domains is observed when consistent speed information is available (Cai & Connell, 2015; Homma & Ashida, 2015). In my study, self-motion was presented with constant velocity. This led to a symmetric link between perceived self-motion distance and duration, making counting a likely applied task-solving strategy. Israël et al. (2013)

placed participants blindfolded on a motion platform and displaced them for certain distances that had to be identified. They found that subjects were counting to evaluate their displacement distance. However, this strategy was interrupted when varying velocity profiles were introduced, suggesting that counting was only a reliable strategy for constant velocity profiles. This is also evident from a study by Von Hopffgarten & Bremmer (2011) who were able to show that distance reproduction from varying velocity profiles was not based on counting, but on the integration of distance- and speed features of simulated self-motion.

During navigation through a natural environment, observers heavily rely on environmental cues for position estimation (e.g., Sjolund et al., 2018). In my study, self-motion was simulated over a dotted 2D ground that consisted of white random dots, thus no external spatial cues were available. In Israël et al. (2013), participants were moved while blindfolded. In both studies, the absence of landmarks (or visual information at all) might have increased the reliance on counting as a strategy to estimate elapsed time for traveled distance. Further experimental approaches for uncoupling travel distance and duration are necessary to disentangle neural correlates of different self-motion parameters (for example, see Kautzky & Thurley, 2016).

5.2.3. *Influence of cognitive demand*

In my imaging study (study 3), I found that neural correlates of visual and tactile path integration are influenced by the task at hand. Enhancement and suppression of self-motion related BOLD signals varied as a function of predictability and cognitive demands. Cognitive demand was manipulated by introducing two different tasks. Participants either had to reproduce a previously observed distance (Repro task, higher demand), or they had to drive a freely chosen distance (Self task, lower demand). In the Repro task, each trial started with a passive part, where subjects were shown the target distance (encoding) which was followed by the active part of reproduction. In the Self task, subjects first actively traveled a distance which was recorded and played back to them in the following passive part. The reproduction of travel distance is characterized by higher cognitive task demand because subjects had to engage attentional and working memory resources to match their reproduction to the target distance. In the production task, cognitive demand was lower given that subjects produced a self-chosen distance. However, subjects had to stay in a predefined distance limit when producing self-chosen distances which had been trained in a behavioral pretesting. Thus, the production

of self-chosen distances was still characterized by cognitive demands, i.e., by being required to stay in the preset distance limit, however, task demands where lower compared to the Repro task where specific target distances had to be replicated. This difference in cognitive demands was accompanied by BOLD enhancement of the anterior insular cortex (AIC) for active re-production as compared to active production of distances in both modalities. Enhanced AIC activation during reproduction (compared to production) might represent higher alertness and attentional allocation towards the target distance and the actually traveled distance (Albanese et al., 2009; Sterzer & Kleinschmidt, 2010). The AIC has been described as part of a 'salience network' which identifies the most salient stimuli by employment of attentional and working memory resources to generate adequate behavioral responses. In that sense, the AIC indicates the processing of salient events by employing attentional and memory resources towards important stimuli, thereby facilitating their processing (for a review see Menon & Uddin, 2010). In my study, higher cognitive demands in the Repro compared to the Self task are supported by corresponding enhancement of AIC activation.

5.2.3.1. Predictive coding

Following the predictive coding account, BOLD response in active compared to passive trials should be suppressed, given that prediction is thought to attenuate self-generated action signals. However, a previous study by Krala et al., (2019) showed a reversed effect of prediction most likely due to engagement of attentional resources in early sensory cortical areas. This was interpreted as a sharpening of prediction signals for task solving (Jiang et al., 2013; Kok et al., 2012).

Different cognitive parameters are employed into the task-solving processes of distance reproduction. A reproduction task requires the participant to keep a target distance in the working memory. Simultaneously, the currently traveled distance must be monitored and compared to the memorized target distance which requires attention allocation towards the current distance. Conversely, when participants are free to travel a self-chosen distance, attention and working memory are not required to the extent as it is the case for reproduction. During reproduction, attentional resources are more strongly engaged compared to simple production because there is no target distance that has to be encoded. Spatial attention is a top-down mechanism that is key for selecting relevant information for a task. The perception of signals presented at the attended location is enhanced by means of faster reaction times

and higher accuracy (Jehu et al., 2015; Prinzmetal et al., 2005). Observers prioritize processing information relevant to their current goals. Only recently an increasing number of studies has started to investigate the interaction between attention and prediction. Generally, attention and prediction are thought to interact synergistically. Predictions are defined as top-down signals that can facilitate perception (and appropriate reactions) by employing information from prediction error signals. Prediction errors are defined as discrepancies between top-down predictions and actual incoming bottom-up sensory evidence (Friston, 2005; Friston & Kiebel, 2009). According to the predictive coding framework, attention enhances the detection of perceptual prediction errors (Garrido et al., 2018; Zuanazzi & Noppeney, 2020), thereby reversing the attenuating effect of predictions (Auksztulewicz & Friston, 2015; Smout et al., 2019). In my study 3, for both tasks, the comparison between active and passive trials showed enhanced BOLD responses in early sensory cortices, while higher-order areas showed BOLD suppression. These results are in line with the fact that active trials of both tasks were behaviorally more demanding compared to the passive trials. In line with the assumption that the Repro task engaged behavioral demands more strongly than the Self task, active trials in the Repro task showed enhanced BOLD responses in the anterior insular cortex (AIC), suggesting that behavioral demands are reflected in activity of higher order areas in amodal distance encoding.

Suppression of the IPL across modalities suggests that areas located on the IPL are involved in the encoding of prediction conformity irrespective of sensory modality. Areas that have been found to show suppressed neural activity for active compared to passive parts are the angular gyrus (AG) and the supramarginal gyrus (SMG) along the lateral intraparietal sulcus. The SMG has been reported to mediate attentional allocation during temporal processing (Wiener et al., 2010) as well as in the spatial domain (Kashkouli et al., 2015; Silk et al., 2010). In my study, suppressed BOLD response of the SMG might have reflected amodal comparison of predictions to actual incoming sensory feedback about traveled duration in that area. Likewise, suppressed BOLD response of the angular gyrus (AG) suggests this area to play a major role in prediction processing. The AG, lying in the posterior region of the IPL, has been found to be engaged into attentional allocation towards task-relevant stimuli (Ciaramelli et al., 2008; Gottlieb, 2007) as well as maintaining attention towards salient events (Singh-Curry & Husain, 2009). Imaging studies have also described a role of the AG in short-term storing multimodal memory content (Humphreys et al., 2021) and memory retrieval (Ciaramelli et al., 2008; Rugg

& King, 2018). This makes the engagement of the AG crucial for task solving of both tasks of study 3, the Repro and the Self task, given that attentional on-line tracking of travelled distance and retrieval of- and comparison to target distance are mandatory for successful solving the path integration task. For the visual and auditory modality, the AG has been described to compare predicted to actual incoming sensory feedback, suggesting a common mechanism for the encoding of prediction errors in different modalities (van Kemenade et al., 2017). The fact that the AG has been also identified to encode agency supports the view of a role of the AG in the amodal encoding of predictions (Kim, 2010; Sperduti et al., 2011). My data adds to these findings by providing evidence for visuo-tactile prediction encoding in the AG. In accordance with recent studies, the attenuating effects of predictions that is proposed by the predictive coding framework has been reversed by increasing behavioral demand during task solving thereby enhancing prediction error responses.

5.3. Limitations and outlook towards naturalistic stimuli

Various senses contribute to the perception of self-motion. However, in the majority of experiments investigating self-motion, including my studies, self-motion is artificially simulated in a laboratory. This has the advantage of a setting that allows for the control of external factors. However, visually and tactilely simulating self-motion in an artificial environment also has a number of disadvantages.

When visual locomotion is simulated by an optic flow pattern, the field of view (FOV) (as given by screen size) has a large influence on the degree of vection experienced by the observer. Smaller screen sizes lead to heading estimation errors and impaired precision of heading judgements (Li et al., 2002; Warren & Kurtz, 1992). However, comparison with previous studies suggests that the screen sizes in my heading studies (81° by 33° for studies 1 & 2, respectively) were sufficiently large to allow for reliable self-motion perception (Andersen & Braunstein, 1985; Pretto et al., 2009). Generally, research suggests that larger screens enhance the impression of vection (Allison et al., 1999; Trutoiu et al., 2009). In my third study, participants viewed the screen via an angled mirror which covered a field of view of 21.7° × 12.3°. Although the FOV was relatively small, behavioral accuracy and precision of heading responses suggest that the optic flow stimulus provided sufficient information for distance judgements. The optic flow stimulus consisted of dots scaling in size with the distance to the observer.

One method to overcome this limitation is to employ stimulus presentation using a virtual reality (VR) headset which allows for simulation of a 360° surrounding space, thereby overcoming limitations induced by FOV size (see e.g. Engel et al., 2020, 2021; Student et al., 2022). Another advantage of self-motion presented in VR systems is that they allow for the presentation of more naturalistic stimulus environments. Using VR makes it also possible to simulate self-motion in upright pose, which is characteristic for walking (Jörges & Harris, 2022). It has long been known that photorealistic stimuli enhance perceived vection (Trutoiu et al., 2009). Furthermore, walking involves constantly looking around for obstacles and foot placement. Usually, during translatory movement, the eyes do not statically fixate at one predefined point at the horizon (as it is the case in artificial self-motion experiments that demand static fixation of a central fixation point), but humans flexibly adjust their gaze towards new destination as the path changes (Calow & Lappe, 2008; Hollands et al., 2002). Recent studies on eye movements during visually perceived self-motion provide evidence for interactions between the execution of ocular movements and self-motion perception, providing new insights into how the latter differs between natural vision and 2D artificial stimulus environments (Matthis et al., 2022).

The benefits of bringing the investigation of the processing of self-motion information to a more realistic setting should also be considered for tactile flow stimulation. Multisensory perception of vection is facilitated if information from two modalities is contextually congruent. Yahata et al., (2021) showed that hot wind compared to normal temperature, or no wind provided by a fan towards the subjects' upper body strongly facilitated perceived vection when participants walked in corridors made of fire in VR. In my heading studies, it would not have been possible to let subjects wear a VR headset given the design of the tactile stimulation devices, since the headset would have covered the area to be stimulated. In future studies, providing tactile flow towards the whole body by means of for example a wind corridor would allow for employment of a VR headset.

The nature of tactile self-motion stimuli employed in my experiments evokes the question how valid the stimulus in simulating self-motion was. In study 1, tactile flow was provided as a rather narrow air stream by small tubes and met the forehead very selectively, subjects indicated a strong impression of vection in the unimodal tactile trials. In the imaging study, tactile flow was provided by the same nozzle as applied in that first study. In my second, behavioral heading study, the tactile flow stimulus was arguably more naturalistic through the

use of a wider air stream, similar to how it would be experienced in the natural world by, for example, wind produced by bike riding. One open question is whether tactile flow is primarily encoded in the context of self-motion or secondarily as a stimulus perceived in the peripersonal space. For example, studies on non-human primates provide evidence that neurons of monkey area VIP encode tactile stimulation evoked by a touching the skin/fur of the head (Bremmer et al., 2002a; Duhamel et al., 1998). Thus, apart from actual air flow, there may be cues signaling self-motion through contact with objects in the environment. An example would be locomotion through the woods, where sticks and twigs brush over the body in congruence with the actors' motion. In that sense, those stimuli represent obstacles or objects in the surrounding. This is evidenced by findings showing that electrical micro-stimulation of macaque area VIP elicits defensive movements by the animal (Cooke et al., 2003). These results are also related to the concept of looming. Looming describes the perceptual effect when an approaching stimulus of one modality increases sensitivity in another modality during the period when the stimulus would reach the observer. In human observers, looming has indeed been found for the interaction of, among others, visuo-tactile stimuli (Cléry et al., 2015; Kandula et al., 2015). Imaging studies on human participants revealed activation of area hVIP by looming visual stimuli during tactile perception (Cléry et al., 2017). Along the same vein, a recent imaging study also suggested that area hVIP encodes not only of self-motion, but also object motion (Field et al., 2020). Thus, in my imaging study, activation of area hVIP might also indicate looming due to object encoding in the near peripersonal space of the face/head rather than self-motion perception. Further studies might resolve this question by systematically manipulating the nature of tactile stimuli. The current trend is moving towards the use of more naturalistic stimuli by the employment of VR techniques. This may help to solve the dilemma between standardized laboratory settings and the generalization of findings to the real world.

5.4. Conclusion

In conclusion, my thesis has demonstrated that tactile flow plays a significant role for both, heading perception and the perception of travel distance. In two studies on visuo-tactile heading perception I was able to demonstrate that behaviorally relevant as well as behavioral irrelevant tactile flow is used for heading estimations. For the combination of heading cues from both modalities, heading perception was mainly driven by visual stimuli with tactile

stimuli showing a significant impact on heading judgements. Perceived heading in both modalities has been subject to centripetal heading biases. For heading judgements, stimuli of both modalities have not been integrated optimally in a Bayesian sense but showed significant interaction. By this, I have provided first evidence on visuo-tactile flow as a reliable heading cue in the perception of self-motion.

In my third study, brain areas involved in the encoding of visual and tactile path integration have been identified by means of human fMRI. Neural processing of visual and tactile self-motion stimuli showed similarities between - and across - both modalities. Neural correlates of visual and tactile path integration differed as a function of behavioral demands. In summary, with my thesis, I have shown that the tactile modality is more strongly related to self-motion perception than previously thought and should receive more attention in future studies.

6. SUMMARY

Humans obtain and process sensory information from various modalities to ensure successful navigation through the environment. While visual, vestibular, and auditory self-motion perception have been extensively investigated, studies on tactile self-motion perception are comparably rare. In my thesis, I have investigated tactile self-motion perception and its interaction with the visual modality. In one of two behavioral studies, I analyzed the influence of a tactile heading stimulus introduced as a distractor on visual heading perception. In the second behavioral study, I analyzed visuo-tactile perception of self-motion direction (heading). In both studies, visual self-motion was simulated as forward motion over a 2D ground plane. Tactile self-motion was simulated by airflow towards the subjects' forehead, mimicking the experience of travel wind, e.g., during a bike ride. In the analysis of the subjects' perceptual reports, I focused on possible visuo-tactile interactions and applied different models to describe the integration of visuo-tactile heading stimuli. Lastly, in a functional magnetic resonance imaging study (fMRI), I investigated neural correlates of visual and tactile perception of traveled distance (path integration) and its modulation by prediction and cognitive task demands.

In my first behavioral study, subjects indicated perceived heading from unimodal visual (optic flow), unimodal tactile (tactile flow) or from a combination of stimuli from both modalities, simulating either congruent or incongruent heading (bimodal condition). In the bimodal condition, the subjects' task was to indicate *visually* perceived heading. Hence, here tactile stimuli were behaviorally irrelevant. In bimodal trials, I found a significant interaction of stimuli from both modalities. Visually perceived heading was biased towards tactile heading direction for an offset of up to 10° between both heading directions.

The relative weighting of stimuli from both modalities in the visuo-tactile interaction were examined in my second behavioral study. Subjects indicated perceived heading from unimodal visual, unimodal tactile and bimodal trials. Here, in bimodal trials, stimuli form both modalities were presented as behaviorally relevant. By varying eye- relative to head position during stimulus presentation, possible influences of different reference frames of the visual and tactile modality were investigated. In different sensory modalities, incoming information is encoded relative to the reference system of

the receiving sensory organ (e.g., relative to the retina in vision or relative to the skin in somatosensation).

In unimodal tactile trials, heading perception was shifted towards eye-position. In bimodal trials, varying head- and eye-position had no significant effect on perceived heading: subjects indicated perceived heading based on both, the visual and tactile stimulus, independently of the behavioral relevance of the tactile stimulus. In sum, results of both studies suggest that the tactile modality plays a greater role in self-motion perception than previously thought.

Besides the perception of travel direction (heading), information about traveled speed and duration are integrated to achieve a measure of the distance traveled (path integration). One previous behavioral study has shown that tactile flow can be used for the reproduction of travel distance (Churan et al., 2017). However, studies on neural correlates of tactile distance encoding in humans are lacking entirely. In my third study, subjects solved two path integration tasks from unimodal visual and unimodal tactile self-motion stimuli. Brain activity was measured by means of functional magnetic resonance imaging (fMRI). Both tasks varied in the engagement of cognitive task demands. In the first task, subjects replicated (Active trial) a previously observed traveled distance (Passive trial) (= Reproduction task). In the second task, subjects traveled a self-chosen distance (Active trial) which was then recorded and played back to them (Passive trial) (= Self task). The predictive coding theory postulates an internal model which creates predictions about sensory outcomes-based mismatches between predictions and sensory input which enables the system to sharpen future predictions (Teufel et al., 2018). Recent studies suggested a synergistical interaction between prediction and cognitive demands, thereby reversing the attenuating effect of prediction. In my study, this hypothesis was tested by manipulating cognitive demands between both tasks. For both tasks, Active trials compared to Passive trials showed BOLD enhancement of early sensory cortices and suppression of higher order areas (e.g., the intraparietal lobule (IPL)). For both modalities, enhancement of early sensory areas might facilitate task solving processes at hand, thereby reversing the hypothesized attenuating effect of prediction. Suppression of the IPL indicates this area as an amodal comparator of predictions and incoming self-motion signals.

In conclusion, I was able to show that tactile self-motion information, i.e., tactile flow, provides significant information for the processing of two key features of self-motion perception: Heading and path integration. Neural correlates of tactile path-integration were investigated by means of fMRI, showing similarities between visual and tactile path integration on early processing stages as well as shared neural substrates in higher order areas located in the IPL. Future studies should further investigate the perception of different self-motion parameters in the tactile modality to extend the understanding of this less researched – but important – modality.

7. ZUSAMMENFASSUNG

Bei der Wahrnehmung von Eigenbewegungen liefern uns unterschiedliche Sinnesmodalitäten Informationen über u.a. unsere Bewegungsrichtung und die Geschwindigkeit, mit der wir uns bewegen. Während der Beitrag von visueller und vestibulärer Information zur Verarbeitung von Eigenbewegung bereits gut untersucht ist, ist die Rolle der taktilen Modalität fast unergründet. In meiner Arbeit habe ich zusätzlich zu visuell simulierter Eigenbewegung den Beitrag taktiler Reize in Form von simuliertem Fahrtwind auf die Verarbeitung von Eigenbewegung untersucht.

In zwei Verhaltensstudien wurde wahrgenommene Bewegungsrichtung in rein visuellen Durchgängen, in rein taktilen Durchgängen und in Durchgängen, in denen Eigenbewegungsrichtung gleichzeitig in beiden Modalitäten präsentiert wurde (bimodal) abgefragt. In bimodalen Durchgängen konnten die Bewegungsrichtungen entweder in beiden Modalitäten übereinstimmen oder mit einem räumlichen Versatz zwischen der visuellen und taktilen Bewegungsrichtung präsentiert werden. In der ersten Studie sollten Probanden in den bimodalen Durchgängen die „*visuell* empfundene Bewegungsrichtung“ angeben. Damit sollte untersucht werden, welchen Einfluss ein behavioral **ir**relevanter taktiler Richtungsreiz auf die visuell wahrgenommene Bewegungsrichtung hat. In den bimodalen Durchgängen zeigte sich ein signifikanter Einfluss eines behavioral unbeachteten taktilen Richtungsreizes auf die visuell wahrgenommene Bewegungsrichtung. Dies verdeutlicht die bis jetzt wenig untersuchte Rolle von taktilen Reizen für die Eigenbewegungswahrnehmung. Die Interaktion von visuellen und taktilen Reizen habe ich im zweiten Verhaltensexperiment weiter untersucht. Im Vergleich zum ersten Experiment wurde in dieser Studie in bimodalen Durchgängen der taktile Reiz als behavioral relevant präsentiert, indem die Probanden gebeten wurden, die ‚wahrgenommene Bewegungsrichtung‘ anzugeben. Die Interaktion wurde in Abhängigkeit von verschiedenen Augen- und Kopfpositionen untersucht, um mögliche Referenzrahmen bei der Eigenbewegungswahrnehmung zu betrachten. Für die bimodalen Durchgänge habe ich die relative Gewichtung beider Sinnesmodalitäten in der Richtungswahrnehmung analysiert. Ich konnte zeigen, dass sich in den bimodalen Durchgängen die Probanden stärker auf die visuelle Modalität verlassen haben, obwohl es einen signifikanten Einfluss der taktilen Bewegungsrichtungen gab. Es gab keinen Einfluss der Augen- und Kopf-Position auf unimodal visuelle und bimodale Verarbeitung. Unimodal taktile Richtungswahrnehmung hingegen wurde in Richtung der

Augen-Position beeinflusst. Dies könnte durch die visuelle Antwortgabe in meinem Experiment begründet sein.

In der dritten Studie habe ich die neuronalen Korrelate von taktiler und visueller Verarbeitung von zurückgelegter Distanz mittels Magnetresonanztomografie untersucht. Dabei war der Einfluss der kognitiven Anforderungen beim Lösen der Aufgabe von Interesse. Die ‚predictive coding' Theorie besagt, dass das Gehirn Vorhersagen über zukünftige Ereignisse trifft, welche dann mit tatsächlich eintreffenden sensorischen Informationen abgeglichen werden. Wenn beides übereinstimmt, werden die vorhergesagten neuronalen Signale gedämpft. Dieser Abgleich wird dann dazu genutzt, das interne Modell an die aktuelle Situation anzupassen und unsere Wahrnehmung der Welt so effizient wie möglich zu organisieren. Neue Studien legen nah, dass dieser verringernde Effekt durch hohe Aufgabenanforderungen umgedreht werden kann. Dies könnte dadurch begründet sein, dass das System kognitive Ressourcen zum Lösen der Aufgabe aufwendet, die somit zu einer Erhöhung (anstatt Dämpfung) der Erregungsübertragung führen. In meiner Studie habe ich den Einfluss kognitiver Anforderungen auf die Reproduktion von zurückgelegter Distanz experimentell manipuliert. Jede Versuchsperson löste zwei Aufgaben, die sich in ihrer Lösungsschwierigkeit unterschieden und jeweils aus aktiven und passiven Durchgängen bestanden. Für beide Aufgaben zeigte sich eine Verstärkung neuronaler Aktivierung in frühen sensorischen Arealen für visuelle wie auch taktile Durchgänge für den Vergleich zwischen aktiven (Re-/Produzieren einer Distanz) mit passiven (Enkodieren/ Betrachten einer Distanz) Durchgängen. Dies spricht für eine Beteiligung dieser Areale am Aufgabenlösen und somit einer Umkehr der durch die ‚predictive coding' Theorie vorhergesagten neuronalen Aktivitätsverringerung. Somit konnte ich vorherige Studien, die eine Umkehr von Dämpfung der neuronalen Aktivierung durch kognitive Anforderungen gezeigt haben, durch meine Ergebnisse ergänzen. Des Weiteren konnte ich neuronale Korrelate taktiler Distanzwahrnehmung identifizieren und Gemeinsamkeiten zur visuellen Distanzwahrnehmung aufzeigen.

Zusammenfassend habe ich in meiner Arbeit erste Befunde zur Rolle der taktilen Modalität bei der Eigenbewegungsverarbeitung aufgezeigt. Taktile Reize in Form von simuliertem Fahrtwind dienen als valider Reiz zur Einschätzung von Bewegungsrichtung als auch zur adäquaten Wahrnehmung von zurückgelegter Distanz. Somit spielt die taktile Modalität einen wesentlich größeren Einfluss bei Eigenbewegungsverarbeitung als bisher herausgestellt und sollte in zukünftigen Untersuchungen von Eigenbewegung stärker beachtet werden.

8. REFERENCES

Acerbi, L., Dokka, K., Angelaki, D. E., & Ma, W. J. (2018). Bayesian comparison of explicit and implicit causal inference strategies in multisensory heading perception. In *PLoS Computational Biology* (Vol. 14, Issue 7). https://doi.org/10.1371/journal.pcbi.1006110

Aedo-Jury, F., Cottereau, B. R., Celebrini, S., & Séverac Cauquil, A. (2020). Antero-Posterior vs. Lateral Vestibular Input Processing in Human Visual Cortex. *Frontiers in Integrative Neuroscience*, *14*(August), 1–14. https://doi.org/10.3389/fnint.2020.00043

Ahissar, M., Ahissar, E., Bergman, H., & Vaadia, E. (1992). Encoding of sound-source location and movement: Activity of single neurons and interactions between adjacent neurons in the monkey auditory cortex. *Journal of Neurophysiology*, *67*(1), 203–215. https://doi.org/10.1152/jn.1992.67.1.203

Alais, D., & Burr, D. (2004). The Ventriloquist Effect Results from Near-Optimal Bimodal Integration. *Current Biology*, *14*(3), 257–262. https://doi.org/10.1016/j.cub.2004.01.029

Alais, D., & Burr, D. (2019). *Cue Combination Within a Bayesian Framework*. 9–31. https://doi.org/10.1007/978-3-030-10461-0_2

Albanese, M. C., Duerden, E. G., Bohotin, V., Rainville, P., & Duncan, G. H. (2009). Differential effects of cognitive demand on human cortical activation associated with vibrotactile stimulation. *Journal of Neurophysiology*, *102*(3), 1623–1631. https://doi.org/10.1152/jn.91295.2008

Albright, T. D. (1984). Direction and orientation selectivity of neurons in visual area MT of the macaque. *Journal of Neurophysiology*, *52*(6), 1106–1130. https://doi.org/10.1152/jn.1984.52.6.1106

Alefantis, P., Lakshminarasimhan, K. J., Avila, E., Noel, J.-P., Pitkow, X., & Angelaki, D. E. (2022). Sensory evidence accumulation using optic flow in a naturalistic navigation task. *The Journal of Neuroscience*, *42*(27), JN-RM-2203-21. https://doi.org/10.1523/jneurosci.2203-21.2022

Alexander, A. S., Carstensen, L. C., Hinman, J. R., Raudies, F., William Chapman, G., & Hasselmo, M. E. (2020). Egocentric boundary vector tuning of the retrosplenial cortex. *Science Advances*, *6*(8). https://doi.org/10.1126/sciadv.aaz2322

Allison, R. S., Gillam, B. J., & Vecellio, E. (2009). Binocular depth discrimination and

estimation beyond interaction space. *Journal of Vision*, *9*(1), 1–14. https://doi.org/10.1167/9.1.10

Allison, R. S., Howard, I. P., & Zacher, J. E. (1999). Effect of field size, head motion, and rotational velocity on roll vection and illusory self-tilt in a tumbling room. *Perception*, *28*(3), 299–306. https://doi.org/10.1068/p2891

Amedi, A., Malach, R., Hendler, T., Peled, S., & Zohary, E. (2001). Visuo-haptic object-related activation in the ventral visual pathway. *Nature Neuroscience*, *4*(3), 324–330. https://doi.org/10.1038/85201

Andersen, G. J., & Braunstein, M. L. (1985). Induced Self-Motion in Central Vision. *Journal of Experimental Psychology: Human Perception and Performance*, *11*(2), 122–132. https://doi.org/10.1037/0096-1523.11.2.122

Anderson, P. W., & Zahorik, P. (2014). Auditory/visual distance estimation: Accuracy and variability. *Frontiers in Psychology*, *5*(SEP), 1–11. https://doi.org/10.3389/fpsyg.2014.01097

Angelaki, D. E., Gu, Y., & DeAngelis, G. C. (2009). Multisensory integration: psychophysics, neurophysiology, and computation. *Current Opinion in Neurobiology*, *19*(4), 452–458. https://doi.org/10.1016/j.conb.2009.06.008

Angelaki, D. E., Gu, Y., & DeAngelis, G. C. (2011). Visual and vestibular cue integration for heading perception in extrastriate visual cortex. *Journal of Physiology*, *589*(4), 825–833. https://doi.org/10.1113/jphysiol.2010.194720

Annett, J. (1996). On knowing how to do things: a theory of motor imagery. *Cognitive brain research*, *3*(2), 65-69. https://doi.org/10.1016/0926-6410(95)00030-5

Arikan, B. E., van Kemenade, B. M. V., Podranski, K., Steinsträter, O., Straube, B., & Kircher, T. (2019). Perceiving your hand moving: BOLD suppression in sensory cortices and the role of the cerebellum in the detection of feedback delays. *Journal of Vision*, *19*(14), 1–22. https://doi.org/10.1167/19.14.4

Arnold, A. E. G. F., Burles, F., Bray, S., Levy, R. M., & Iaria, G. (2014). Differential neural network configuration during human path integration. *Frontiers in Human Neuroscience*, *8*(1 APR), 1–12. https://doi.org/10.3389/fnhum.2014.00263

Aronson, E., & Lee, D. N. (1974). Visual proprioceptive control of standing in human infants.

Perception & Psychophysics, *15*(3), 529–532. https://doi.org/10.3758/BF03199297

Auksztulewicz, R., & Friston, K. (2015). Attentional enhancement of auditory mismatch responses: A DCM/MEG study. *Cerebral Cortex*, *25*(11), 4273–4283. https://doi.org/10.1093/cercor/bhu323

Avillac, M., Denève, S., Olivier, E., Pouget, A., & Duhamel, J. R. (2005). Reference frames for representing visual and tactile locations in parietal cortex. *Nature Neuroscience*, *8*(7), 941–949. https://doi.org/10.1038/nn1480

Avillac, M., Hamed, S. Ben, & Duhamel, J. R. (2007). Multisensory integration in the ventral intraparietal area of the macaque monkey. *Journal of Neuroscience*, *27*(8), 1922–1932. https://doi.org/10.1523/JNEUROSCI.2646-06.2007

Battaglia, P. W., Jacobs, R. A., & Aslin, R. N. (2003). Bayesian integration of visual and auditory signals for spatial localization. *Journal of the Optical Society of America A*, *20*(7), 1391. https://doi.org/10.1364/josaa.20.001391

Beauchamp, M. S., LaConte, S., & Yasar, N. (2009). Distributed representation of single touches in somatosensory and visual cortex. *Human Brain Mapping*, *30*(10), 3163–3171. https://doi.org/10.1002/hbm.20735

Beauchamp, M. S., Yasar, N. E., Kishan, N., & Ro, T. (2007). Human MST but not MT responds to tactile stimulation. *Journal of Neuroscience*, *27*(31), 8261–8267. https://doi.org/10.1523/JNEUROSCI.0754-07.2007

Benoit, M. M. K., Raij, T., Lin, F. H., Jääskeläinen, I. P., & Stufflebeam, S. (2010). Primary and multisensory cortical activity is correlated with audiovisual percepts. *Human Brain Mapping*, *31*(4), 526–538. https://doi.org/10.1002/hbm.20884

Berthoz, A., Israël, I., Georges-François, P., Grasso, R., & Tsuzuku, T. (1995). Spatial memory of body linear displacement: What is being stored? *Science*, *269*(5220), 95–98. https://doi.org/10.1126/science.7604286

Bettencourt, K. C., & Xu, Y. (2015). Decoding the content of visual short-term memory under distraction in occipital and parietal areas. *Nature Neuroscience*, *19*(1), 150–157. https://doi.org/10.1038/nn.4174

Blauert, J. (1996). *Spatial Hearing. The Psychophysics of Human Sound Localization*. The MIT Press. https://doi.org/10.7551/mitpress/6391.001.0001

Boccia, M., Guariglia, C., Sabatini, U., & Nemmi, F. (2016). Navigating toward a novel environment from a route or survey perspective: neural correlates and context-dependent connectivity. *Brain Structure and Function*, *221*(4), 2005–2021. https://doi.org/10.1007/s00429-015-1021-z

Bodegård, A., Geyer, S., Grefkes, C., Zilles, K., & Roland, P. E. (2001). Hierarchical processing of tactile shape in the human brain. *Neuron*, *31*(2), 317–328. https://doi.org/10.1016/S0896-6273(01)00362-2

Bonato, M., Zorzi, M., & Umiltà, C. (2012). When time is space: Evidence for a mental time line. *Neuroscience and Biobehavioral Reviews*, *36*(10), 2257–2273. https://doi.org/10.1016/j.neubiorev.2012.08.007

Bottini, R., & Doeller, C. F. (2020). Knowledge Across Reference Frames: Cognitive Maps and Image Spaces. *Trends in Cognitive Sciences*, *24*(8), 606–619. https://doi.org/10.1016/j.tics.2020.05.008

Boussaoud, D., Ungerleider, L. G., & Desimone, R. (1990). Pathways for motion analysis: Cortical connections of the medial superior temporal and fundus of the superior temporal visual areas in the macaque. *Journal of Comparative Neurology*, *296*(3), 462–495. https://doi.org/10.1002/cne.902960311

Bradfield, L. A., & Hart, G. (2020). Rodent medial and lateral orbitofrontal cortices represent unique components of cognitive maps of task space. *Neuroscience and Biobehavioral Reviews*, *108*, 287–294. https://doi.org/10.1016/j.neubiorev.2019.11.009

Bradley, D. C., & Goyal, M. S. (2008). Velocity computation in the primate visual system. *Nature Reviews Neuroscience*, *9*(9), 686–695. https://doi.org/10.1038/nrn2472

Brainard, D. H. (1997). The Psychophysics Toolbox. *Spatial Vision*, *10*(4), 433–436. https://doi.org/10.1163/156856897X00357

Bremmer, F., Graf, W., Hamed, S. Ben, & Duhamel, J. R. (1999). Eye position encoding in the macaque ventral intraparietal area (VIP). *NeuroReport*, *10*(4), 873–878. https://doi.org/10.1097/00001756-199903170-00037

Bremmer, F., & Lappe, M. (1999). The use of optical velocities for distance discrimination and reproduction during visually simulated self motion. *Experimental Brain Research*, *127*(1), 33–42. https://doi.org/10.1007/s002210050771

Bremmer, F., Churan, J., & Lappe, M. (2017). Heading representations in primates are compressed by saccades. *Nature Communications*, *8*(1). https://doi.org/10.1038/s41467-017-01021-5

Bremmer, F., Duhamel, J. R., Ben Hamed, S., & Graf, W. (2002a). Heading encoding in the macaque ventral intraparietal area (VIP). *European Journal of Neuroscience*, *16*(8), 1554–1568. https://doi.org/10.1046/j.1460-9568.2002.02207.x

Bremmer, F., Klam, F., Duhamel, J. R., Ben Hamed, S., & Graf, W. (2002). Visual-vestibular interactive responses in the macaque ventral intraparietal area (VIP). *European Journal of Neuroscience*, *16*(8), 1569–1586. https://doi.org/10.1046/j.1460-9568.2002.02206.x

Bremmer, F., Kubischik, M., Pekel, M., Hoffmann, K. P., & Lappe, M. (2010). Visual selectivity for heading in monkey area MST. *Experimental Brain Research*, *200*(1), 51–60. https://doi.org/10.1007/s00221-009-1990-3

Bremmer, F., Schlack, A., Kaminiarz, A., & Hoffmann, K. P. (2013). Encoding of movement in near extrapersonal space in primate area VIP. *Frontiers in Behavioral Neuroscience*, *7*(JANUARY 2013), 1–10. https://doi.org/10.3389/fnbeh.2013.00008

Bremmer, F., Schlack, A., Shah, N. J., Zafiris, O., Kubischik, M., Hoffmann, K.-P., Zilles, K., & Fink, G. R. (2001). Polymodal Motion Processing in Posterior Parietal and Premotor Cortex. *Neuron*, *29*(1), 287–296. https://doi.org/10.1016/s0896-6273(01)00198-2

Bresciani, J. P., Dammeier, F., & Ernst, M. O. (2006). Vision and touch are automatically integrated for the perception of sequences of events. *Journal of Vision*, *6*(5), 554–564. https://doi.org/10.1167/6.5.2

Brett, M., Anton, J. L., Valabregue, R., & Poline, J. B. (2002). Region of interest analysis using an SPM toolbox. *NeuroImage*, *16*, 497.

Britten, K. H. (2008). Mechanisms of self-motion perception. *Annual Review of Neuroscience*, *31*, 389–410. https://doi.org/10.1146/annurev.neuro.29.051605.112953

Bushara, K. O., Grafman, J., & Hallett, M. (2001). Neural correlates of auditory-visual stimulus onset asynchrony detection. *Journal of Neuroscience*, *21*(1), 300–304. https://doi.org/10.1523/jneurosci.21-01-00300.2001

Butler, J. S., Campos, J. L., & Bülthoff, H. H. (2015). Optimal visual–vestibular integration under conditions of conflicting intersensory motion profiles. *Experimental Brain*

Research, *233*(2), 587–597. https://doi.org/10.1007/s00221-014-4136-1

Butler, J. S., Smith, S. T., Campos, J. L., & Bülthoff, H. H. (2010). Bayesian integration of visual and vestibular signals for heading. *Journal of Vision*, *10*(11), 1–13. https://doi.org/10.1167/10.11.23

Butler, R. A., & Flannery, R. (1980). The spatial attributes of stimulus frequency and their role in monaural localization of sound in the horizontal plane. *Perception & Psychophysics*, *28*(5), 449–457. https://doi.org/10.3758/BF03204889

Cabeza, R., Ciaramelli, E., Olson, I. R., & Moscovitch, M. (2008). The parietal cortex and episodic memory: An attentional account. *Nature Reviews Neuroscience*, *9*(8), 613–625. https://doi.org/10.1038/nrn2459

Cai, Z. G., & Connell, L. (2015). Space-time interdependence: Evidence against asymmetric mapping between time and space. *Cognition*, *136*, 268–281. https://doi.org/10.1016/j.cognition.2014.11.039

Cai, Z. G., & Connell, L. (2016). On magnitudes in memory: An internal clock account of space-time interaction. *Acta Psychologica*, *168*, 1–11. https://doi.org/10.1016/j.actpsy.2016.04.003

Calow, D., & Lappe, M. (2008). Efficient encoding of natural optic flow. *Network: Computation in Neural Systems*, *19*(3), 183–212. https://doi.org/10.1080/09548980802368764

Caruso, V. C., Pages, D. S., Sommer, M. A., & Groh, J. M. (2021). Compensating for a shifting world: Evolving reference frames of visual and auditory signals across three multimodal brain areas. *Journal of Neurophysiology*, *126*(1), 82–94. https://doi.org/10.1152/jn.00385.2020

Chaplin, T. A., Rosa, M. G. P., & Lui, L. L. (2018). Auditory and visual motion processing and integration in the primate cerebral cortex. *Frontiers in Neural Circuits*, *12*(October), 1–9. https://doi.org/10.3389/fncir.2018.00093

Chen, A., DeAngelis, G. C., & Angelaki, D. E. (2011). *Representation of Vestibular and Visual Cues to Self-Motion in Ventral Intraparietal Cortex*. *31*(33), 12036–12052. https://doi.org/10.1523/JNEUROSCI.0395-11.2011

Chen, A., DeAngelis, G. C., & Angelaki, D. E. (2013). Functional specializations of the ventral

intraparietal area for multisensory heading discrimination. *Journal of Neuroscience*, *33*(8), 3567–3581. https://doi.org/10.1523/JNEUROSCI.4522-12.2013

Chen, X., DeAngelis, G. C., & Angelaki, D. E. (2013a). Diverse spatial reference frames of vestibular signals in parietal cortex. *Neuron*, *80*(5), 1310–1321. https://doi.org/10.1016/j.neuron.2013.09.006

Chen, X., DeAngelis, G. C., & Angelaki, D. E. (2013b). Eye-centered representation of optic flow tuning in the ventral intraparietal area. *Journal of Neuroscience*, *33*(47), 18574–18582. https://doi.org/10.1523/JNEUROSCI.2837-13.2013

Chen, X., DeAngelis, G. C., & Angelaki, D. E. (2014). Eye-centered visual receptive fields in the ventral intraparietal area. *Journal of Neurophysiology*, *112*(2), 353–361. https://doi.org/10.1152/jn.00057.2014

Chen, X., DeAngelis, G. C., & Angelaki, D. E. (2018). Flexible egocentric and allocentric representations of heading signals in parietal cortex. *Proceedings of the National Academy of Sciences of the United States of America*, *115*(14), E3305–E3312. https://doi.org/10.1073/pnas.1715625115

Chow, H. M., Knöll, J., Madsen, M., & Spering, M. (2021). Look where you go: Characterizing eye movements toward optic flow. *Journal of Vision*, *21*(3), 1–15. https://doi.org/10.1167/jov.21.3.19

Chrastil, E. R., Nicora, G. L., & Huang, A. (2019). Vision and proprioception make equal contributions to path integration in a novel homing task. *Cognition*, *192*(June), 103998. https://doi.org/10.1016/j.cognition.2019.06.010

Chrastil, E. R., Sherrill, K. R., Hasselmo, M. E., & Stern, C. E. (2015). There and back again: Hippocampus and retrosplenial cortex track homing distance during human path integration. *Journal of Neuroscience*, *35*(46), 15442–15452. https://doi.org/10.1523/JNEUROSCI.1209-15.2015

Churan, J., Kaminiarz, A., Schwenk, J. C. B., & Bremmer, F. (2021). Action-dependent processing of self-motion in parietal cortex of macaque monkeys. *Journal of Neurophysiology*, *125*(6), 2432–2443. https://doi.org/10.1152/jn.00049.2021

Churan, J., Paul, J., Klingenhoefer, S., & Bremmer, F. (2017). Integration of visual and tactile information in reproduction of traveled distance. *Journal of Neurophysiology*, *118*(3),

1650–1663. https://doi.org/10.1152/jn.00342.2017

Ciaramelli, E., Grady, C. L., & Moscovitch, M. (2008). Top-down and bottom-up attention to memory: A hypothesis (AtoM) on the role of the posterior parietal cortex in memory retrieval. *Neuropsychologia*, *46*(7), 1828–1851. https://doi.org/10.1016/j.neuropsychologia.2008.03.022

Cléry, J., Guipponi, O., Odouard, S., Pinède, S., Wardak, C., & Hamed, S. Ben. (2017). The prediction of impact of a looming stimulus onto the body is subserved by multisensory integration mechanisms. *Journal of Neuroscience*, *37*(44), 10656–10670. https://doi.org/10.1523/JNEUROSCI.0610-17.2017

Cléry, J., Guipponi, O., Wardak, C., & Ben Hamed, S. (2015). Neuronal bases of peripersonal and extrapersonal spaces, their plasticity and their dynamics: Knowns and unknowns. *Neuropsychologia*, *70*, 313–326. https://doi.org/10.1016/j.neuropsychologia.2014.10.022

Coleman, P. D. (1963). An analysis of cues to auditory depth perception in free space. *Psychological Bulletin*, *60*(3), 302–315. https://doi.org/10.1037/h0045716

Colonius, H., & Diederich, A. (2020). Formal models and quantitative measures of multisensory integration: a selective overview. *European Journal of Neuroscience*, *51*(5), 1161–1178. https://doi.org/10.1111/ejn.13813

Cooke, D. F., Taylor, C. S. R., Moore, T., & Graziano, M. S. A. (2003). Complex movements evoked by microstimulation of the ventral intraparietal area. *Proceedings of the National Academy of Sciences of the United States of America*, *100*(10), 6163–6168. https://doi.org/10.1073/pnas.1031751100

Crane, B., T. (2012). Direction Specific Biases in Human Visual and Vestibular Heading Perception. *PLoS ONE*, *7*(12), 1–15. https://doi.org/10.1371/journal.pone.0051383

Crane, B., T. (2017). Effect of eye position during human visual-vestibular integration of heading perception. *Journal of Neurophysiology*, *118*(3), 1609–1621. https://doi.org/10.1152/jn.00037.2017

Crane, B., T. (2015). Coordinates of human visual and inertial heading perception. *PLoS ONE*, *10*(8), 1–14. https://doi.org/10.1371/journal.pone.0135539

Cullen, K. E. (2004). Sensory signals during active versus passive movement. *Current Opinion*

in Neurobiology, *14*(6), 698–706. https://doi.org/10.1016/j.conb.2004.10.002

Cullen, K. E. (2019). Vestibular processing during natural self-motion: implications for perception and action. *Nature Reviews Neuroscience*, *20*(6), 346–363. https://doi.org/10.1038/s41583-019-0153-1

Cullen, K. E., & Zobeiri, O. A. (2021). Proprioception and the predictive sensing of active self-motion. *Current Opinion in Physiology*, *20*, 29–38. https://doi.org/10.1016/j.cophys.2020.12.001

Cuturi, L. F., & MacNeilage, P. R. (2013). Systematic Biases in Human Heading Estimation. *PLoS ONE*, *8*(2). https://doi.org/10.1371/journal.pone.0056862

D'Avossa, G., & Kersten, D. (1996). Evidence in human subjects for independent coding of aximuth and elevatio for direction of optic flow. *Vision Research*, *36*(18), 2915–2924.

Dacey, D., M.; Liao, HW.; Peterson, B. B.; Robinson, F., R.; Smith, V., C.; Pokorny, J.; Yau, K-W.; Gamlin, P. D. (2005). Melanopsin-expressing ganglion cells in primate retina signal colour and irradiance and project to the LGN. *Nature*, *433*(7027), 749–754. https://doi.org/10.1038/nature03387

Dahm, S. F., & Rieger, M. (2016). Is there symmetry in motor imagery? Exploring different versions of the mental chronometry paradigm. *Attention, Perception, and Psychophysics*, *78*(6), 1794–1805. https://doi.org/10.3758/s13414-016-1112-9

De Haan, E. H. F., Fabri, M., Dijkerman, H. C., Foschi, N., Lattanzi, S., & Pinto, Y. (2020). Unified tactile detection and localisation in split-brain patients. *Cortex*, *124*, 217–223. https://doi.org/10.1016/j.cortex.2019.11.010

De Winkel, K. N., Soyka, F., Barnett-Cowan, M., Bülthoff, H. H., Groen, E. L., & Werkhoven, P. J. (2010). Integration of visual and inertial cues in the perception of angular self-motion. *Experimental Brain Research*, *231*(2), 209–218. https://doi.org/10.1007/s00221-013-3683-1

De Winkel, K. N., Katliar, M., & Bülthoff, H. H. (2015). Forced fusion in multisensory heading estimation. *PLoS ONE*, *10*(5), 1–20. https://doi.org/10.1371/journal.pone.0127104

De Winkel, K. N., Katliar, M., & Bülthoff, H. H. (2017). Causal inference in multisensory heading estimation. *PLoS ONE*, *12*(1), 1–20. https://doi.org/10.1371/journal.pone.0169676

Del Gratta, C., Della Penna, S., Tartaro, A., Ferretti, A., Torquati, K., Bonomo, L., Romani, G. L., & Rossini, P. M. (2000). Topographic organization of the human primary and secondary somatosensory areas: An fMRI study. *NeuroReport*, *11*(9), 2035–2043. https://doi.org/10.1097/00001756-200006260-00046

Delmas, P., Hao, J., & Rodat-Despoix, L. (2011). Molecular mechanisms of mechanotransduction in mammalian sensory neurons. *Nature Reviews Neuroscience*, *12*(3), 139–153. https://doi.org/10.1038/nrn2993

Deneve, S., & Pouget, A. (2004). Bayesian multisensory integration and cross-modal spatial links. *Journal of Physiology Paris*, *98*(1-3 SPEC. ISS.), 249–258. https://doi.org/10.1016/j.jphysparis.2004.03.011

Derbie, A. Y., & Dejenie, M. A. (2022). Intra Parietal Sulcus Area 1–2 and Angular Gyrus Differentiates Visual Short-Term Memory and Sustained Attention Activities. *Annals of Neurosciences*, 097275312110723. https://doi.org/10.1177/09727531211072301

Di Marco, S., Fattori, P., Galati, G., Galletti, C., Lappe, M., Maltempo, T., Serra, C., Sulpizio, V., & Pitzalis, S. (2021). Preference for locomotion-compatible curved paths and forward direction of self-motion in somatomotor and visual areas. *Cortex*, *137*, 74–92. https://doi.org/10.1016/j.cortex.2020.12.021

DiCarlo, J. J., & Johnson, K. O. (2000). Spatial and temporal structure of receptive fields in primate somatosensory area 3b: Effects of stimulus scanning direction and orientation. *Journal of Neuroscience*, *20*(1), 495–510. https://doi.org/10.1523/jneurosci.20-01-00495.2000

Disbrow, E., Roberts, T. P. L., Slutsky, D., Rowley, H., & Krubitzer, L. (2000). A comparison of fMRI and electrophysiology in the anesthetized macaque monkey. *NeuroImage*, *11*(5 PART II), 2000. https://doi.org/10.1016/s1053-8119(00)91735-x

Dokka, K., DeAngelis, G. C., & Angelaki, D. E. (2015). Multisensory integration of visual and vestibular signals improves heading discrimination in the presence of a moving object. *Journal of Neuroscience*, *35*(40), 13599–13607. https://doi.org/10.1523/JNEUROSCI.2267-15.2015

Driver, J., & Noesselt, T. (2008). Multisensory Interplay Reveals Crossmodal Influences on "Sensory-Specific" Brain Regions, Neural Responses, and Judgments. *Neuron*, *57*(1), 11–

23. https://doi.org/10.1016/j.neuron.2007.12.013

Duffy, C. J., & Wurtz, R. H. (1991). Sensitivity of MST neurons to optic flow stimuli. II. Mechanisms of response selectivity revealed by small-field stimuli. *Journal of Neurophysiology*, *65*(6), 1346–1359. https://doi.org/10.1152/jn.1991.65.6.1346

Duhamel, J. R., Bremmer, F., BenHamed, S., & Graf, W. (1997). Spatial invariance of visual receptive fields in parietal cortex neurons. *Nature*, *389*(6653), 845–848. https://doi.org/10.1038/39865

Duhamel, J. R., Colby, C. L., & Goldberg, M. E. (1998). Ventral intraparietal area of the macaque: Congruent visual and somatic response properties. *Journal of Neurophysiology*, *79*(1), 126–136. https://doi.org/10.1152/jn.1998.79.1.126

Dukelow, S. P., DeSouza, J. F., Culham, J. C., van den Berg, A. V., Menon, R. S., Vilis, T., (2001). Distinguishing subregions of the human MT+ complex using visual fields and pursuit eye movements. *Journal of Neurophysiology*, *86*(4), 1991-2000.

Eickhoff, S. B., Stephan, K. E., Mohlberg, H., Grefkes, C., Fink, G. R., Amunts, K., & Zilles, K. (2005). A new SPM toolbox for combining probabilistic cytoarchitectonic maps and functional imaging data. *NeuroImage*, *25*(4), 1325–1335. https://doi.org/10.1016/j.neuroimage.2004.12.034

Ekstrom, A. D., & Ranganath, C. (2018). Space, time, and episodic memory: The hippocampus is all over the cognitive map. *Hippocampus*, *28*(9), 680–687. https://doi.org/10.1002/hipo.22750

Engel, D., Schütz, A., Krala, M., Schwenk, J. C. B., Morris, A. P., & Bremmer, F. (2020). Inter-trial phase coherence of visually evoked postural responses in virtual reality. *Experimental Brain Research*, *238*(5), 1177–1189. https://doi.org/10.1007/s00221-020-05782-2

Engel, D., Student, J., Schwenk, J. C. B., Morris, A. P., Waldthaler, J., Timmermann, L., & Bremmer, F. (2021). Visual perturbation of balance suggests impaired motor control but intact visuomotor processing in Parkinson's disease. *Journal of Neurophysiology*, *126*(4), 1076–1089. https://doi.org/10.1152/jn.00183.2021

Ericson, J. D., & Warren, W. H. (2020). Probing the Invariant Structure of Spatial Knowledge : Support for the cognitive graph hypothesis. *Cognition*, *200*, 104276

https://doi.org/10.1016/j.cognition.2020.104276

Ernst, M. O., & Banks, M. S. (2002). Humans integrate visual and haptic information in a. *Nature*, *415*(January), 429–433. https://doi.org/10.1038/415429a

Bartlett, F. C. (1932). Remembering: A study in experimental and socialpsychology. Cambridge, UK: Cambridge University Press

Farkhatdinov, I., & Hayward, V. (2013). *Vibrotactile Inputs To The Feet Can Modulate Vection*. 677–681. https://doi.org/10.1109/WHC.2013.6548490

Feng, M., & Lindeman, R. W. (2016). *An Initial Exploration of a Multi-Sensory Design Space : Tactile Support for Walking in Immersive Virtual Environments*. 95–104.

Fermin, A. S. R., Friston, K., & Yamawaki, S. (2022). An insula hierarchical network architecture for active interoceptive inference. *Royal Society Open Science*, *9*(6). https://doi.org/10.1098/rsos.220226

Ferrari, A., & Noppeney, U. (2021). Attention controls multisensory perception via 2 distinct mechanisms at different levels of the cortical hierarchy. In *PLoS Biology* (Vol. 19, Issue 11). https://doi.org/10.1371/journal.pbio.3001465

Fetsch, C. R., DeAngelis, G. C., & Angelaki, D. E. (2010). *Visual – vestibular cue integration for heading perception : applications of optimal cue integration theory*. *31*, 1721–1729. https://doi.org/10.1111/j.1460-9568.2010.07207.x

Fetsch, C. R., Turner, A. H., DeAngelis, G. C., & Angelaki, D. E. (2009). Dynamic reweighting of visual and vestibular cues during self-motion perception. *Journal of Neuroscience*, *29*(49), 15601–15612. https://doi.org/10.1523/JNEUROSCI.2574-09.2009

Fetsch, C. R., Wang, S., Gu, Y., DeAngelis, G. C., & Angelaki, D. E. (2007). Spatial reference frames of visual, vestibular, and multimodal heading signals in the dorsal subdivision of the medial superior temporal area. *Journal of Neuroscience*, *27*(3), 700–712. https://doi.org/10.1523/JNEUROSCI.3553-06.2007

Field, D. T., Biagi, N., & Inman, L. A. (2020). The role of the ventral intraparietal area (VIP/pVIP) in the perception of object-motion and self-motion. *NeuroImage*, *213*(August 2019). https://doi.org/10.1016/j.neuroimage.2020.116679

Finnerty, G. T., Shadlen, M. N., Jazayeri, M., Nobre, A. C., & Buonomano, D. V. (2015). Time in cortical circuits. *Journal of Neuroscience*, *35*(41), 13912–13916.

https://doi.org/10.1523/JNEUROSCI.2654-15.2015

Fitzgerald, P. J., Lane, J. W., Thakur, P. H., & Hsiao, S. S. (2006). Receptive field properties of the macaque second somatosensory cortex: Representation of orientation on different finger pads. *Journal of Neuroscience*, *26*(24), 6473–6484. https://doi.org/10.1523/JNEUROSCI.5057-05.2006

Flandin, G., & Friston, K. J. (2019). Analysis of family-wise error rates in statistical parametric mapping using random field theory. *Human Brain Mapping*, *40*(7), 2052–2054. https://doi.org/10.1002/hbm.23839

Foster, C., Sheng, W. A., Heed, T., & Ben Hamed, S. (2022). The macaque ventral intraparietal area has expanded into three homologue human parietal areas. *Progress in Neurobiology*, *209*, 102185. https://doi.org/10.1016/j.pneurobio.2021.102185

French, R. L., & DeAngelis, G. C. (2020). Multisensory neural processing: from cue integration to causal inference. *Current Opinion in Physiology*, *16*, 8–13. https://doi.org/10.1016/j.cophys.2020.04.004

Frenz, H., Bührmann, T., Lappe, M., & Kolesnik, M. (2007). Estimation of Travel Distance from Visual Motion in Virtual Environments. *ACM Transactions on Applied Perception*, *4*(1), 3. https://doi.org/10.1145/1227134.1227137

Frenz, H., & Lappe, M. (2005). Absolute travel distance from optic flow. *Vision Research*, *45*(13), 1679–1692. https://doi.org/10.1016/j.visres.2004.12.019

Friston, K. (2005). A theory of cortical responses. *Philosophical Transactions of the Royal Society B: Biological Sciences*, *360*(1456), 815–836. https://doi.org/10.1098/rstb.2005.1622

Friston, K. J., Holmes, A., Poline, J. B., Price, C. J., & Frith, C. D. (1996). Detecting activations in pet and fMRI: Levels of inference and power. *NeuroImage*, *4*(3), 223–235. https://doi.org/10.1006/nimg.1996.0074

Friston, K., & Kiebel, S. (2009). Predictive coding under the free-energy principle. *Philosophical Transactions of the Royal Society B: Biological Sciences*, *364*(1521), 1211–1221. https://doi.org/10.1098/rstb.2008.0300

Friston, K. J., Ashburner, J., Frith, C. D., Poline, J. -B, Heather, J. D., & Frackowiak, R. S. J. (1995). Spatial registration and normalization of images. *Human Brain Mapping*, *3*(3),

165–189. https://doi.org/10.1002/hbm.460030303

Garrido, M. I., Rowe, E. G., Halász, V., & Mattingley, J. B. (2018). Bayesian Mapping Reveals That Attention Boosts Neural Responses to Predicted and Unpredicted Stimuli. *Cerebral Cortex*, *28*(5), 1771–1782. https://doi.org/10.1093/cercor/bhx087

Garvert, M. M., Saanum, T., Schulz, E., Schuck, N. W., & Doeller, C. F. (2021). Hippocampal spatio-temporal cognitive maps adaptively guide reward generalization. *BioRxiv*, *26*(April), 2021.10.22.465012. https://doi.org/10.1038/s41593-023-01283-x

Gepshtein, S., Burge, J., Ernst, M. O., & Banks, M. S. (2005). The combination of vision and touch depends on spatial proximity. *Journal of Vision*, *5*(11), 1013–1023. https://doi.org/10.1167/5.11.7

Gottlieb, J. (2007). From Thought to Action: The Parietal Cortex as a Bridge between Perception, Action, and Cognition. *Neuron*, *53*(1), 9–16. https://doi.org/10.1016/j.neuron.2006.12.009

Gu, Y. (2018). Vestibular signals in primate cortex for self-motion perception. *Current Opinion in Neurobiology*, *52*, 10–17. https://doi.org/10.1016/j.conb.2018.04.004

Gu, Y., Angelaki, D. E., & DeAngelis, G. C. (2008). *Neural correlates of multisensory cue integration in macaque MSTd*. *11*(10), 1201–1210. https://doi.org/10.1038/nn.2191

Gu, Y., DeAngelis, G. C., & Angelaki, D. E. (2012). Causal links between dorsal medial superior temporal area neurons and multisensory heading perception. *Journal of Neuroscience*, *32*(7), 2299–2313. https://doi.org/10.1523/JNEUROSCI.5154-11.2012

Gu, Y., Watkins, P. V., Angelaki, D. E., & DeAngelis, G. C. (2006). Visual and nonvisual contributions to three-dimensional heading selectivity in the medial superior temporal area. *Journal of Neuroscience*, *26*(1), 73–85. https://doi.org/10.1523/JNEUROSCI.2356-05.2006

Guipponi, O., Cléry, J., Odouard, S., Wardak, C., & Ben Hamed, S. (2015). Whole brain mapping of visual and tactile convergence in the macaque monkey. *NeuroImage*, *117*, 93–102. https://doi.org/10.1016/j.neuroimage.2015.05.022

Guipponi, O., Wardak, C., Ibarrola, D., Comte, J. C., Sappey-Marinier, D., Pinède, S., & Hamed, S. Ben. (2013). Multimodal convergence within the intraparietal sulcus of the macaque monkey. *Journal of Neuroscience*, *33*(9), 4128–4139.

https://doi.org/10.1523/JNEUROSCI.1421-12.2013

Harrar, V., & Harris, L. R. (2009). Eye position affects the perceived location of touch. *Experimental Brain Research*, *198*(2–3), 403–410. https://doi.org/10.1007/s00221-009-1884-4

Harrar, V., & Harris, L. R. (2010). Touch used to guide action is partially coded in a visual reference frame. *Experimental Brain Research*, *203*(3), 615–620. https://doi.org/10.1007/s00221-010-2252-0

Harris, L. R., Sakurai, K., & Beaudot, W. H. A. (2017). Tactile Flow Overides Other Cues to Self Motion. *Scientific Reports*, *7*(1), 1–8. https://doi.org/10.1038/s41598-017-01111-w

Harrison, S. J., & Davis, T. J. (2023). Homing tasks performed using variations of crawling gait patterns reveal a role for attention in podokinetic path integration. *Experimental Brain Research*, *241*(3), 825–838. https://doi.org/10.1007/s00221-023-06558-0

Harrison, S. J., Reynolds, N., Bishoff, B., & Stergiou, N. (2021). Assessing the relative contribution of vision to odometry via manipulations of gait in an over-ground homing task. *Experimental Brain Research*, *239*(4), 1305–1316. https://doi.org/10.1007/s00221-021-06066-z

Ho, C., & Spence, C. (2007). Head orientation biases tactile localization. *Brain Research*, *1144*(1), 136–141. https://doi.org/10.1016/j.brainres.2007.01.091

Hollands, M., Patla, A., & Vickers, J. (2002). “Look where you’re going!”: Gaze behaviour associated with maintaining and changing the direction of locomotion. *Experimental Brain Research*, *143*(2), 221–230. https://doi.org/10.1007/s00221-001-0983-7

Homma, C. T., & Ashida, H. (2015). What makes space-time interactions in human vision asymmetrical? *Frontiers in Psychology*, *6*(JUN), 1–8. https://doi.org/10.3389/fpsyg.2015.00756

Hou, H., & Gu, Y. (2020). Multisensory Integration for Self-Motion Perception. In *The Senses: A Comprehensive Reference* (Issue February). https://doi.org/10.1016/b978-0-12-809324-5.23879-0

Hsu, Y. F., Hämäläinen, J. A., & Waszak, F. (2014). Both attention and prediction are necessary for adaptive neuronal tuning in sensory processing. *Frontiers in Human Neuroscience*, *8*(MAR), 1–9. https://doi.org/10.3389/fnhum.2014.00152

Huang, R. S., Chen, C. F., & Sereno, M. I. (2015). Neural substrates underlying the passive observation and active control of translational egomotion. *Journal of Neuroscience*, *35*(10), 4258–4267. https://doi.org/10.1523/JNEUROSCI.2647-14.2015

Hubel, D. H., & Wiesel, T. N. (1968). Receptive fields and functional architecture of monkey striate cortex. *The Journal of Physiology*, *195*(1), 215–243. https://doi.org/10.1113/jphysiol.1968.sp008455

Huk, A. C., Dougherty, R. F., & Heeger, D. J. (2002). *Retinotopy and Functional Subdivision of Human Areas MT and MST*. *22*(16), 7195–7205. https://doi.org/10.1523/JNEUROSCI.22-16-07195.2002

Humphreys, G. F., Lambon Ralph, M. A., & Simons, J. S. (2021). A Unifying Account of Angular Gyrus Contributions to Episodic and Semantic Cognition. *Trends in Neurosciences*, *44*(6), 452–463. https://doi.org/10.1016/j.tins.2021.01.006

Iamshchinina, P., Kaiser, D., Yakupov, R., Haenelt, D., Sciarra, A., Mattern, H., Luesebrink, F., Duezel, E., Speck, O., Weiskopf, N., & Cichy, R. M. (2021). Perceived and mentally rotated contents are differentially represented in cortical depth of V1. *Communications Biology*, *4*(1), 1–8. https://doi.org/10.1038/s42003-021-02582-4

Ilg, U. J., & Schumann, S. (2022). *Primate Area MST-l Is Involved in the Generation of Goal-Directed Eye and Hand Movements*. 761–771. https://doi.org/10.1152/jn.00278.2006.

Indovina, I., Maffei, V., Mazzarella, E., Sulpizio, V., Galati, G., & Lacquaniti, F. (2016). Path integration in 3D from visual motion cues: A human fMRI study. *NeuroImage*, *142*, 512–521. https://doi.org/10.1016/j.neuroimage.2016.07.008

Israël, I., Capelli, A., Priot, A. E., & Giannopulu, I. (2013). Spatial linear navigation: Is vision necessary? *Neuroscience Letters*, *554*, 34–38. https://doi.org/10.1016/j.neulet.2013.08.060

Jehu, D. A., Desponts, A., Paquet, N., & Lajoie, Y. (2015). Prioritizing attention on a reaction time task improves postural control and reaction time. *International Journal of Neuroscience*, *125*(2), 100–106. https://doi.org/10.3109/00207454.2014.907573

Jiang, J., Summerfield, C., & Egner, T. (2013). Attention sharpens the distinction between expected and unexpected percepts in the visual brain. *Journal of Neuroscience*, *33*(47), 18438–18447. https://doi.org/10.1523/JNEUROSCI.3308-13.2013

Jones, S. A., Beierholm, U., Meijer, D., & Noppeney, U. (2019). Older adults sacrifice response speed to preserve multisensory integration performance. *Neurobiology of Aging*, *84*, 148–157. https://doi.org/10.1016/j.neurobiolaging.2019.08.017

Jörges, B., & Harris, L. R. (2022). Object speed perception during lateral visual self-motion. *Attention, Perception, and Psychophysics*, *84*(1), 25–46. https://doi.org/10.3758/s13414-021-02372-4

Kaminiarz, A., Schlack, A., Hoffmann, K., Lappe, M., & Bremmer, F. (2022). *Visual selectivity for heading in the macaque ventral intraparietal area*. 2470–2480. https://doi.org/10.1152/jn.00410.2014

Kandula, M., Hofman, D., & Dijkerman, H. C. (2015). Visuo-tactile interactions are dependent on the predictive value of the visual stimulus. *Neuropsychologia*, *70*, 358–366. https://doi.org/10.1016/j.neuropsychologia.2014.12.008

Kashkouli Nejad, K., Sugiura, M., Nozawa, T., Kotozaki, Y., Furusawa, Y., Nishino, K., Nukiwa, T., & Kawashima, R. (2015). Supramarginal activity in interoceptive attention tasks. *Neuroscience Letters*, *589*(February), 42–46. https://doi.org/10.1016/j.neulet.2015.01.031

Kautzky, M., & Thurley, K. (2016). Estimation of self-motion duration and distance in rodents. *Royal Society Open Science*, *3*(5). https://doi.org/10.1098/rsos.160118

Keshavarz, B., Hettinger, L. J., Vena, D., & Campos, J. L. (2014). Combined effects of auditory and visual cues on the perception of vection. *Experimental Brain Research*, *232*(3), 827–836. https://doi.org/10.1007/s00221-013-3793-9

Kim, T., Bair, W., & Pasupathy, A. (2022). Perceptual Texture Dimensions Modulate Neuronal Response Dynamics in Visual Cortical Area V4. *The Journal of Neuroscience : The Official Journal of the Society for Neuroscience*, *42*(4), 631–642. https://doi.org/10.1523/JNEUROSCI.0971-21.2021

Kleiner M., Brainard D., Pelli D., Ingling A., Murray R., Broussard C. (2007). What's new in Psychtoolbox-3? *Perception*, *36*, ECVP Abstract Supplement.

Kleinschmidt, A., Thilo, K. V., Büchel, C., Gresty, M. A., Bronstein, A. M., & Frackowiak, R. S. J. (2002). Neural correlates of visual-motion perception as object- or self-motion. *NeuroImage*, *16*(4), 873–882. https://doi.org/10.1006/nimg.2002.1181

Knill, D. C., & Pouget, A. (2004). The Bayesian brain: The role of uncertainty in neural coding and computation. *Trends in Neurosciences*, *27*(12), 712–719. https://doi.org/10.1016/j.tins.2004.10.007

Kok, P., Rahnev, D., Jehee, J. F. M., Lau, H. C., & De Lange, F. P. (2012). Attention reverses the effect of prediction in silencing sensory signals. *Cerebral Cortex*, *22*(9), 2197–2206. https://doi.org/10.1093/cercor/bhr310

Körding, K. P., & Wolpert, D. M. (2006). Bayesian decision theory in sensorimotor control. *Trends in Cognitive Sciences*, *10*(7), 319–326. https://doi.org/10.1016/j.tics.2006.05.003

Kovács, G., Raabe, M., & Greenlee, M. W. (2008). Neural correlates of visually induced self-motion illusion in depth. *Cerebral Cortex*, *18*(8), 1779–1787. https://doi.org/10.1093/cercor/bhm203

Krala, M., van Kemenade, B., Straube, B., Kircher, T., & Bremmer, F. (2019). Predictive coding in a multisensory path integration task: An fMRI study. *Journal of Vision*, *19*(11), 13. https://doi.org/10.1167/19.11.13

Krüger, B., Hegele, M., & Rieger, M. (2022). The multisensory nature of human action imagery. *Psychological Research*, *ii*. https://doi.org/10.1007/s00426-022-01771-y

Kubovy, M., Holcombe, A. O., & Wagemans, J. (1998). On the Lawfulness of Grouping by Proximity. *Cognitive Psychology*, *35*(1), 71–98. https://doi.org/10.1006/cogp.1997.0673

Kuehn, E., & Pleger, B. (2020). Encoding schemes in somatosensation: From micro- to meta-topography. *NeuroImage*, *223*(August). https://doi.org/10.1016/j.neuroimage.2020.117255

Lacey, S., Flueckiger, P., Stilla, R., Lava, M., & Sathian, K. (2010). Object familiarity modulates the relationship between visual object imagery and haptic shape perception. *NeuroImage*, *49*(3), 1977–1990. https://doi.org/10.1016/j.neuroimage.2009.10.081

Lacey, S., Lin, J. B., & Sathian, K. (2011). Object and spatial imagery dimensions in visuo-haptic representations. *Experimental Brain Research*, *213*(2–3), 267–273. https://doi.org/10.1007/s00221-011-2623-1

Lambrechts, A., Walsh, V., & Van Wassenhove, V. (2013). Evidence accumulation in the magnitude system. *PLoS ONE*, *8*(12). https://doi.org/10.1371/journal.pone.0082122

Lappe, M., Bremmer, F., Pekel, M., Thiele, A., & Hoffmann, K. P. (1996). Optic flow

processing in monkey STS: a theoretical and experimental approach. *Journal of Neuroscience*, *16*(19), 6265-6285. https://doi.org/10.1523/JNEUROSCI.16-19-06265.1996

Lappe, M., Bremmer, F., & Van Den Berg, A. V. V. (1999). Perception of self motion from visual flow. *Trends in Cognitive Sciences*, *3*(9), 329–336. https://doi.org/10.1016/S1364-6613(99)01364-9

Lappe, M., Jenkin, M., & Harris, L. R. (2007). Travel distance estimation from visual motion by leaky path integration. *Experimental Brain Research*, *180*(1), 35–48. https://doi.org/10.1007/s00221-006-0835-6

Lappe, M., & Rauschecker, J. P. (1993). *A neural network for the processing of optic flow from ego-motion in man and higher mammals* (Vol. 5, pp. 374–391). https://doi.org/10.1162/neco.1993.5.3.374

Lappe, M., & Rauschecker, J. P. (1994). Heading detection from optic flow. *Nature*, *369*, 712–713. https://doi.org/10.1038/369712a0

Layton, O. W., & Fajen, B. R. (2016). Sources of bias in the perception of heading in the presence of moving objects: Object-based and border-based discrepancies. *Journal of Vision*, *16*(1), 1–18. https://doi.org/10.1167/16.1.9

Layton, O. W., Mingolla, E., & Browning, N. A. (2012). A motion pooling model of visually guided navigation explains human behavior in the presence of independently moving objects. *Journal of Vision*, *12*(1), 1–19. https://doi.org/10.1167/12.1.20

Li, L., Peli, E., & Warren, W. H. (2002). Heading perception in patients with advanced retinitis pigmentosa. *Optometry and Vision Science*, *79*(9), 581–589. https://doi.org/10.1097/00006324-200209000-00009

Lich, M., & Bremmer, F. (2014). Self-motion perception in the elderly. *Frontiers in Human Neuroscience*, *8*(September), 1–15. https://doi.org/10.3389/fnhum.2014.00681

Lutfi, R. A., & Wang, W. (1999). Correlational analysis of acoustic cues for the discrimination of auditory motion. *The Journal of the Acoustical Society of America*, *106*(2), 919–928. https://doi.org/10.1121/1.428033

Ma, W. J., Beck, J. M., Latham, P. E., & Pouget, A. (2006). Bayesian inference with probabilistic population codes. *Nature Neuroscience*, *9*(11), 1432–1438. https://doi.org/10.1038/nn1790

MacKay, D. J. (2013). Information theory, inference and learning algorithms. In *Cambridge university press.* (Vol. 13). https://doi.org/10.1166/asl.2012.3830

Mao, D. (2023). Neural Correlates of Spatial Navigation in Primate Hippocampus. *Neuroscience Bulletin*, *39*(2), 315–327. https://doi.org/10.1007/s12264-022-00968-w

Matthis, J. S., Muller, K. S., Bonnen, K., & Hayhoe, M. M. (2020). Retinal optic flow during natural locomotion. *BioRxiv*, 2020.07.23.217893. https://doi.org/10.1101/2020.07.23.217893

Matthis, J. S., Muller, K. S., Bonnen, K. L., & Hayhoe, M. M. (2022). Retinal optic flow during natural locomotion. In *PLoS Computational Biology* (Vol. 18, Issue 2). https://doi.org/10.1371/journal.pcbi.1009575

Mauk, M. D., & Buonomano, D. V. (2004). The neural basis of temporal processing. *Annual Review of Neuroscience*, *27*, 307–340. https://doi.org/10.1146/annurev.neuro.27.070203.144247

Maunsell, J. H. R., & Van Essen, D. C. (1983). The Connections of the Middel Temporal Visual Area (MT) and Their Relationship to a Cortical Hie. *Journal of Neuroscience*, *3*(12), 2563–2586. http://www.jneurosci.org/content/jneuro/3/12/2563.full.pdf

McKerrow, P. (2008). Acoustic flow. *2008 IEEE/RSJ International Conference on Intelligent Robots and Systems, IROS*, 1365–1370. https://doi.org/10.1109/IROS.2008.4650800

Meijer, D., Veselič, S., Calafiore, C., & Noppeney, U. (2019). Integration of audiovisual spatial signals is not consistent with maximum likelihood estimation. *Cortex*, *119*, 74–88. https://doi.org/10.1016/j.cortex.2019.03.026

Merchant, H., Harrington, D. L., & Meck, W. H. (2013). Neural basis of the perception and estimation of time. *Annual Review of Neuroscience*, *36*, 313–336. https://doi.org/10.1146/annurev-neuro-062012-170349

Meredith, M. A., & Stein, B. E. (1986). Visual, auditory, and somatosensory convergence on cells in superior colliculus results in multisensory integration. *Journal of neurophysiology*, *56*(3), 640-662. https://doi.org/10.1152/jn.1986.56.3.640

Mergner, T., & Rosemeier, T. (1998). Interaction of vestibular, somatosensory and visual signals for postural control and motion perception under terrestrial and microgravity conditions - A conceptual model. *Brain Research Reviews*, *28*(1–2), 118–135.

https://doi.org/10.1016/S0165-0173(98)00032-0

Mertz, S., Belkhenchir, S., & Lepecq, J. C. (2000). Evidence of imagined passive self-motion through imagery-perception interaction. *Acta Psychologica*, *105*(1), 57–78. https://doi.org/10.1016/S0001-6918(00)00048-2

Mishkin, M., Ungerleider, L. G., & Macko, K. A. (1983). Object vision and spatial vision: two cortical pathways. *Trends in neurosciences*, *6*, 414-417. https://doi.org/10.1016/0166-2236(83)90190-X

Moraresku, S., & Vlcek, K. (2020). The Use of Egocentric and Allocentric Reference Frames in Static and Dynamic Conditions in Humans. *Physiological Research*, *69*(5), 787–801. https://doi.org/10.33549/physiolres.934528

Morillon, B., Arnal, L. H., Schroeder, C. E., & Keitel, A. (2019). Prominence of delta oscillatory rhythms in the motor cortex and their relevance for auditory and speech perception. *Neuroscience and Biobehavioral Reviews*, *107*, 136–142. https://doi.org/10.1016/j.neubiorev.2019.09.012

Morris, A. P., Kubischik, M., Hoffmann, K. P., Krekelberg, B., & Bremmer, F. (2012). Dynamics of eye-position signals in the dorsal visual system. *Current Biology*, *22*(3), 173–179. https://doi.org/10.1016/j.cub.2011.12.032

Müller, R., & Schnitzler, H.-U. (2000). Acoustic flow perception in cf-bats: Extraction of parameters. *The Journal of the Acoustical Society of America*, *108*(3), 1298. https://doi.org/10.1121/1.1287842

Mullette-Gillman, O. A., Cohen, Y. E., & Groh, J. M. (2005). Eye-centered, head-centered, and complex coding of visual and auditory targets in the intraparietal sulcus. *Journal of Neurophysiology*, *94*(4), 2331–2352. https://doi.org/10.1152/jn.00021.2005

Mumford, D. (1992). On the computational architecture of the neocortex - II The role of cortico-cortical loops. *Biological Cybernetics*, *66*(3), 241–251. https://doi.org/10.1007/BF00198477

Murata, K., Seno, T., Ozawa, Y., & Ichihara, S. (2014). Self-Motion Perception Induced by Cutaneous Sensation Caused by Constant Wind. *Psychology*, *05*(15), 1777–1782. https://doi.org/10.4236/psych.2014.515184

Murovec, B., Spaniol, J., & Campos, J. L. (2021). *Multisensory Effects on Illusory Self-Motion (*

Vection): the Role of Visual , Auditory , and Tactile Cues. 0–2. https://doi.org/10.1163/22134808-bja10058

Näätänen, R., & Michie, P. T. (1979). Early selective-attention effects on the evoked potential: A critical review and reinterpretation. *Biological Psychology*, *8*(2), 81–136. https://doi.org/10.1016/0301-0511(79)90053-X

Nadler, J. W., Barbash, D., Kim, H. G. R., Shimpi, S., Angelaki, D. E., & DeAngelis, G. C. (2013). Joint representation of depth from motion parallax and binocular disparity cues in macaque area MT. *Journal of Neuroscience*, *33*(35), 14061–14074. https://doi.org/10.1523/JNEUROSCI.0251-13.2013

Nakamura, H., Kuroda, T., Wakita, M., Kusunoki, M., Kato, A., Mikami, A., Sakata, H., & Itoh, K. (2001). From Three-Dimensional Space Vision to Prehensile Hand Movements : The Lateral Intraparietal Area Links the Area V3A and the Anterior Intraparietal Area in Macaques. *Journal of Neuroscience*, *21*(20), 8174–8187.

Nakhla, N., Korkian, Y., Krause, M. R., & Pack, C. C. (2021). Neural selectivity for visual motion in macaque area v3a. *ENeuro*, *8*(1), 1–14. https://doi.org/10.1523/ENEURO.0383-20.2020

Nau, M., Navarro Schröder, T., Bellmund, J. L. S., & Doeller, C. F. (2018). Hexadirectional coding of visual space in human entorhinal cortex. *Nature Neuroscience*, *21*(2), 188–190. https://doi.org/10.1038/s41593-017-0050-8

Nau, M., Schindler, A., & Bartels, A. (2018). Real-motion signals in human early visual cortex. *NeuroImage*, *175*, 379–387. https://doi.org/10.1016/j.neuroimage.2018.04.012

Nichols, T., Brett, M., Andersson, J., Wager, T., & Poline, J. B. (2005). Valid conjunction inference with the minimum statistic. *NeuroImage*, *25*(3), 653–660. https://doi.org/10.1016/j.neuroimage.2004.12.005

Nielson, D. M., Smith, T. A., Sreekumar, V., Dennis, S., & Sederberg, P. B. (2015). Human hippocampus represents space and time during retrieval of real-world memories. *Proceedings of the National Academy of Sciences of the United States of America*, *112*(35), 11078–11083. https://doi.org/10.1073/pnas.1507104112

Noel, J. P., & Angelaki, D. E. (2022). Cognitive, Systems, and Computational Neurosciences of the Self in Motion. *Annual Review of Psychology*, *73*, 103–129.

https://doi.org/10.1146/annurev-psych-021021-103038

O'Keefe, J., Dostrovsky, J., & J. O'Keefe, J. D. (1971). Short Communications The hippocampus as a spatial map . Preliminary evidence from unit activity in the freely-moving rat. *Brain Research*, *34*(1), 171–175. https://doi.org/10.1016/0006-8993(71)90358-1

O'Keefe, John. (1976). Place units in the hippocampus of the freely moving rat. *Experimental Neurology*, *51*(1), 78–109. https://doi.org/10.1016/0014-4886(76)90055-8

O'Keefe, John, & Nadel, L. (1979). The Hippocampus as a Cognitive Map. In *American Journal of Psychiatry* (Vol. 136, Issue 10). https://doi.org/10.1176/ajp.136.10.1353

Oldfield, R. C. (1971). The assessment and analysis of handedness: the Edinburgh inventory. *Neuropsychologia*, *9*(1), 97-113. https://doi.org/10.1016/0028-3932(71)90067-4

Orban, G. A., Fize, D., Peuskens, H., Denys, K., Nelissen, K., Sunaert, S., Todd, J., & Vanduffel, W. (2003). Similarities and differences in motion processing between the human and macaque brain: Evidence from fMRI. *Neuropsychologia*, *41*(13), 1757–1768. https://doi.org/10.1016/S0028-3932(03)00177-5

Ouarti, N., Lécuyer, A., & Berthoz, A. (2014, February). Haptic motion: Improving sensation of self-motion in virtual worlds with force feedback. In *2014 IEEE Haptics Symposium (HAPTICS)* (pp. 167-174). IEEE. https://doi.org/10.1109/HAPTICS.2014.6775450

Pack, C. C., & Bensmaia, S. J. (2015). Seeing and Feeling Motion: Canonical Computations in Vision and Touch. *PLoS Biology*, *13*(9), 1–11. https://doi.org/10.1371/journal.pbio.1002271

Palmisano, S., Allison, R. S., Schira, M. M., & Barry, R. J. (2015). Future challenges for vection research: Definitions, functional significance, measures, and neural bases. *Frontiers in Psychology*, *6*(FEB), 1–15. https://doi.org/10.3389/fpsyg.2015.00193

Paolini, M., Distler, C., Bremmer, F., Lappe, M., & Hoffmann, K. (2000). Responses to continuously changing optic flow in area MST. *Journal of Neurophysiology*, *84*(2), 730–743. https://doi.org/10.1152/jn.2000.84.2.730

Pei, Y. C., & Bensmaia, S. J. (2014). The neural basis of tactile motion perception. *Journal of Neurophysiology*, *112*(12), 3023–3032. https://doi.org/10.1152/jn.00391.2014

Pei, Y. C., Hsiao, S. S., Craig, J. C., & Bensmaia, S. J. (2010). Shape invariant coding of motion

direction in somatosensory cortex. *PLoS Biology*, *8*(2). https://doi.org/10.1371/journal.pbio.1000305

Perrone, J. A., & Thiele, A. (2001). Speed skills: Measuring the visual speed analyzing properties of primate MT neurons. *Nature Neuroscience*, *4*(5), 526–532. https://doi.org/10.1038/87480

Pitzalis, S., Sereno, M. I., Committeri, G., Fattori, P., Galati, G., Patria, F., & Galletti, C. (2010). Human V6: The medial motion area. *Cerebral Cortex*, *20*(2), 411–424. https://doi.org/10.1093/cercor/bhp112

Pitzalis, S., Sdoia, S., Bultrini, A., Committeri, G., Di Russo, F., Fattori, P., Galletti, C., & Galati, G. (2013). Selectivity to Translational Egomotion in Human Brain Motion Areas. *PLoS ONE*, *8*(4), 1–14. https://doi.org/10.1371/journal.pone.0060241

Pitzalis, S., Serra, C., Sulpizio, V., Committeri, G., de Pasquale, F., Fattori, P., Galletti, C., Sepe, R., & Galati, G. (2020). Neural bases of self- and object-motion in a naturalistic vision. *Human Brain Mapping*, *41*(4), 1084–1111. https://doi.org/10.1002/hbm.24862

Poirier, C., Baumann, S., Dheerendra, P., Joly, O., Hunter, D., Balezeau, F., Sun, L., Rees, A., Petkov, C. I., Thiele, A., & Griffiths, T. D. (2017). Auditory motion-specific mechanisms in the primate brain. *PLoS Biology*, *15*(5), 1–24. https://doi.org/10.1371/journal.pbio.2001379

Poucet, B. (1993). Spatial Cognitive Maps in Animals: New Hypotheses on Their Structure and Neural Mechanisms. *Psychological Review*, *100*(2), 163–182. https://doi.org/10.1037/0033-295X.100.2.163

Pretto, P., Ogier, M., Bülthoff, H. H., & Bresciani, J. P. (2009). Influence of the size of the field of view on motion perception. *Computers and Graphics (Pergamon)*, *33*(2), 139–146. https://doi.org/10.1016/j.cag.2009.01.003

Prinzmetal, W., Park, S., & Garrett, R. (2005). Involuntary attention and identification accuracy. *Perception and Psychophysics*, *67*(8), 1344–1353. https://doi.org/10.3758/BF03193639

Pritchett, L. M., & Harris, L. R. (2011). Perceived touch location is coded using a gaze signal. *Experimental Brain Research*, *213*(2–3), 229–234. https://doi.org/10.1007/s00221-011-2713-0

Raftery, A. E. (2016). *Bayesian Model Selection in Social Research Author (s): Adrian E . Raftery Source : Sociological Methodology , Vol . 25 (1995), pp . 111-163 Published by : American Sociological Association Stable URL : http://www.jstor.org/stable/271063 Accessed : 29*. *25*(1995), 111–163.

Rahnev, D., & Denison, R. N. (2018). Suboptimality in perceptual decision making. *Behavioral and Brain Sciences*, *41*. https://doi.org/10.1017/S0140525X18000936

Ramkhalawansingh, R., Butler, J. S., & Campos, J. L. (2018). Visual-vestibular integration during self-motion perception in younger and older adults. *Psychology and Aging*, *33*(5), 798–813. https://doi.org/10.1037/pag0000271

Rao, R. P. N., & Ballard, D. H. (1999). Predictive coding in the visual cortex: A functional interpretation of some extra-classical receptive-field effects. *Nature Neuroscience*, *2*(1), 79–87. https://doi.org/10.1038/4580

Redlick, F. P., Jenkin, M., & Harris, L. R. (2001). Humans can use optic flow to estimate distance of travel. *Vision Research*, *41*(2), 213–219. https://doi.org/10.1016/S0042-6989(00)00243-1

Reznik, D. (2021). Action-Locked Neural Responses in Auditory Cortex to Self-Generated Sounds. *International Journal of Psychophysiology*, *168*, S92. https://doi.org/10.1016/j.ijpsycho.2021.07.283

Riecke, B. E., Västfjäll, D., Larsson, P., & Schulte-Pelkum, J. (2005, July). Top-down and multi-modal influences on self-motion perception in virtual reality. In *Proceedings of HCI international 2005* (pp. 1-10).

Riecke, B. E., Feuereissen, D., & Rieser, J. J. (2008, August). Auditory self-motion illusions (" circular vection") can be facilitated by vibrations and the potential for actual motion. In *Proceedings of the 5th Symposium on Applied Perception in Graphics and Visualization* (pp. 147-154).

Rieger, M., & Massen, C. (2014). Tool characteristics in imagery of tool actions. *Psychological Research*, *78*(1), 10–17. https://doi.org/10.1007/s00426-013-0481-0

Riemer, M., Achtzehn, J., Kuehn, E., & Wolbers, T. (2022). Cross-dimensional interference between time and distance during spatial navigation is mediated by speed representations in intraparietal sulcus and area hMT+. *NeuroImage*, *257*(March),

119336. https://doi.org/10.1016/j.neuroimage.2022.119336

Riemer, M., Shine, J. P., & Wolbers, T. (2018). On the (a)symmetry between the perception of time and space in large-scale environments. *Hippocampus*, *28*(8), 539–548. https://doi.org/10.1002/hipo.22954

Rodriguez, R., & Crane, B. T. (2019). Effect of range of heading differences on human visual–inertial heading estimation. *Experimental Brain Research*, *237*(5), 1227–1237. https://doi.org/10.1007/s00221-019-05506-1

Rodriguez, R., & Crane, B. T. (2021). Effect of timing delay between visual and vestibular stimuli on heading perception. *Journal of Neurophysiology*, *126*(1), 304–312. https://doi.org/10.1152/jn.00351.2020

Rolls, E. T. (2020). Spatial coordinate transforms linking the allocentric hippocampal and egocentric parietal primate brain systems for memory, action in space, and navigation. *Hippocampus*, *30*(4), 332–353. https://doi.org/10.1002/hipo.23171

Rosenblum, L., Grewe, E., Churan, J., & Bremmer, F. (2022). Influence of Tactile Flow on Visual Heading Perception. *Multisensory Research*, *79*(8), 1–18. https://doi.org/10.1163/22134808-bja10071

Rosenblum, L., Kreß, A., Arikan, B.E., Straube, B., Bremmer, F. (2023). Neural correlates of visual and tactile path integration and their task related modulation. *Sci Rep, 13*(9913) https://doi.org/10.1038/s41598-023-36797-8

Rosenblum, L., Kreß, A., Schwenk, J. C., & Bremmer, F. (2022). Visuo-tactile heading perception. *Journal of Neurophysiology*, *128*(5), 1355-1364. https://doi.org/10.1152/jn.00231.2022

Royden, C. S., & Hildreth, E. C. (1996). Human heading judgments in the presence of moving objects. *Perception and Psychophysics*, *58*(6), 836–856. https://doi.org/10.3758/BF03205487

Rugg, M. D., & King, D. R. (2018). Ventral lateral parietal cortex and episodic memory retrieval. *Cortex*, *107*, 238–250. https://doi.org/10.1016/j.cortex.2017.07.012

Ruiz, S., Crespo, P., & Romo, R. (1995). Representation of moving tactile stimuli in the somatic sensory cortex of awake monkeys. *Journal of Neurophysiology*, *73*(2), 525–537. https://doi.org/10.1152/jn.1995.73.2.525

Saito, H. A., Yukie, M., Tanaka, K., Hikosaka, K., Fukada, Y., & Iwai, E. (1986). Integraton of direction signals of image motion in the superior temporal sulcus of the Macaque monkey. *Journal of Neuroscience*, *6*(1), 145–157. https://doi.org/10.1523/jneurosci.06-01-00145.1986

Sasaki, R., Angelaki, D. E., & DeAngelis, G. C. (2017). Dissociation of self-motion and object motion by linear population decoding that approximates marginalization. *Journal of Neuroscience*, *37*(46), 11204–11219. https://doi.org/10.1523/JNEUROSCI.1177-17.2017

Sasaki, R., Angelaki, D. E., & DeAngelis, G. C. (2019). Processing of object motion and self-motion in the lateral subdivision of the medial superior temporal area in macaques. *Journal of Neurophysiology*, *121*(4), 1207–1221. https://doi.org/10.1152/jn.00497.2018

Sasaki, R., Anzai, A., Angelaki, D. E., & DeAngelis, G. C. (2020). Flexible coding of object motion in multiple reference frames by parietal cortex neurons. *Nature Neuroscience*, *23*(8), 1004–1015. https://doi.org/10.1038/s41593-020-0656-0

Sathian, K., & Zangaladze, A. (2002). Feeling with the mind's eye: Contribution of visual cortex to tactile perception. *Behavioural Brain Research*, *135*(1–2), 127–132. https://doi.org/10.1016/S0166-4328(02)00141-9

Sathian, K., Zangaladze, A., Hoffman, J. M., & Grafton, S. T. (1997). Feeling with the mind's eye. *NeuroReport*, *8*(18), 3877–3881. https://doi.org/10.1097/00001756-199712220-00008

Saunders, J. A. (2014). Reliability and relative weighting of visual and nonvisual information for perceiving direction of self-motion during walking. *Journal of Vision*, *14*(3), 1–17. https://doi.org/10.1167/14.3.24

Schlack, A., Hoffmann, K. P., & Bremmer, F. (2002). Interaction of linear vestibular and visual stimulation in the macaque ventral intraparietal area (VIP). *European Journal of Neuroscience*, *16*(10), 1877–1886. https://doi.org/10.1046/j.1460-9568.2002.02251.x

Schlack, A., Sterbing-D'Angelo, S. J., Hartung, K., Hoffmann, K. P., & Bremmer, F. (2005). Multisensory space representations in the macaque ventral intraparietal area. *Journal of Neuroscience*, *25*(18), 4616–4625. https://doi.org/10.1523/JNEUROSCI.0455-05.2005

Schmidt, R. A. (1975). A schema theory of discrete motor skill learning. *Psychological Review*, *82*(4), 225–260. https://doi.org/10.1037/h0076770

Schmitt, C., Baltaretu, B. R., Crawford, J. D., & Bremmer, F. (2020). A Causal Role of Area hMST for Self-Motion Perception in Humans. *Cerebral Cortex Communications*, *1*(1), 1–14. https://doi.org/10.1093/texcom/tgaa042

Schmitt, C., Krala, M., & Bremmer, F. (2022). Neural signatures of actively controlled self-motion and the subjective encoding of distance. *ENeuro*, *9*(6). https://doi.org/10.1523/ENEURO.0137-21.2022

Schmitt, C., Schwenk, J. C. B., Schütz, A., Churan, J., Kaminiarz, A., & Bremmer, F. (2021). Preattentive processing of visually guided self-motion in humans and monkeys. *Progress in Neurobiology*, *205*(June). https://doi.org/10.1016/j.pneurobio.2021.102117

Schröger, E., Marzecová, A., & Sanmiguel, I. (2015). Attention and prediction in human audition: A lesson from cognitive psychophysiology. *European Journal of Neuroscience*, *41*(5), 641–664. https://doi.org/10.1111/ejn.12816

Seno, T., Ogawa, M., Ito, H., & Sunaga, S. (2011). Consistent air flow to the face facilitates vection. *Perception*, *40*, 1237–1241. https://doi.org/10.1068/p7055

Sereno, M. I., & Huang, R. S. (2006). A human parietal face area contains aligned head-centered visual and tactile maps. *Nature Neuroscience*, *9*(10), 1337–1343. https://doi.org/10.1038/nn1777

Shams, L., Ma, W. J., & Beierholm, U. (2005). Sound-induced flash illusion as an optimal percept. *NeuroReport*, *16*(17), 1923–1927. https://doi.org/10.1097/01.wnr.0000187634.68504.bb

Shao, M., DeAngelis, G. C., Angelaki, D. E., & Chen, A. (2022). Higher Neural Functions and Behavior Clustering of heading selectivity and perception-related activity in the ventral intraparietal area, *Journal of neurophysiology*, *119*(3), 1113-1126. https://doi.org/10.1152/jn.00556.2017

Shibata, T. (2002). Head mounted display. *Displays*, *23*(1–2), 57–64. https://doi.org/10.1016/S0141-9382(02)00010-0

Shinder, M. E., & Taube, J. S. (2019). Three-dimensional Tuning of Head Direction Cells in Rats. *Journal of Neurophysiology*, *121*(1), 1–345. https://doi.org/10.1152/jn.00880.2017

Silk, T. J., Bellgrove, M. A., Wrafter, P., Mattingley, J. B., & Cunnington, R. (2010). Spatial working memory and spatial attention rely on common neural processes in the

intraparietal sulcus. *NeuroImage*, *53*(2), 718–724. https://doi.org/10.1016/j.neuroimage.2010.06.068

Simoncelli, E. P., & Heeger, D. J. (1998). A Model of Neural Responses in Area MT. *Vision Research*, *38*(5), 743–761. https://doi.org/10.1016/S0042-6989(97)00183-1

Singh-Curry, V., & Husain, M. (2009). The functional role of the inferior parietal lobe in the dorsal and ventral stream dichotomy. *Neuropsychologia*, *47*(6), 1434–1448. https://doi.org/10.1016/j.neuropsychologia.2008.11.033

Sirigu, A., & Desmurget, M. (2021). Somatosensory awareness in the parietal operculum. *Brain : A Journal of Neurology*, *144*(12), 3558–3560. https://doi.org/10.1093/brain/awab415

Sjolund, L. A., Kelly, J. W., & McNamara, T. P. (2018). Optimal combination of environmental cues and path integration during navigation. *Memory and Cognition*, *46*(1), 89–99. https://doi.org/10.3758/s13421-017-0747-7

Smith, A. T. (2021). Cortical visual area CSv as a cingulate motor area: a sensorimotor interface for the control of locomotion. *Brain Structure and Function*, *226*(9), 2931–2950. https://doi.org/10.1007/s00429-021-02325-5

Smout, C. A., Tang, M. F., Garrido, M. I., & Mattingley, J. B. (2019). Attention promotes the neural encoding of prediction errors. *PLoS Biology*, *17*(2), 1–22. https://doi.org/10.1371/journal.pbio.2006812

Sperry, R. W. (1950). Neural basis of the spontaneous optokinetic response produced by visual inversion. *Journal of comparative and physiological psychology*, *43*(6), 482. https://doi.org/10.1037/h0055479

Stangl, M., Kanitscheider, I., Riemer, M., Fiete, I., & Wolbers, T. (2020). Sources of path integration error in young and aging humans. *Nature Communications*, *11*(1). https://doi.org/10.1038/s41467-020-15805-9

Stengard, E., & Van Den Berg, R. (2019). Imperfect Bayesian inference in visual perception. *PLoS Computational Biology*, *15*(4), 1–27. https://doi.org/10.1371/journal.pcbi.1006465

Sterzer, P., & Kleinschmidt, A. (2010). Anterior insula activations in perceptual paradigms: often observed but barely understood. *Brain Structure & Function*, *214*(5–6), 611–622. https://doi.org/10.1007/s00429-010-0252-2

Straube, B., Van Kemenade, B. M., Arikan, B. E., Fiehler, K., Leube, D. T., Harris, L. R., & Kircher, T. (2017). Predicting the multisensory consequences of one's own action: Bold suppression in auditory and visual cortices. *PLoS ONE*, *12*(1), 1–25. https://doi.org/10.1371/journal.pone.0169131

Student, J., Engel, D., Timmermann, L., Bremmer, F., & Waldthaler, J. (2022). Visual Perturbation Suggests Increased Effort to Maintain Balance in Early Stages of Parkinson's to be an Effect of Age Rather Than Disease. *Frontiers in Human Neuroscience*, *16*(March), 1–13. https://doi.org/10.3389/fnhum.2022.762380

Studer, B., Cen, D., & Walsh, V. (2014). The angular gyrus and visuospatial attention in decision-making under risk. *NeuroImage*, *103*, 75–80. https://doi.org/10.1016/j.neuroimage.2014.09.003

Subramanian, D., Alers, A., & Sommer, M. A. (2019). Corollary Discharge for Action and Cognition. *Biological Psychiatry: Cognitive Neuroscience and Neuroimaging*, *4*(9), 782–790. https://doi.org/10.1016/j.bpsc.2019.05.010

Sun, Q., Zhang, H., Alais, D., & Li, L. (2020). Serial dependence and center bias in heading perception from optic flow. *Journal of Vision*, *20*(10), 1–15. https://doi.org/10.1167/JOV.20.10.1

Sunaert, S., Van Hecke, P., Marchal, G., & Orban, G. A. (2000). Attention to speed of motion, speed discrimination, and task difficulty: An fMRI study. *NeuroImage*, *11*(6 I), 612–623. https://doi.org/10.1006/nimg.2000.0587

Taoka, M., Toda, T., Hihara, S., Tanaka, M., Iriki, A., & Iwamura, Y. (2016). A systematic analysis of neurons with large somatosensory receptive fields covering multiple body regions in the secondary somatosensory area of macaque monkeys. *Journal of Neurophysiology*, *116*(5), 2152–2162. https://doi.org/10.1152/jn.00241.2016

Telford, L., Howard, I. P., & Ohmi, M. (1995). Heading judgments during active and passive self-motion. *Experimental Brain Research*, *104*(3), 502–510. https://doi.org/10.1007/BF00231984

Teufel, C., Dakin, S. C., & Fletcher, P. C. (2018). Prior object-knowledge sharpens properties of early visual feature-detectors. *Scientific Reports*, *8*(1), 1–12. https://doi.org/10.1038/s41598-018-28845-5

Teufel, C., & Fletcher, P. C. (2020). Forms of prediction in the nervous system. *Nature Reviews Neuroscience*, *21*(4), 231–242. https://doi.org/10.1038/s41583-020-0275-5

Thaler, L., Schütz, A. C., Goodale, M. A., & Gegenfurtner, K. R. (2013). What is the best fixation target? The effect of target shape on stability of fixational eye movements. *Vision Research*, *76*, 31–42. https://doi.org/10.1016/j.visres.2012.10.012

Tolman, E. C. (1948). Cognitive maps in rats and men. *Psychological Review*, *55*(4), 189–208. https://doi.org/10.1037/h0061626

Tootell, R., B. H.; Mendola, J., D.; Hadjikhani, N., K.; Ledden, P., J.; Liu, A., K.; Reppas, J., B.; Sereno, M., I.; Dale, A. M. (1997). Functional Analysis of V3A and Related Areas in Human Visual Cortex. *The Journal of Neuroscience*, *71*(18), 7060–7078. https://doi.org/doi:10.1523/jneurosci.17-18-07060.1997

Trees, J., Snider, J., Falahpour, M., Guo, N., Lu, K., Johnson, D. C., Poizner, H., & Liu, T. T. (2014). Game controller modification for fMRI hyperscanning experiments in a cooperative virtual reality environment. *MethodsX*, *1*, 292–299. https://doi.org/10.1016/j.mex.2014.10.009

Trutoiu, L. C., Mohler, B. J., Schulte-Pelkum, J., & Bülthoff, H. H. (2009). Circular, linear, and curvilinear vection in a large-screen virtual environment with floor projection. *Computers and Graphics (Pergamon)*, *33*(1), 47–58. https://doi.org/10.1016/j.cag.2008.11.008

Tuthill, J. C., & Azim, E. (2018). Proprioception. *Current Biology*, *28*(5), R194–R203. https://doi.org/10.1016/j.cub.2018.01.064

Tzourio-Mazoyer, N., Landeau, B., Papathanassiou, D., Crivello, F., Etard, O., Delcroix, N., Mazoyer, B., & Joliot, M. (2002). Automated anatomical labeling of activations in SPM using a macroscopic anatomical parcellation of the MNI MRI single-subject brain. *NeuroImage*, *15*(1), 273–289. https://doi.org/10.1006/nimg.2001.0978

Uhlmann, L., Pazen, M., van Kemenade, B. M., Steinsträter, O., Harris, L. R., Kircher, T., & Straube, B. (2020). Seeing your own or someone else's hand moving in accordance with your action: The neural interaction of agency and hand identity. *Human Brain Mapping*, *41*(9), 2474–2489. https://doi.org/10.1002/hbm.24958

Van Kemenade, B. M., Arikan, B. E., Kircher, T., & Straube, B. (2017). The angular gyrus is a

supramodal comparator area in action–outcome monitoring. *Brain Structure and Function*, *222*(8), 3691–3703. https://doi.org/10.1007/s00429-017-1428-9

Vicario, C. M., Nitsche, M. A., Salehinejad, M. A., Avanzino, L., & Martino, G. (2020). Time processing, interoception, and insula activation: A mini-review on clinical disorders. *Frontiers in Psychology*, *11*(August), 1–8. https://doi.org/10.3389/fpsyg.2020.01893

Von Hopffgarten, A., & Bremmer, F. (2011). Self-motion reproduction can be affected by associated auditory cues. *Seeing and Perceiving*, *24*(3), 203–222. https://doi.org/10.1163/187847511X571005

Wall, M. B., & Smith, A. T. (2008). The Representation of Egomotion in the Human Brain. *Current Biology*, *18*(3), 191–194. https://doi.org/10.1016/j.cub.2007.12.053

Wallace, M. T., Meredith, M. A., & Stein, B. E. (1998). Multisensory integration in the superior colliculus of the alert cat. *Journal of Neurophysiology*, *80*(2), 1006–1010. https://doi.org/10.1152/jn.1998.80.2.1006

Wandell, B. A., Dumoulin, S. O., & Brewer, A. A. (2007). Visual field maps in human cortex. *Neuron*, *56*(2), 366–383. https://doi.org/10.1016/j.neuron.2007.10.012

Wang, C., Chen, X., & Knierim, J. J. (2020). Egocentric and allocentric representations of space in the rodent brain. *Current Opinion in Neurobiology*, *60*, 12–20. https://doi.org/10.1016/j.conb.2019.11.005

Warren, S., Hamalainen, H. A., & Gardner, E. P. (1986). Objective classification of motion- and direction-sensitive neurons in primary somatosensory cortex of awake monkeys. *Journal of Neurophysiology*, *56*(3), 598–622. https://doi.org/10.1152/jn.1986.56.3.598

Warren Jr, W. H. (1995). Self-motion: Visual perception and visual control. In *Perception of space and motion* (pp. 263-325). Academic Press. https://doi.org/10.1016/B978-012240530-3/50010-9

Warren, W. H., & Kurtz, K. J. (1992). The role of central and peripheral vision in perceiving the direction of self-motion. *Perception & Psychophysics*, *51*(5), 443–454. https://doi.org/10.3758/BF03211640

Warren, W. H., Morris, M. W., & Kalish, M. (1988). Perception of Translational Heading From Optical Flow. *Journal of Experimental Psychology: Human Perception and Performance*, *14*(4), 646–660. https://doi.org/10.1037/0096-1523.14.4.646

Wiener, M., Hamilton, R., Turkeltaub, P., Matell, M. S., & Coslett, H. B. (2010). Fast forward: Supramarginal gyrus stimulation alters time measurement. *Journal of Cognitive Neuroscience*, *22*(1), 23–31. https://doi.org/10.1162/jocn.2009.21191

Wikenheiser, A. M., & Schoenbaum, G. (2016). Over the river, through the woods: Cognitive maps in the hippocampus and orbitofrontal cortex. *Nature Reviews Neuroscience*, *17*(8), 513–523. https://doi.org/10.1038/nrn.2016.56

Wittmann, M., Simmons, A. N., Aron, J. L., & Paulus, M. P. (2010). Accumulation of neural activity in the posterior insula encodes the passage of time. *Neuropsychologia*, *48*(10), 3110–3120. https://doi.org/10.1016/j.neuropsychologia.2010.06.023

Worsley, K. J., Marrett, S., Neelin, P., Vandal, A. C., Friston, K. J., & Evans, A. C. (1996). A unified statistical approach for determining significant signals in images of cerebral activation. *Human Brain Mapping*, *4*(1), 58–73. https://doi.org/10.1002/(SICI)1097-0193(1996)4:1<58::AID-HBM4>3.0.CO;2-O

Wu, H., Jin, H., Sun, Y., Wang, Y., Ge, M., Chen, Y., & Chi, Y. (2016). Evaluating stereoacuity with 3D shutter glasses technology. *BMC Ophthalmology*, *16*(1), 4–11. https://doi.org/10.1186/s12886-016-0223-3

Yahata, R., Takeya, W., Seno, T., & Tamada, Y. (2021). Hot Wind to the Body Can Facilitate Vection Only When Participants Walk Through a Fire Corridor Virtually. *Perception*, *50*(2), 154–164. https://doi.org/10.1177/0301006620987087

Zheng, Q., Zhou, L., & Gu, Y. (2021). Temporal synchrony effects of optic flow and vestibular inputs on multisensory heading perception. *Cell Reports*, *37*(7), 109999. https://doi.org/10.1016/j.celrep.2021.109999

Zhu, S. L., Lakshminarasimhan, K. J., & Angelaki, D. E. (2023). Computational cross-species views of the hippocampal formation. *Hippocampus*, *February*. https://doi.org/10.1002/hipo.23535

Zuanazzi, A., & Noppeney, U. (2020). Modality-specific and multisensory mechanisms of spatial attention and expectation. *Journal of Vision*, *20*(8), 1–16. https://doi.org/10.1167/JOV.20.8.1

9. VERZEICHNIS DER AKADEMISCHEN LEHRER/-INNEN

Meine akademischen Lehrenden in Marburg waren:

Bremmer
Endres
Jansen
Kircher
Oertel
Schübo
Sommer
Straube

In Giessen:

Fiehler
Fleming
Gegenfurtner
Munzert
Schwarzer

In Frankfurt:

Vo

In Toronto, Kanada:

Crawford
Harris
Henriques

In Kingston, Kanada:

Blohm
Munoz
Troje

In Berlin:

Penzel
Fietze
Glos

In Magdeburg:

Kaiser
Krippl
Merkel
Müller
Noesselt
Pollmann
Ullsperger

In Münster:

Bruchmann
Schloßmacher
Straube

In Osnabrück:

Becker
Düsing
Gruber
Klanke
Kuhl
Müller
Schöne
Schumacher
Staufenbiel
Straatmann
Stockhorst
Schöttke

10. DANKSAGUNG

Zuallererst möchte ich meinem Betreuer und Supervisor, Prof. Dr. Frank Bremmer, für seine Unterstützung, seine Geduld und seine ständige Hilfsbereitschaft danken. Dafür, dass er sich Zeit genommen hat, meine Forschungsinhalte- und Ideen, meine Karriere und meine Pläne mit mir zu diskutieren. Dafür, dass er stets verständnisvoll und hilfsbereit war und dafür, dass er mir in allen Bereichen mit Ratschlägen zur Seite gestanden hat. Ich bedanke mich herzlich für die Zeit in Marburg, in der AG Neurophysik. Außerdem möchte ich ihm und Prof. Dr. Katja Fiehler für die Möglichkeit danken, Teil einer einzigartigen, internationalen Forschergruppe, dem ‚IRTG', gewesen sein zu dürfen.

Ganz besonderer Dank gilt Dr. Jakob C. B. Schwenk für seine Hilfe in absolut allen Bereichen, für all seine investierte Mühe und alles, was er für mich getan hat.

Ich möchte mich ebenfalls bei meinem Zweitbetreuer, Prof. Dr. Benjamin Straube für seine engagierte und hilfreiche Betreuung und dafür, dass er mir jederzeit mit seiner Hilfe und fachlicher Expertise zur Seite gestanden hat, bedanken.

Special thanks to my colleagues Dr. Jan Churan, Alexander Kreß, Dr. André Kaminiarz and Dr. Baptiste Caziot for providing help and important input throughout my PhD. I would like to thank the whole AG Neurophysik for wonderful three years at the Lahnberge: Dr. David Engel, Dr. Constanze Schmitt, Renate Reisenegger, Sadra Fatkhhani (+ Pari), Georg Blanke, Elisa Grewe, Oliver Beckert, Frau Thomas and Sarah Bindbeutel.

Herzlicher Dank gilt Alexander Platzner für seine tatkräftige Unterstützung, ohne die meine Forschungstätigkeit nicht möglich gewesen wäre, sowie Samira Zander für ihren großartigen Einsatz bei der Durchführung meiner Experimente.

Außerdem bedanken möchte ich mich bei der Gruppe der Klinik für Psychiatrie und Psychotherapie unter Leitung von Prof. Dr. Thilo Kircher. Ich danke Dr. Ezgi B. Arikan für ihre Anleitung und für ihre extreme Hilfsbereitschaft. Ebenfalls bedanken möchte ich mich bei Prof. Dr. Bianca van Kemenade für ihren Einsatz und ihre wertvolle Hilfestellung. Besonderer Dank gilt Dr. Jens Sommer. Der Erfolg meiner Dissertation ist durch seine exakte und lehrreiche Arbeit mitgetragen.

Ich danke auch Prof. Dr. Thomas Penzel und Prof. Dr. Ingo Fietze für Ihre Unterstützung und Geduld!

Особую благодарность я хочу выразить моим родителям, Елене и Игорю Розенблюм. Всё то, чего я достигла в своей жизни и каким человеком я стала, произошло только благодаря вам. Вы - мои примеры для подражания, мои учителя, мои друзья